ELUCIDATING THE ROLE OF MOR-1K IN OPIOID-INDUCED HYPERALGESIA

Folabomi Abiola Oladosu

A dissertation submitted to the faculty at the University of North Carolina at Chapel Hill in partial fulfillment of the requirements for the degree of Philosophy in the Curriculum of Neurobiology in the school of Medicine

Chapel Hill
2016

Approved by:
Andrea G. Nackley
Linda Dykstra
Ru-Rong Ji
William Maixner
Mark Zylka

ABSTRACT

Folabomi Abiola Oladosu: Elucidating the Role of MOR-1K in Opioid-Induced Hyperalgesia
(Under the direction of Andrea G. Nackley)

Opioids commonly used in the treatment of acute and chronic pain have been reported to produce a paradoxical opioid-induced hyperalgesia (OIH) in a subset of the population. Recent evidence indicates a potential role for MOR-1K, an alternative splice variant of MOR-1, in OIH. Unlike its parent receptor, MOR-1K has a genetic association with increased pain sensitivity and facilitates cellular excitation upon opioid activation. Because of these properties, we hypothesize that MOR-1K contributes to OIH in genetically susceptible individuals. First, using a murine model of OIH alongside RNA interference-mediated knockdown and virally-mediated overexpression, we established MOR-1K plays a role in OIH development in a strain-specific manner, such that the 129S6 strain demonstrated an exclusively analgesic pain profile with decreased MOR-1K transcript levels, while the CXB7/ByJ strain demonstrated an exclusively hyperalgesic pain profile with increased MOR-1K transcript levels. These strain-specific divergences prompted subsequent genetic and molecular biologic studies, revealing a functional single nucleotide polymorphism in the MOR-1K gene locus that is associated with OIH and MOR-1K expression. Additionally, we have characterized MOR-1K cellular expression, demonstrating that the splice variant is expression in satellite glial cells in the dorsal root ganglion. Together, our findings suggest that MOR-1K is an essential contributor to OIH development. With further research, MOR-1K could be exploited as a target for development of antagonists that reduce or prevent OIH.

ACKNOWLEDGEMENTS

"It takes a whole village to raise a child."

~African Proverb

Even though the bulk of this text consists of all the work I've done for the past six years of my life, I consider this particular section to be the most important, because this section acknowledges all the people who have made this document possible. First, I thank my parents for bringing me into this world and nurturing my sense of curiosity, even though in got me into trouble, and for introducing me into the world of math and science. Second, I thank all the mentors I've had throughout my life that encouraged me to learn and gave me the confidence to push forward. Of note, I want to acknowledge Drs. Kelly Giovanello, Parastoo Hashemi, Elyse Dankowski, Ed Smith, Dave Harrison, Ashalla Freeman, Jessica Harrell, Samatha Segall, and Carolina Meloto. I also want to acknowledge my friends within and outside the world of academic research. These were the people who stood by my side in times both good and bad. Last, but not least, I must thank my lab family. Drs. Jane Hartung and Brittney Ciszek: I could not have asked for better lab sisters and better friends and I cannot wait to see what future successes come your way. Sandra O'Buckley: Even though you arrived in the lab half way through my grad school career, I could not imagine arriving at the end of this experience without you. You have provided me with an abundance knowledge and support. Dr. Andrea Nackley: At first, I thought that you chose me because you were

doing me a kindness, giving me a shot. I was wrong; you saw what I could not see in myself and helped me to realize my capabilities and my potential. You instilled in me the confidence I need to be successful in whatever I approach. For that, I cannot thank you enough.

All these people have each made their own impact in my life and have helped shaped me to become who I am today and will continue to do so in the future, long after this text is published and bound, collecting dust.

TABLE OF CONTENTS

LIST OF TABLES

LIST OF FIGURES

LIST OF ABBREVIATIONS

αAR: Alpha Adrenergic receptor

βAR: Beta Adrenergic receptor

2-AG: 2-Arachidonoylglycerol

5-HT: Serotonin

AAV: Adeno-associated Virus

AC: Adenylyl Cyclase

bHLH: basic helix-loop-helix

C-term: Carboxyl Terminus

Ca^{++}: Calcium

cAMP: Cyclic Adenosine Monophosphate

CB: Cannabinoid

CTFI: corrected total fluorescent intensity

DAMGO: [D-Ala^2, N-$MePhe^4$, Gly-ol]-enkephalin

DF: Dorsolateral Funiculus

E-Box: Enhancer Box

EL: Extracellular Loop

Epi: Epinephrine

GI: Gastrointestinal

GPCR: G-protein coupled receptor

HEK: Human Embryonic Kidney

HIF: Hypoxia-inducible Factor

HRP: Horseradish Peroxidase

IBNtxA: Iodobenzoylnaltrexamide

LPI: Lysophosphatidylinositol

LSD: Lysergic Acid Diethylamide

LTP: Long Term Potentiation

MAO: Monoamine Oxidase

MC1R: Melanocortin 1 Receptor

MOR-1: Mu Opioid Receptor 1

mRNA: Messenger Ribonucleic Acid

N-term: Amino Terminus

NADA: *N*-Arachidonoyl Dopamine

NMDA: *N*-methyl-D-aspartate

NE: Norepinephrine

NET: Norepinephrine Transporter

OAE: *O*-Arachidonoyl Ethanolamine

OIH: Opioid-induced Hyperalgesia

OP: Opioid

PAG: Periaqueductal Grey

PBS: Phosphate-buffered Saline

PBS-T: Phosphate-buffered Saline with Triton-X

PLC β: Phospholipase C β

ROI: Region of Interest

RVM: Rostral ventral Medulla

SERT: Serotonin Transporter

Sc: Spinal Cord

SGC: Satellite Glial Cell

siRNA: Small Interfering Ribonucleic Acid

SNP: Single Nucleotide Polymorphism

SP: Substance P

THC: Tetrahydrocannabinol

TM: Transmembrane

TRVP1: Transient Receptor Potential Cation Channel Subfamily V Member 1

Introduction

Defining Acute and Chronic Pain

Pain is a multidimensional sensory and emotional experience that can generally be categorized into one of four types(1). *Nociceptive pain* is an acute response to environmental stimuli that warns of potential or actual tissue damage. This type of pain provides is considered adaptive, as it facilitates in the avoidance of potentially noxious stimuli. In the event of actual damage, inflammatory and/or neuropathic pain may occur. *Inflammatory pain* occurs in response to damage of tissues or the presence of infection. The presence of noxious stimuli (i.e. capsaicin, mustard oil, acid, etc.) or pro-inflammatory mediators (i.e. Substance P, cytokines, proteases) released from immune cells produce a pronociceptive signal accompanied by edema at the site of injury(2). *Neuropathic pain* occurs in response to direct insult of peripheral nerves. This damage, usually caused by lesioning or substantial pressure against the nerve, creates increased spontaneous firing, which is associated with unwarranted widespread pain, spontaneous sharp or burning pain, and tactile hypersensitivity(3). Inflammatory and neuropathic pain typically serve to promote wound healing and repair; however, in many cases the pain outlasts the stimulus and becomes chronic. Examples of chronic inflammatory and neuropathic pain disorders include complex regional pain syndrome; rheumatoid arthritis; diabetic neuropathy; chemotherapy induced neuropathy; and post-surgical neuropathic pain. Unlike three aforementioned types of pain, *functional or idiopathic pain* is characterized by perpetual abnormalities in sensory processing that occur in the absence of direct inflammation or nerve damage. Chronic pain disorders characterized by functional or idiopathic pain include fibromyalgia, migraine, temporomandibular joint disorder, irritable bowel syndrome, and vulvodynia(4).

Acute and chronic pain are primarily treated with pharmacologic agents that promote analgesia. The principle target of a variety of analgesic drugs including opioids, cannabinergics, and anti-depressants is G-protein coupled receptors (GPCRs). Upon activation, GPCRs initiate molecular changes resulting in excitation or inhibition of nerve, immune, and glial cells important for the onset and maintenance of pain. For example, mu opioid receptors modulate the onset and maintenance of pain due to their expression in primary afferent nociceptors, spinal cord, and brain. Given its expression in the primary afferents, activation of the mu opioid receptor (MOR-1) quells excitatory signaling in pronociceptive Aδ and C fibers. In the spinal cord, MOR-1 activation quells pronociceptive signaling via the inhibition of Substance P release and hyperpolarization lamina II interneuron. In conjunction with antinociception in the periphery and spinal cord, MOR-1 activation in key supraspinal regions affect the perception (i.e. anterior insula, anterior cingulate cortex) and descending modulation (i.e. periaqueductal gray, rostral ventromedial medulla) of antinociception(5).

While the critical role of GPCRs in pain biology and management is well-established, reliably effective therapeutics with minimal side-effects are lacking. Inter-individual variability in response to a given analgesic is largely due to variation at the genetic level. Of particular interest are genetic variants in alternative splice regions that alter protein coding of the mRNA, giving rise to proteins which differ in form and function (i.e., alternative splice variants). Chapter 1 will highlight the importance of alternative splicing of GPCRs, including MOR-1, in the transmission and modulation of pain. Chapters 2 through 4 will then focus on molecular, cellular, and behavioral studies that demonstrate a role for MOR-1K, a MOR-1 alternative splice variant, in the development of opioid induced hyperalgesia.

Defining Opioid-induced Hyperalgesia

Opioids are amongst the most frequently prescribed treatment for acute and chronic pain. As of 2012, 259 million prescriptions were written exclusively in the United States(6). The favorability of opioids over other types of pain management treatments is due to its potent analgesia. Opioids

produce their analgesic effects primarily by targeting MOR-1. MOR-1 is a seven transmembrane GPCR, that, upon opioid binding, utilize $G_{i/o}$ signaling to reduce cyclic adenosine monophosphate levels (cAMP) and intra-cellular Ca^{2+} levels, thus inhibiting pronociceptive signaling(7). MOR-1s are located in central, spinal, and peripheral regions where they can modulate the perception, transmission, and transduction of pain. Centrally and spinally, MOR-1s are ubiquitously expressed in the brain, especially concentrated in somatosensory cortex, the periaqueductal grey, striatum, nucleus accumbens, the superficial dorsal horn of the spinal cord(8,9) and in glial cells(10,11). In the periphery, MOR-1s are expressed in a variety of cell types: lymphocytes(12,13), dendritic cells(14), and endothelial cells(15). Given its vast expression, MOR-1s have the ability to greatly impact pain transmission throughout the body.

Despite its analgesic properties, opioids come with unwanted side effects that complicate pain management. These problematic side effects include opioid tolerance, respiratory depression, opioid-induced constipation, opioid dependence, opioid withdrawal, and addiction(16). Another emerging side effect is opioid-induced hyperalgesia (OIH), a paradoxical condition in which opioids produce pain. This chapter will review the etiology and known mechanisms of OIH and will also provide the foundation for the hypothesis that MOR-1K contributes OIH development in genetically susceptible individuals.

The clinical prevalence of OIH

Opioid-induced hyperalgesia, or OIH, is defined as increased pain sensitivity following acute or chronic opioid administration that is also distinct from the originally reported pain(17). This paradoxical condition was first reported in 1986(18); since this initial report, debate still exists over the relevance of OIH as a real clinical concern. One point of contention is if OIH is simply another presentation of opioid tolerance. Clinical studies have shown that these conditions are indeed different. With opioid tolerance, increasing the administered dose to a higher concentration provides analgesia that was formerly achieved with a lower concentration. With OIH, however, the

administration of an increased amount/or concentration of drug would further exacerbate the patient's reported pain (19,20).

Although the occurrence of OIH within the general population is unknown, clinical studies have revealed three populations that present with OIH: post-surgical patients; former opioid addicts; and chronic pain patients. A meta-analysis of twenty seven studies investigating post-operative OIH found that high doses of remifentanil administration were associated with increased pain sensitivity and that remifentanil-induced pain persisted for at least 24 hours following surgery (21). These data demonstrate that acute opioid administration following surgery/injury can produce increased pain sensitivity. Similarly, chronic opioid administration also produces increased pain sensitivity, specifically in former opioid addicts and in chronic pain patients. When compared to opioid naïve participants, both methadone-maintained subjects and opioid-treated chronic pain patients demonstrated greater pain responses to thermal cold stimuli(22,23). Furthermore, investigations of long-term opioid treatment for chronic pain revealed that OIH manifests differently based on the type of chronic pain. For example, within the migraine and IBS populations, OIH can manifest as medication overuse headache and narcotic bowel syndrome, respectively (24-26).

The clinical use of opioids is a critical component of acute and chronic pain management. The prevalence of OIH, however, compromises the efficacy of opioid analgesia. If opioids are to remain a standard of acute and chronic pain management, it is essential to separate OIH from opioid analgesia and prevent its occurrence. In order to achieve this goal, it is necessary to define the mechanisms that produce this paradoxical pain.

The molecular mechanisms of OIH

The culmination of basic science research suggests that OIH is due to neuroplastic changes in the central and peripheral nervous system, ultimately promoting pronociceptive signaling. Despite this knowledge, the complete mechanism that causes this opioid-induced sensitization is partially formed.

Thus far, the molecular changes related to the central glutamatergic system, the descending facilitation system, or the norepinephrine system the have been implicated in OIH.

Glutamate, one of the most abundant excitatory neurotransmitters, modulates synaptic plasticity and long-term potentiation (LTP) via activation of *N*-methyl-D-aspartate (NMDA) receptor (27). Given that LTP is involved in OIH(28), it is no surprise that NMDA receptor also contribute to OIH. Following chronic morphine administration in Sprague Dawley rats, Mao and colleagues discovered an opioid-induced inhibition in spinal glutamate reuptake transporters, increase synaptic glutamate levels(29). A separate study exploring the role of the NMDA receptor in OIH revealed that the co-administration of s-ketamine or MK-801, both NMDA receptor antagonists, with morphine prevented mechanical hyperalgesia and increased *NMDAR1* mRNA expression(30,31). S-ketamine, when administered preventatively, also blocks remifentanil-induced hyperalgesia clinically(32,33). These studies demonstrate that the central glutamatergic system is necessary for OIH development.

The descending facilitation pathway also contributes to OIH. This pathway, including the periaqueductal grey (PAG), rostral ventral medulla (RVM), and the dorsolateral funiculus (DF), modulates transmission via the release of endogenous opioids(20). Dysfunction in the descending facilitation pathway is known to promote chronic pain conditions and also contributes to OIH. Morphine-induced hyperalgesia was found to be blocked via lidocaine injection into RVM(34) or via bilateral lesioning of the dorsolateral funiculus(35). Spinal dynorphin, an endogenous opioid peptide neurotransmitter involved in descending facilitation, also contribute to the mechanism that drives OIH. The pre-emptive intrathecal administration of dynorphin antiserum in rats blocked [D-Ala^2, N-MePhe^4, Gly-ol]-enkephalin (DAMGO) induced pain and tolerance(36).

In addition to glutamatergic activity and descending facilitation, norepinephrine and beta-adrenergic receptor activity also enable the development of OIH. A preclinical study examining gene associations with OIH in mice found a significant correlation between gene *ADRB2,* which codes for

beta 2-adrenergic receptor (β2AR), and morphine-induced hyperalgesia(37). A subsequent clinical study found that co-administration of propranolol with remifentanil reduced mechanical hyperalgesia in participants(38).

The aforementioned systems contribute to the central sensitization characteristic of OIH. That said, none of these receptors directly bind to opioids, and therefore, cannot be responsible for initiating the mechanism that drives OIH. Sticking to the principle of Ockham's razor, the most likely initiator would be a receptor within the mu opioid receptor family, given their high binding affinity for opioids. Here, we introduce a likely candidate: a splice variant of the mu opioid receptor, MOR-1K.

CHAPTER 1: The Role of G-Protein Coupled Receptors and Their Alternative Splice Variants in Pain Management[1]

1.1 GPCRs are Relevant for the Treatment of Pain

Drugs that target GPCRs represent the primary treatment strategy for patients with acute and chronic pain; however, there is individual variability in both the efficacy and adverse side effects associated with these drugs. These inconsistencies reflects individuals' variability in alternative splicing of pain-relevant GPCRs. Here, this chapter reviews the importance of GPCRs and their known splice variants to the management of pain.

The human genome encodes approximately 800 distinct GPCRs, 70% of which contribute to pain-related phenotypes(39). GPCRs interact with a variety of signaling mediators, ranging from small molecules to large proteins. Although each receptor has the ability to induce a range of functional intracellular changes, all GPCRs possess distinct and evolutionarily conserved architecture. Each canonical receptor is comprised of seven transmembrane (7TM) proteins that span the cellular membrane. These transmembrane proteins are interconnected by intracellular and extracellular loops (Figure 1.1). In addition, there are amino acid chains known as N-terminus and C-terminus tails, which are attached to the first and last transmembrane, respectively. As alluded by its name, every GPCR is coupled to a G-protein, which acts as a molecular switch to regulate cellular activity.

[1]This chapter previously appeared as an article in Mayo Clinic Proceedings. The original citation is as follows: Oladosu F.A., Maixner W., and Nackley A.G., "Alternative Splicing of G-Protein Coupled Receptors: Relevance to Pain Management" *Mayo Clin Proc* 90, no 8. (August 2015): 1135-1151.

Figure 1.1. GPCR structure and function. **A)** A g-protein coupled receptor (GPCR) is composed of seven transmembranes (grey) interconnected by three intracellular (orange) and three extracellular (purple) loops. On the end of the first and last transmembrane are the N-terminus (blue) and C-terminus (red), respectively. As its name suggests, a GPCR is bound to a trimeric g-protein composed of alpha (α) and beta/gamma (β/γ) subunits. **B)** When a ligand (black) binds to a GPCR, the associated g-protein separates into the α and β/γ subunits. These subunits then stimulate a variety of downstream effectors that produce changes in cellular activity (see Table 1). Abbreviations: GPCR = G-Protein Coupled Receptor

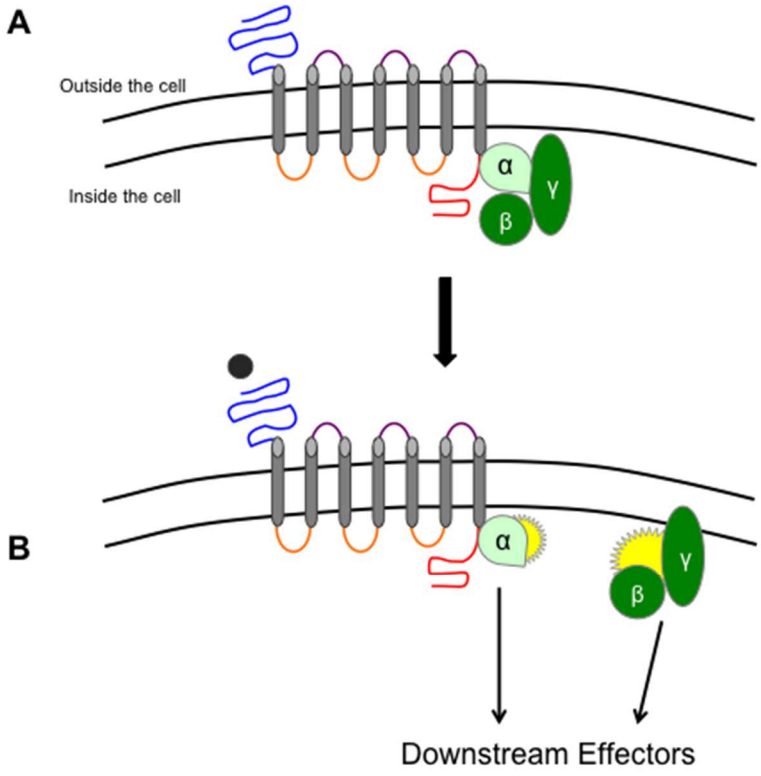
A
Outside the cell
Inside the cell
α
γ
β
B
α
γ
β
Downstream Effectors

Table 1.1. Common G-proteins and Their Intracellular Effects

G protein	Effectors	Overall Impact
$G\alpha_s$	activates adenylyl cyclase → ↑ cAMP[a]	cellular excitation (pro-nociceptive)
$G\alpha_q$	activates PLCβ → ↑ intracellular Ca^{++} levels	cellular excitation (pro-nociceptive)
$G\alpha_{i/o}$	inhibits adenylyl cyclase → ↓ cAMP	cellular inhibition (anti-nociceptive)

[a]Abbreviations: cAMP = cyclic adenosine monophosphate; Ca^{++} = calcium; PLCβ = phospholipase C β.

The resulting structure created by the transmembrane segments and loops provides interactive sites where ligands can bind. Ligands that bind to their receptor and initiate cell signaling are referred to as agonists. Upon binding, agonists produce a conformational change of the GPCR and subsequent uncoupling of the associated g-protein. Once uncoupled, the g-protein separates into two subunits (the alpha (α) and beta/gamma (β/γ) subunits), each of which initiates a chain of molecular reactions that affect cellular activity(40). Depending on the type of g-protein, the initiated downstream effects can promote cellular excitation or inhibition (Table 1.1). In general, agonists that activate pain-relevant GPCRs coupled to G_s typically produce pain, while those coupled to G_i typically inhibit pain(39). Other ligands, known as antagonists, compete with agonists for the GPCR binding site and impede g-protein uncoupling and downstream signaling events. Because of their ability to modulate cellular activity at each step of the pain pathway, GPCRs represent a popular pharmacologic target for the management of clinical pain. In fact, over 60% of commonly prescribed analgesics work by binding to GPCRs(40). Table 1.2 provides a summary of these GPCRs (opioid, cannabinoid, adrenergic, and serotoninergic receptors) along with their associated g-protein, endogenous ligands, and analgesic compounds.

Table 1.2. GPCRs Commonly Targeted for Clinical Pain Management

GPCR	G-protein	Endogenous Ligands	Prescribed Analgesics			Known Splice Variant
			Reuptake Inhibitors	Agonist	Antagonist	
Cannabinoid (CB) Receptors						
CB1	$G\alpha_i(41)$	2-AG Anandamide		Nabilone THC	Cannabidiol	Yes
CB2	$G\alpha_i(41)$	LPI NADA OAE		Nabilone THC	Cannabidiol	Yes
Adrenergic (AR) Receptors						
α_1AR	$G\alpha_q(42)$	Epinepherine Norepinephrine	Amitriptyline (NET) Despiramine (NET) Desvenlafaxine (NET) Duloxetine (NET) Levorphanol (MAO) Meperidine (NET) Nortriptyline (NET) Tapentadol (NET) Venlafixine (NET)		Amitriptyline Promethazine Nortriptyline Trazodone	Yes
α_2AR	$G\alpha_i(42)$			Clonidine	Trazodone	No
β_1AR	$G\alpha_s(43)$				Atenolol Nadolol Metoprolol	No

					Propanolol Timolol	
β_2AR	$G\alpha_{s,}$ $G\alpha_i$(43)				Nadolol Propanolol Timolol	No
β_3AR	$G\alpha_s$(43)				Nadolol Propanolol Timolol	Yes
Serotonin (5-HT) Receptors						
5-HT_1	$G\alpha_i$(44)	Serotonin	Amitriptyline (SERT) Despiramine (SERT) Desvenlafaxine (SERT) Duloxetine (SERT) Levorphanol (MAO) Nortriptyline (SERT) Trazodone (SERT) Venlafaxine (SERT)	Almotriptan Dihydroergotamine Eletriptan Frovatriptan Naratriptan Rizatriptan Sumatriptan Zolmitriptan	Trazodone	No
5-HT_2	$G\alpha_q$(44)			Dihydroergotamine	Amitriptyline	Yes

				Methylergometrine	Nortriptyline Promethazine Trazodone	
5-HT_4	$G\alpha_s$(44)			Mosapride		Yes
5-HT_6	$G\alpha_s$(44)				Amitriptyline Nortriptyline Trazodone	Yes
5-HT_7	$G\alpha_s$(44)				Amitriptyline Trazodone	Yes
Mu-Opioid Receptor						
MOR-1[a]	$G\alpha_i$(45)	α-endorphin β-endorphin γ-endorphin		Alfentanil Buprenorphine Codeine Fentanyl Hydrocodone Hydromorphone Levorphanol	Naloxone Naltrexone	Yes

				Meperidine Methadone Morphine Oxycodone Oxymorphone Remifentanil Sufentanil Tapentadol Tramadol		

Abbreviations: 2-AG = 2-Arachidonoylglycerol; 5-HT = Serotonin; CB = Cannabinoid; LPI = Lysophosphatidylinositol; MAO = Monoamine Oxidase; MOR-1 = Mu Opioid Receptor NADA = *N*-Arachidonoyl Dopamine; NET = Norepinephrine Transporter; OAE = *O*-Arachidonoyl ethanolamine; SERT = Serotonin Transporter; THC = Tetrahydrocannabinol**;** αAR = Alpha adrenergic receptor; βAR = Beta adrenergic receptor

Cannabinoid receptors share similar signaling properties with MOR-1, making them attractive targets for clinical pain management. There are two cannabinoid (CB) receptor subtypes, CB_1 and CB_2, both of which couple to $G_{\alpha i}$. CB receptors play a significant role in promoting analgesia in response to endocannabinoids such as 2-Arachidonoylglycerol (2-AG), and anandamide. Commercially available CB agonists such as nabilone and tetrahydrocannabidol, which bind to both CB subtypes, are used to treat fibromyalgia and neuropathic pain(46).

Adrenergic receptors, which mediate the physiological responses to epinephrine (Epi) and norepinephrine (NE), represent another frequently targeted class of GPCRs. The adrenergic superfamily includes three subtypes respectively of α_1ARs (α_{1A}AR, α_{1B}AR, α_{1D}AR), α_2ARs (α_{2A}AR, α_{2B}AR, α_{2C}AR), and βARs (β_1ARs, β_2ARs, β_3ARs). The α_2AR couples to $G_{\alpha i}$ and promotes analgesia *via* cellular inhibition. Hence α_2AR agonists such as trazodone are used to promote analgesia. In contrast, α_1AR, which is coupled to $G_{\alpha q}$, facilitates cellular excitation of pronociceptive neurons, resulting in increased pain signaling. The βARs also facilitate pain signaling *via* $G_{\alpha s}$ signaling. To attenuate their excitatory contributions, α_1AR and βARs are commonly used to treat a range of chronic pain disorders such as migraine, neuropathic pain, and fibromyalgia.

Serotonin receptors, which mediate physiological responses to the monoamine serotonin (5-HT) play an important role in pain management(44). The serotonin superfamily is quite large, including seven general members: 5-HT_1 (5-HT_{1A}, 5-HT_{1B}, 5-HT_{1D}, 5-HT_{1E}, 5-HT_{1F}), 5-HT_2 (5-HT_{2A}, 5-HT_{2B}, 5-HT_{2C}), 5-HT_3, 5-HT_4, 5-HT_5, 5-HT_6, and 5-HT_7. With the exception of the 5-HT_3 receptor, a ligand-gated ion channel, all 5-HT receptors are GPCRs. The effects of the 5-HT receptor family on pain are heavily dependent upon the receptor subtype. Triptans target $G_{\alpha i}$-coupled 5-HT_1 receptors, which promote analgesia *via* cellular inhibition, and normalize vascular changes associated with migraine headache(47). Antidepressants promote chronic synaptic serotonin release that causes the downregulation of $G_{\alpha q}$ coupled 5-HT_2 receptors, thus attenuating their excitatory contributions to pain signaling. 5-HT antagonists that target 5-HT_4 receptors in the central nervous system and the

gastrointestinal (GI) tract are used in the treatment of migraine(48) and IBS(49). Meanwhile, the net effect of 5-HT_7 activation on pain is highly dependent on the location of the receptor. Activation of 5-HT_7 receptors on peripheral nerve terminals produces pain(50,51), while activation in midbrain structures such as the periaqueductal gray alleviates pain associated with nerve injury(52).

Finally, opioid receptors are among the most well known GPCRs that regulate the transmission and perception of pain. There are four opioid receptor subtypes, including: the mu opioid receptor (MOR-1), the delta opioid receptor, the kappa opioid receptor, and the nociceptin receptor (ORL-1). Of these subtypes, MOR-1 is the classic receptor responsible for analgesic responses to endogenous endorphins as well as exogenous drugs. Upon agonist binding to MOR-1, its associated $G_{\alpha i}$ protein is activated and produces cellular inhibition of pronociceptive neurons(7). For this reason, opioids are used in the management of acute pain (such as that associated with surgery) as well as chronic pain disorders such as low back pain, extremity pain, and osteoarthritis(53). Opioid antagonists, usually co-administered with opioid agonists to reduce the development of unwanted opioid side effects, are also capable of producing analgesia independently of MOR-1(54).

While these conventional therapeutics are able to alleviate pain, their efficacy is limited to a subset of the population(55). Additionally, their use is constrained by adverse side effects, such as altered mental state, nausea, constipation, sedation, and life-threatening respiratory depression. Variability in patient response and side-effect profiles is, in part, due to variability in alternative splicing of GPCRs expressed in tissues that regulate pain processing. By expanding our understanding of GPCR alternative splice variants and their associated pharmacodynamic responses, we will be able to better predict patient-centered treatment outcomes.

1.2 The Impact of Alternative Splicing on GPCR Signaling

1.2.1 Alternative splicing adds to the diversity of GPCR signaling

Alternative splicing is an important mechanism of gene regulation, affecting approximately 90% of all genes within the human genome(56). A single gene is able to generate exponential protein coding capabilities *via* alternative splicing. Prior to alternative splicing, a gene is first transcribed into precursor messenger ribonucleic acid (pre-mRNA). The pre-mRNA sequence contains short protein coding regions known as exons. Interspersed between the exons are longer non-coding regions known as introns (Figure 1.2). Before the sequence can be translated to produce protein, the introns and alternative exons within pre-mRNA are removed, or spliced, and the constitutive exons are brought together, resulting in the canonical mRNA transcript ready for protein synthesis. When alternative splicing occurs, however, the pre-mRNA is edited such that constitutive exons are removed from, or introns are retained, in the final mRNA transcript. The most common type of alternative splicing within the human genome is exon skipping(57). Here, constitutive exons are excluded from the final mRNA transcript. Another common type of alternative splicing is splice site selection, in which the portion of an exon is spliced out due the presence of a nucleotide sequence that facilitates splicing activity(57). Intron retention is another type of alternative splicing in which an intron remains in the final mRNA transcript. Each type of alternative splicing will render an mRNA transcript and corresponding protein that is structurally different than the canonical protein produced from the standard template (Figure 1.3).

Figure 1.2. Different types of alternative splicing. The most common type of alternative splicing in animals is **A)** exon skipping, in which a constitutive exon is spliced from the final mRNA transcript. Alternative **B)** 3' and **C)** 5' splice sites provide additional junctions within an exon, resulting in partial splicing of the exonic mRNA sequence. **D)** Intron retention is a rare type of alternative splicing that occurs when an intron remains within the final mRNA transcript. Abbreviations: mRNA = Messenger Ribonucleic Acid

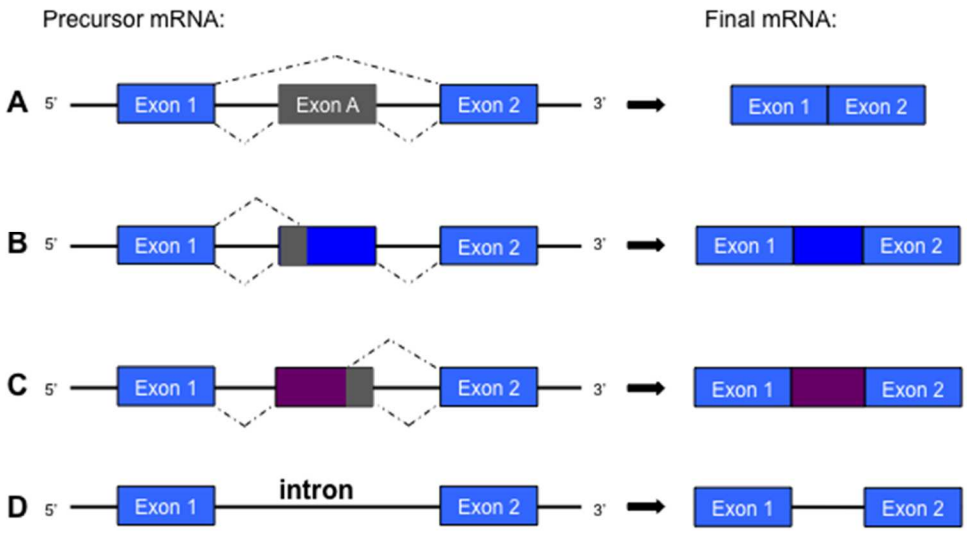
Precursor mRNA:
Final mRNA:
A
5'
Exon 1
Exon A
Exon 2
3'
Exon 1
Exon 2
B
5'
Exon 1
Exon 2
3'
Exon 1
Exon 2
C
5'
Exon 1
Exon 2
3'
Exon 1
Exon 2
D
5'
Exon 1
intron
Exon 2
3'
Exon 1
Exon 2

Figure 1.3. Structural variations in GPCRs as a result of alternative splicing. Exons within the mRNA transcript serve as coding regions for specific sections of protein. Alternative splicing events that change or remove exonic sequences can produce GPCR splice variants with corresponding changes in protein composition and/or structure. **A)** For example, splicing events that lead to alterations in exon 1 can yield GPCRs with truncated N-termini that affect ligand binding, while events that lead to alterations in exon 4 can yield GPCRs with truncated C-termini that affect g-protein coupling and signaling. **B)** Splicing events can also lead to skipping of an exon that codes for an unit of the GPCR, such as a transmembrane, thus yielding a truncated GPCR lacking the encoded section, such as a 6 transmembrane (6TM) splice variant. Abbreviations: GPCR = G-Protein Coupled Receptor; TM = Transmembrane

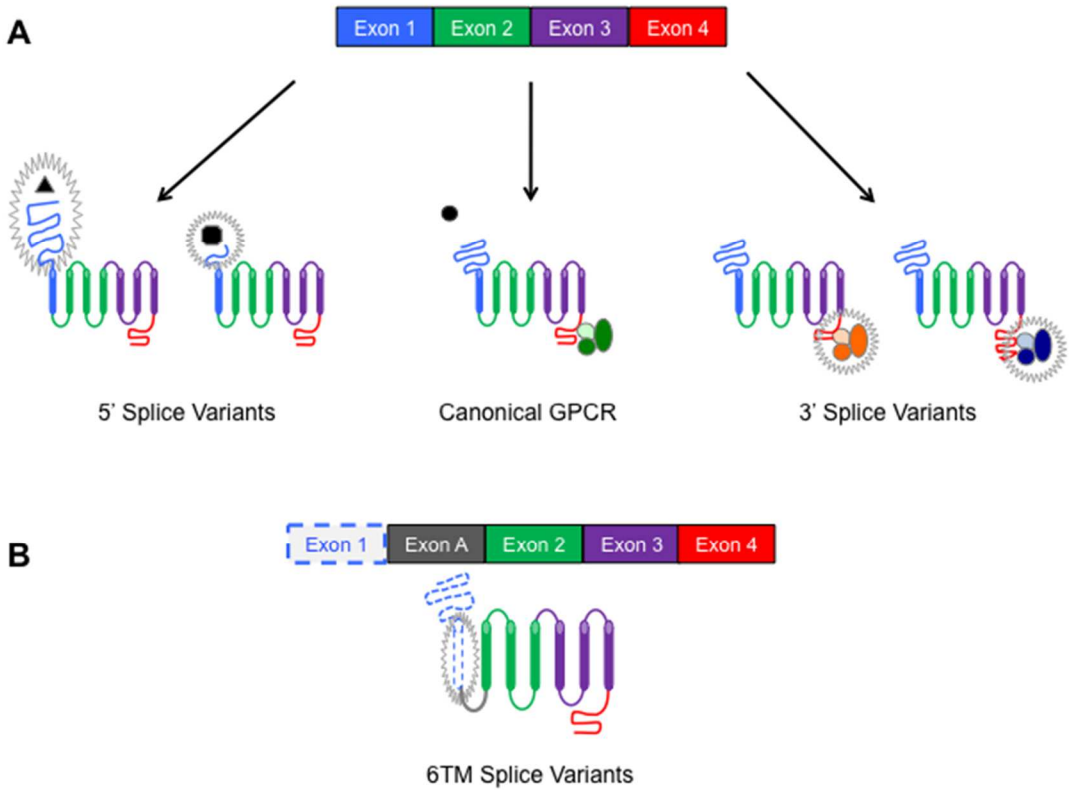
A
Exon 1
Exon 2
Exon 3
Exon 4
5' Splice Variants
Canonical GPCR
3' Splice Variants
B
Exon 1
Exon A
Exon 2
Exon 3
Exon 4
6TM Splice Variants

Accumulating evidence suggests that alternative splicing significantly adds to the functional diversity of the human genome and that variations in these processes produce pathological states(58). The presence of multiple GPCR splice variants allows for essential, precisely regulated differences in expression (e.g., tissue-specific expression)(59), as well as in agonist binding(60), agonist-induced internalization[21], and intracellular signaling dynamics(61,62). Some alternative splice variants even display functional characteristics opposite to the canonical form(63-65) (Table 1.3). Polymorphisms that alter the ratio of functionally distinct protein isoforms through alternative splicing may produce changes in the direction of pain-relevant GPCR pharmacodynamics (e.g. coupling to stimulatory vs. inhibitory G protein effector systems), yet remain understudied. A PubMed search of "alternative splicing pain" yields only 87 relevant original research articles. Most are focused on ion channels such as voltage-gated calcium channels(66) and transient receptor potential channels(67,68), with only 12 articles focusing on GPCRs. This is an important area of study as identification of GPCR splice variants differentially expressed in individuals with altered pain perception and/or analgesic responses will help elucidate novel targets for the development of individualized treatment strategies.

1.2.2 Alternative splicing creates functional GPCR variants

Examples of alternative splice variants of pain-relevant GPCRs that exhibit diversity in expression and signaling profiles include the aforementioned cannabinoid receptors, adrenergic receptors, serotonin receptors, and opioid receptors. Accumulating evidence from *in vitro*, pre-clinical, and clinical studies suggests that alternative splicing of these and other GPCR transcripts adds additional layers of complexity to GPCR signaling and pharmacodynamics responses.

Table 1.3. Signaling, Tissue Distribution, and Function of Known GPCR Splice Variants.

Receptor Variants	G-protein	Tissue Distribution	Functional Characteristics
Cannabinoid Receptors			
CB1	$G\alpha_i$(41)	brain, sc, DRG > pituitary > heart, lung, uterus, testis, spleen, tonsils(69)	
N-term variants			↓ agonist binding, ↓ $GTP\gamma S$ activity(70)
CB1a		similar distribution to CB1+ kidney(70,71)	↓ agonist binding, ↓ $GTP\gamma S$ activity(70)
CB1b		fetal brain > GI tract, uterus, muscle > adult brain(70)	
CB2	$G\alpha_i$(41)	immune cells/tissues > glia and macrophages in brain/sc(69,72-74)	
N-term variants			?
CB2A		testis > spleen, leukocytes > brain(75)	?
CB2B		spleen > leukocytes(75)	
Adrenergic Receptors			
α_{1A}	$G\alpha_q$(42)	liver, heart, brain > prostate, kidney, bladder(42)	
C-term variants	$G\alpha_i$(43)	liver, heart > prostrate, kidney(76,77)	pharmacology similar to α_{1A}(43,76,77,79)

α_{1A-2} α_{1A-3} α_{1A-4} α_{1A-5} 6TM variants (-TM7) α_{1A-6} α_{1A-7} α_{1A-8} α_{1A-9} α_{1A-10} α_{1A-11} α_{1A-12} α_{1A-13} α_{1A-14} α_{1A-15} α_{1A-16}	$G\alpha_i$(43) $G\alpha_i$(43)	liver > heart, prostrate (absent in kidney)(76,77) liver, heart > prostrate, (absent in kidney)(76,77) liver, heart, hippocampus, and prostate; expressed intracellularly(78)	 impair α_{1A} binding & cell surface expression(78)
α_{1B} 6TM variant (-	$G\alpha_q$(42)	liver, heart, brain (including cortex) (42)	

TM7) α_{1B-2}		expressed in hippocampus, but absent in cortex(80)	?
β_3 C-term variants β_{3a} (mouse) β_{3b} (mouse)	$G\alpha_s$, $G\alpha_i$(81,82) $G\alpha_s$(43,83) $G\alpha_s$, $G\alpha_i$(43,83)	fat, immune cells/tissues > GI tract, DRG(81,84) fat > ileum > brain(85) brain > fat, ileum(85)	 ? ?
Serotonin Receptors			
5-HT_{2A} 6TM variant (-TM4) 5-HT_{2A-tr}	$G\alpha_q$(44)	cortex, hippocampus, brainstem, olfactory > basal ganglia, limbic(44) hippocampus, caudate, corpus collosum, amygdala, substania nigra(86)	impaired 5-HT-induced Ca^{++} signaling(86)
5-HT_{2C} 6TM variant (-TM4) 5-HT_{2CT}	$G\alpha_q$(44)	choroid plexus, striatum, hippocampus, hypothalamus, olfactory, sc(44,87) choroid plexus, striatum, hippocampus, hypothalamus, olfactory, sc(87)	impaired 5-HT ligand binding(87)

C-term variant 5-HT$_{2AC\text{-}R\text{-}COOH\Delta}$		sc, cortex, cerebellum, medulla, caudate, amygdala, corpus collosum(88)	impaired 5-HT ligand binding(88)
5-HT$_4$	Gα_s(44)	intestine > brain > pit > uterus, testis > spleen > heart, kidney, lung, sc(96)	
C-term variants	Gα_s(89)		↑ constitutive AC activity, ↑ isomerization, ↓ agonist internalization(98,99)
5-HT$_{4a}$	Gα_s, Gα_i(89,90)	intestine, brain > pit > uterus, testis > heart > spleen, lung, sc(96)	
5-HT$_{4b}$	Gα_s(89)		↑ constitutive AC activity(89)
5-HT$_{4c}$	Gα_s(89)	intestine, brain > pit > uterus > heart, spleen, lung, sc(96)	↑ constitutive AC activity(89)
5-HT$_{4d}$	Gα_s(91)	intestine > pit > brain > uterus, testis, heart, spleen, sc(96)	20-fold ↑ in agonist-induced cAMP activity(100)
5-HT$_{4e}$	Gα_s(92)	ileum, colon, but absent in brain(95,97)	↑ constitutive AC activity(91)
5-HT$_{4f}$	Gα_s(93)	brain > testis > sc > intestine, pit, heart, prostate ileum, colon(97)	?
5-HT$_{4g}$	Gα_s(94)		?
5-HT$_{4i}$	Gα_s(95)	brain, ileum, colon(97)	↑ constitutive AC activity(101)
5-HT$_{4n}$		brain, heart, ileum, colon(97)	
		brain, ileum, colon, heart(97)	
2nd EL loop variant 5-HT$_{4h}$	Gα_s(92)	brain, heart, esophagus(97)	antagonist GR113808 acts as partial agonist(92)

		GI tract(92)	
5-HT$_6$ 6TM variant (-TM4) 5-HT$_{6\text{-tr}}$	Gα_s (44)	cortex, hippocampus, olfactory, striatum, amygdala, accumbens(44) cortex, hippocampus, cerebellum, thalamus, substantia nigra, caudate(102)	impaired binding to 5-HT and LSD(102)
5-HT$_7$ C-term variants 5-HT$_{7a}$ 5-HT$_{7b}$ 5-HT$_{7d}$	Gα_s(44) Gα_s(103) Gα_s(104) Gα_s(104)	brain, heart, GI tract, muscle, kidney, astrocytoma, glia(105,106) brain, heart, GI tract, spleen, lung, astrocytoma, glia(103,105,106) brain, heart, GI tract, spleen, lung, astrocytoma, glia(104)-(105,106) heart, GI tract, ovary, testis, spleen, lung, astrocytoma(105)	? ↑ constitutive AC activity(104) exhibit agonist-independent internalization(107)
Opioid Receptors			

MOR-1	$G\alpha_i$(45)	brain, spinal cord > adrenal gland > small intestine(109)	
C-term			
variants		brain(110)	OP binding → analgesia(113)
MOR-1A		brain(110)	OP binding → analgesia(113)
MOR-1B		brain(110); agonist-induced reduction(111)	OP binding → analgesia(113)
MOR-1C		brain(110)	OP induced itch(108)
MOR-1D	$G\alpha_i$(108)	brain(110)	OP binding → analgesia(113)
MOR-1E		brain(110)	OP binding → analgesia(113)
MOR-1F		brain(110)	?
MOR-1O		brain(110)	?
MOR-1P		brain(110)	?
MOR-1U		brain(110)	?
MOR-1V		brain(110)	?
MOR-1W		brain(110)	?
MOR-1X		brain(110)	OP binding → analgesia(114)
MOR-1Y			
N-term		brain(110)	Novel opioid binding(115)
variants		brain(110)	OP binding → analgesia(116)
MOR-1G		brain(110)	OP binding → analgesia(116)
MOR-1H		brain(110)	OP binding → analgesia(116)

MOR-1I		brain(110)	contributes to OIH
MOR-1J	$G\alpha_s$(65)	brain(110)	OP binding → analgesia(116)
MOR-1K		brain(110)	?
MOR-1L		brain(110)	?
MOR-1M			
MOR-1N			
		brain(110)	?
Single TM		brain(110)	Stabilization of MOR-1(117)
variants		brain(110)	Stabilization of MOR-1(117)
MOR-1Q		brain(110)	?
MOR-1R		brain(110)	?
MOR-1S		brain (human neuroblastoma cell line)(112)	?
MOR-1T		brain (human neuroblastoma cell line)(112)	?
MOR-1Z			
MOR-1SV1			
MOR-1SV2			

Abbreviations: 5-HT = serotonin; AC = adenylyl cyclase; N-term = amino terminus; Ca^{++} = calcium; C-term = carboxyl terminus; cAMP = cyclic adenosine monophosphate; EL = extracellular loop; GI = gastrointestinal; LSD = lysergic acid diethylamide; OP = opioid; sc = spinal cord; SP = Substance P; TM = transmembrane

Cannabinoid receptors

Both the CB_1 and CB_2 receptors undergo alternative splicing to yield variants differing at their N-terminal region. The CB_{1a} variant is truncated by 61 amino acids, with the first 28 amino acids completely different from the canonical CB_1(71). While its tissue distribution largely overlaps with that of CB_1, CB_{1a} exhibits decreased agonist binding and activity, which might be due to a lack of two glycosylation sites typically important for signal transduction(118). The CB_{1b} variant lacks the first 33 N-terminus amino acids and although it overlaps with CB_1 in a number of tissues, its abundant expression in fetal brain suggests it may play an important role in development(70). Similar to CB_{1a}, CB_{1b} exhibits decreased agonist binding and activity.

The CB_2 variants are generated through the use of alternate promoters located upstream of the major coding exon 3(75). The gene CB_{2A} is initiated from the more distal promoter and includes exons 1a and 1b spliced to exon 3, while CB_{2B} is initiated from the more proximal promoter and includes exon 2 spliced to exon 3. The CB_{2A} variant is predominantly expressed in testes and at lower levels in spleen and brain. In contrast, the CB_{2B} variant is predominantly expressed in spleen with very low expression in brain and no expression in testes. These tissue-specific distribution patterns may indicate specialized roles for the different splice variants with respect to pain modulation, immune response, and spermatogenesis.

Adrenergic receptors

Adrenergic receptors play a key role in pain processing as well as cognition and cardiovascular function. While α_2ARs, β_1ARs, and β_2ARs are highly relevant to the modulation of pain by endogenous and exogenous agonists, the genes encoding these receptors are intronless and not subject to alternative splicing. Among the remaining adrenergic receptors, the α_{1A}AR subtype has best most extensively studied with respect to alternative splicing.

The human $\alpha_{1A}AR$ gene locus is comprised of over 8 exons and codes for 15 known splice

variants(119). The canonical receptor is generated through splicing exon 1 (coding for the N-terminus and transmembranes [TM] 1 to 6) together with exon 2 (coding for TM7 and the C-terminus). Four C-terminus splice variants ($\alpha_{1A\text{-}2}$, $\alpha_{1A\text{-}3}$, $\alpha_{1A\text{-}4}$, $\alpha_{1A\text{-}5}$) have been identified that are generated through the use of additional acceptor sites at varying locations within, and distal to, exon 2. The $\alpha_{1A\text{-}2}$, $\alpha_{1A\text{-}3}$, and $\alpha_{1A\text{-}4}$ variants exhibit ligand binding properties and tissue distribution profiles similar to α_{1A}AR, although $\alpha_{1A\text{-}3}$ and $\alpha_{1A\text{-}4}$ are absent in kidney(76-79). In contrast to α_{1A}AR that couples to $G\alpha_q$, these variants couple to $G\alpha_i$ so as to inhibit AC activity(43). This diversity in α_{1A}AR signaling may contribute to differential responses to α_1AR antagonists used in the treatment of pain.

In addition, eleven 6TM variants ($\alpha_{1A\text{-}6}$, $\alpha_{1A\text{-}7}$, $\alpha_{1A\text{-}8\ldots}$ $\alpha_{1A\text{-}16}$) have been identified that are generated through exon skipping. These variants lack TM7 and their C-terminal tails are located extracellularly(78). The truncated 6TM variants are expressed in similar tissues as α_{1A}AR, but are localized exclusively within the cell and unable to bind α_1AR agonists or directly mediate signal transduction. The 6TM variants do, however, impair α_{1A}AR ligand binding and trafficking to the cell surface. Thus, α_{1A}AR 6TM variants likely play a significant physiological role by modifying the function and expression of their parent 7TM receptors.

One α_{1B}AR splice variant has also been identified in human brain(80). The α_{1B}AR protein is generated through splicing of exons 1 and 2. In contrast to the canonical receptor, the *$\alpha_{1B\text{-}2}$AR* includes an immediately adjacent sequence following exon 1 in its coding sequence and excludes exon 2 that codes for TM7. Tseng-Crank and colleagues also identified low levels of a truncated *α_{1D}AR* transcript, however the result was inconclusive and naturally occurring α_{1D}AR variants were not observed(80). More work is required to determine the potential functional role of α_{1B}AR and α_{1D}AR variants.

The β_3AR is primarily known for its ability to regulate energy metabolism and thermogenesis(80), though evidence for its ability to promote functional and neuropathic pain is

emerging (83,85,120). The gene encoding β_3AR undergoes alternative splicing within the coding region to yield two C-terminal splice variants differing with respect to tissue expression, g-protein signaling profiles, and regulatory properties(79,86,121). The β_{3A}AR and β_{3B}AR splice variants contain completely unique terminal chains that are 13 and 17 amino acids long, respectively. The β_{3A}AR is primarily enriched in fat tissue and couples exclusively to $G\alpha_s$, while the β_{3B}AR is primarily enriched in brain and couples to both $G\alpha_s$ and $G\alpha_i$. In addition, the β_{3A}AR exhibits increased agonist-induced extracellular acidification, a measure of cAMP-independent cellular activity. Their unique tissue distribution and signaling profiles, together with the known functional role of β_3ARs, could indicate that β_{3A}ARs play a greater role in lipolysis/thermogenesis and that β_{3B}AR in brain mediate pain. While these studies were conducted in mouse, it is important to note that the human β_3AR contains a significant number of genetic variants that are predicted to regulate alternative splicing(87,88).

Serotonin receptors

Serotonin receptors play a key role in pain processing as well as mood and GI function(44). Of the 5-HT_1 (A, B, D-F), 5-HT_2 (A-C), 5-HT_4, 5-HT_5, 5-HT_6, and 5-HT_7 GPCR family members, the 5-HT_{2A}, 5-HT_{2C}, 5-HT_4, 5-HT_6, and 5-HT_7 receptors are known to undergo alternative splicing.

The human 5-HT_2 receptor subtypes (5-HT_{2A}, 5-HT_{2B}, and 5-HT_{2C}) couple to $G_{\alpha q}$ proteins to promote the transient release of intracellular calcium. One truncated splice variant of *5-HT_{2A}* (*5-$HT_{2A\text{-}tr}$*) has been identified that utilizes alternate splice donor and acceptor sites to yield a 3TM receptor with 57 unique amino acids in the C-terminal region(86). The 5-$HT_{2A\text{-}tr}$ is co-expressed with 5-HT_{2A} in most brain tissues, however is unable to couple to the calcium pathway. Two truncated splice variants of 5-HT_{2C} (5-HT_{2CT} and 5-$HT_{2C\text{-}R\text{-}COOH\Delta}$) have also been identified. Similar to 5-$HT_{2A\text{-}tr}$, the *5-HT_{2CT}* variant utilizes alternate splice donor and acceptor sites to yield a 3TM receptor with 19 unique amino acids in the C-terminal region(87). The *5-$HT_{2C\text{-}R\text{-}COOH\Delta}$* variant retains an extra 90 nucleotides from intron 5 in the TM4 splice site, resulting in a 3TM receptor with a short C-terminus(88).

Compared to the canonical 5-HT_{2C} receptor, the truncated variants exhibit similar expression patterns but have impaired 5-HT ligand binding and g-protein coupling(87,88). While the relative importance of these truncated 5-HT_2 splice variants in humans remains unknown, they are conserved in rat and mouse(88) where their expression levels increase following nerve injury(122).

The 5-HT_4 receptor couples preferentially to $G_{\alpha s}$ and, while widely expressed, the highest levels are found in intestine(96). Agonists targeting 5-HT_4 are beneficial in alleviating abdominal pain associated with irritable bowel syndrome. Of all the 5-HT receptors, 5-HT_4 possesses the greatest diversity in alternative splicing. At least ten splice variants have been identified that vary with respect to their tissue distribution and function. Nine C-terminus variants (5-HT_{4a}, 5-HT_{4b}, 5-HT_{4c}, 5-HT_{4d}, 5-HT_{4e}, 5-HT_{4f}, 5-HT_{4g}, 5-HT_{4i}, 5-HT_{4n}) have been identified that are identical up to amino acid Leu358, after which they vary in sequence and length(97). Additionally, one variant (*5-HT_{4h}*) has been identified that includes exon h coding for 14 additional amino acids in the second extracellular loop(92). The 5-HT_{4a}, 5-HT_{4b}, 5-HT_{4c}, and 5-HT_{4e} variants are expressed in most tissues, with distribution patterns similar to the canonical form(96,97). In contrast, the 5-HT_{4f} variant is found in the brain and GI tract, but absent in the heart and other tissues[22]. Meanwhile, the 5-HT_{4d} and 5-HT_{4h} variants are expressed exclusively in the GI tract(92,94,97). While all of the 5-HT_4 splice variants display typical ligand binding properties, some show notable functional differences. Both of the GI-specific 5-HT_{4d} and 5-HT_{4h} variants have a tendency to recognize 5-HT antagonists as partial agonists(92,100). Furthermore, the 5-HT_{4d} variant exhibits a remarkable 20-fold increase in cAMP formation following application of the 5-HT_4 agonist renzapride(100). The 5-HT_{4b} variant is unique in its able to couple to $G_{\alpha i}$ as well as $G_{\alpha s}$ proteins, suggesting its diverse signaling capabilities in the GI tract, brain, and other tissues(90). In the absence of ligand binding, the majority of C-terminus variants exhibits heightened constitutive AC activity(89,91,95,98-100). The ability of GPCRs to increase basal AC activity has been previously reported and can result in physiological functions of the receptor that are largely independent of endogenous ligands or exogenous drugs(123).

Collectively, these studies illustrate the high degree of tissue and signaling specificity for a number of 5-HT_4 splice variants that may be represent attractive targets for the development of new more selective drugs for the treatment of irritable bowel syndrome among other conditions.

The 5-HT_6 receptor is unique in that it is expressed almost exclusively in the central nervous system(44). A 3TM splice variant of *5-HT$_6$* (*5-HT$_{6\text{-}tr}$*) has been identified in brain that is generated through different splice donor and acceptor sites(102). The corresponding receptor includes the TM1-3 and 10 unique amino acids in its C-terminus. In contrast to 5-HT_6, the expression of 5-$HT_{6\text{-}tr}$ is limited to substantia nigra and caudate. The 5-$HT_{6\text{-}tr}$ receptor is able to translocate to the membrane, yet unable to bind serotonin. This splice variant may have a yet-to-be-determined function or be indicative of abnormalities due to pathologic state.

The 5-HT_7 receptor is expressed on primary afferent nociceptors, as well as in pain-relevant brain regions where it couples to $G_{\alpha s}$ to mediate the transmission and modulation of pain. Three splice variants of 5-HT_7 (5-HT_{7a}, 5-HT_{7b}, 5-HT_{7d}) have been identified that are all generated through alternative splicing of the second intron located near the C-terminal coding region. The 5-HT_{7a} and 5-HT_{7b} variants have tissue expression profiles and functional characteristics similar to the canonical receptor, though 5-HT_{7b} has been shown to exhibit significantly higher constitutive AC activity when expressed in stable cell lines{Krobert:2002du}. The 5-HT_{7d} variant is predominantly expressed in smooth muscle tissues such as the heart and GI tract(104) and displays unique functional characteristics. Compared to the canonical 5-HT_7 receptor and the 5-HT_{7a} and 5-HT_{7b} variants, the 5-HT_{7d} variant displays agonist-independent internalization (even in the presence of antagonist) and associated reductions in agonist-induced AC activity(107). It has been suggested that differences in the functional characteristics of 5-HT_7 variants is due to specific features of their carboxyl tails, leading to differential interactions with protein partners that mediate their activity, trafficking, and/or internalization(107,124).

Opioid receptors

The pharmacologic manipulation of the mu opioid receptor is an essential component of clinical pain treatment. Although the signaling characteristics of MOR-1 are well established, we are just beginning to understand the complex nature of genetic variants that contribute to alternative splicing. At least 20 MOR-1 splice variants have been identified in mouse and human genomes(61), suggesting an array of potentially functional consequences that may occur with opioid administration.

Pre-clinical studies within the past 15 years have begun to reveal the functional properties of specific MOR-1 splice variants. Pasternak and coworkers provide evidence that the expression of MOR-1 splice variants represent compensatory responses to chronic opioid administration that stabilize or diminish the development of tolerance(125). Additional studies investigating the functional characteristics of MOR-1 splice variants provide evidence that a set of these receptors promote opioid analgesia by providing exclusive binding sites for different opioids. Transgenic mice lacking exon 11, an exon that provides an alternative promoter region for the MOR transcript, demonstrated substantial reductions in the analgesic efficacies of heroin, fentanyl, and the morphine metabolite morphine-6β-glucuronide(60), suggesting that exon-11 containing variants play a critical role in opioid analgesia. Exon 11-containing splice variants also mediate the analgesic effects of iodobenzoylnaltrexamide (IBNtxA), a novel synthetic opioid that produces ten times the analgesic efficacy of morphine without producing respiratory distress, dependence, tolerance, or GI distress in rodents(111,115,126). MOR-1 splice variants also promote analgesia by enhancing canonical receptor function. Single-transmembrane splice variants MOR-1R and MOR-1S structurally enhance MOR-1 function by stabilizing the canonical 7TM receptor at the cellular membrane(117).

Other studies have shown that the presentation of some unwanted side effects are due to the activation of MOR-1 splice variants. For example, Liu and colleagues have demonstrated that because of its distinct C-terminus, the splice variant MOR-1D dimerizes with the gastrin-releasing peptide receptor in the mouse spinal cord to produce opioid-induced itch(108). Another splice variant known

as MOR-1K, a truncated receptor lacking the N-terminus and first transmembrane, has been implicated in the paradoxical increase in pain sensitivity known as opioid-induced hyperalgesia (OIH). In contrast to MOR-1 which typically couples to $G\alpha_i$, MOR-1K couples to $G\alpha_s$ to activate adenylyl cyclase (AC) and increase intracellular calcium, thus engaging pro-nociceptive signaling events that likely drive OIH(65). A subsequent preclinical study in mice revealed that genetic knockdown of MOR-1K hindered the development of OIH and unmasked opioid analgesia(127). The relationship between MOR-1K and OIH is further discussed throughout the remainder of the manuscript.

Conclusion

G-protein coupled receptors play a major role in modulating the activity of a chorus of cells involved in the transmission, modulation and perception of pain. For this reason, GPCRs are the primary target of many pharmacologic interventions used in the management of acute and chronic pain. Nonetheless, the use of these medications is limited due to variability in analgesic efficacy and side effect profiles. These limitations are partly attributed to genetic differences that influence alternative splicing of pain-relevant GPCRs. The functional importance and implications of the diversity of GPCRs in contributing to the pathophysiology of clinical pain is just beginning to emerge. More research, especially in the clinical arena, is necessary to further investigate the functions of specific GPCR splice variants, as well as the dynamic interactions between multiple variants of the same canonical receptor, within the context of pain. This line of inquiry will evolve our understanding of pain mechanisms and inform the design of new and clinically useful drugs that target specific alternative splice variants altered in a subset of patients.

In the next chapter, I provide experimental evidence that points to the mu opioid splice variant MOR-1K as a target for the development of pharmacologic therapies that can be used to manage pain without producing paradoxical opioid induced hyperalgesia

CHAPTER 2: MOR-1K Contributes to OIH in Genetically Susceptible Mice [2]

2.1. Introduction

Accumulating evidence indicates that MOR-1K, a functional splice variant of the canonical mu opioid receptor (MOR-1), may contribute to the emergence of OIH. MOR-1K is a truncated six transmembrane G-protein coupled receptor (GPCR) lacking a N-terminus transmembrane due to the absence of exon 1 within its mRNA transcript (61). Replacing exon 1 are exon 11, which provides an alternative translation start site in several MOR-1 splice variants, and exon 13, which is unique to the *MOR-1K* transcript. The MOR-1 transcript, which encompasses exons that encode for MOR-1K, is highly conserved across species, with a 91% nucleotide sequence homology between human and mouse. Results from a human genetic association study demonstrated that a single nucleotide polymorphism within exon 13 of the human *MOR-1K* transcript is associated with increased pain sensitivity and blunted morphine efficacy (128). Subsequent *in vitro* studies demonstrated that MOR-1K exhibits signaling properties distinct from its parent receptor MOR-1. MOR-1 utilizes $G_{i/o}$ protein to inhibit cyclic adenosine monophosphate (cAMP) levels and intracellular calcium levels to produce cellular inhibition of pronociceptive cells. In contrast, MOR-1K couples to G_s protein, leading to increased cAMP production and intracellular calcium levels, thus promoting cellular excitation (65). Previous studies have shown that G_s-dependent increases in intracellular calcium *via* cAMP production and protein kinase A activation play a critical role in central sensitization (129) and the development of inflammatory, neuropathic, and functional pain (130). The utilization of G_s signaling

[2] This chapter previously appeared as an article in PLoS ONE. The original citation is as follows: Oladosu F.A., Conrad M.S., O'Buckley S.C., Rashid N.U., Slade G.D., and Nackley A.G., "Mu Opioid Splice Variant MOR-1K Contributes to the Development of Opioid-Induced Hyperalgesia" *PLoS ONE* 10, no 8. (August 2015): e0135711

by MOR-1K suggests that the receptor may also contribute to central sensitization associated with OIH.

Given the receptor's genetic association with increased pain sensitivity and its excitatory signaling profile, we hypothesize MOR-1K may contribute to OIH in genetically susceptible individuals. Here, we evaluate MOR-1K in the development of OIH using three genetically diverse mouse strains alongside small interfering RNA (siRNA) knockdown of *MOR-1K*. Our results demonstrate that OIH is associated with increased *MOR-1K* gene expression levels in a strain-specific manner. Disrupting the increase in *MOR-1K* gene expression levels *via* chronic intrathecal (i.t.) siRNA administration not only hinders the development of OIH, but also increases morphine analgesic efficacy. Collectively, these findings demonstrate that MOR-1K is likely a key contributor to OIH.

2.2. Materials and Methods

2.2.1. Ethical Statement

All procedures within this study were approved by the University of North Carolina Animal Care and Use Committee (permit number: 12-319) and adhered to the guidelines of the Committee for Research and Ethical Issues of the International Association of the Study of Pain (http://www.iasp-pain.org/Education/Content.aspx?ItemNumber=1217). All surgeries were performed under isofluorane anesthesia, and all efforts were made to minimize suffering.

2.2.2. Animals

Male and female C57BL/6J (http://jaxmice.jax.org/strain/000664.html) and CXB7/ByJ (http://jaxmice.jax.org/strain/000357.html) mice were obtained from Jackson Labs (Bar Harbor, ME) while 129S6 (http://www.taconic.com/129SVE) mice were obtained from Taconic (Germantown, NY). All mice were 8 -12 weeks old, weighed 20-30 g, were maintained under 12-hour light/dark cycle, and were fed *ad libitum.*

2.2.3. Drugs and Chemicals

Morphine sulfate (Sigma, MO) was dissolved in 0.9% sterile saline (Hospira, IL). Doses of 10 mg/kg, 20 mg/kg, or 40 mg/kg were administered *via* subcutaneous (s.c.) injection in a volume determined by animal weight (1µl/g). Fluorescein-tagged exon 13-antisense siRNA [5'-UCA GUC UUU AUC AGC UCA CCG CCA-3'] or fluorescein-tagged exon 13-sense siRNA (Midland Certified Reagent Co., OH) [5'-AGU CAG AAA UAG UCG AGU GGC GGU-3'] in artificial cerebrospinal fluid was administered at a rate of 0.5µl/hr; 0.291µg/hr/day for a duration of 7 days *via* Alzet osmotic mini-pump (Durect, CA) connected to an i.t. catheter (Durect, CA). Previous studies have successfully administered siRNA in this fashion as well (131,132). Sense siRNA was chosen as a negative control as it is related to the target mRNA sequence of interest but does not affect target mRNA expression (133).

2.2.4. Experimental Design

Experiment 1: The effects of chronic morphine administration on pain behavior and gene expression.

Prior to chronic morphine administration, C57BL/6J, CXB7/ByJ, and 129S6 mice (N=96; 8 males and 8 females per experimental condition) were assessed for baseline responses to mechanical and thermal heat stimuli. Following baseline assessments, mice received morphine similar to the murine OIH protocol described by Liang et al (37). Briefly, mice received vehicle (sterile saline) or escalating doses of morphine (10 mg/kg, 20 mg/kg, 20 mg/kg, and 40 mg/kg) twice daily (8am and 6pm) *via* s.c. injection on days 1, 2, 3, and 4, respectively. Behavioral responses were evaluated prior to and immediately following the 8am injection on days 1-4 and at 8am on days 5-7. Gene expression levels were measured in tissues collected from separate groups of C57BL/6J, 129S6, and CXB7/ByJ mice (N=84; 3-4 males and 3-4 females per experimental condition) sacrificed on day 0, on days 1 or 4 following the 8am injection, or on day 5 at 8am. The experimental design is illustrated in Figure 2A.

Experiment 2: The effects of MOR-1K exon 13 siRNA knockdown on OIH and MOR-1K gene expression.

Prior to chronic morphine administration, CXB7/ByJ mice (N=48; 8 males and 8 females per experimental condition) were assessed for baseline responses to mechanical stimuli. Following baseline assessments, mice underwent surgery for chronic i.t. administration of antisense exon 13 siRNA or sense exon 13 siRNA. Mice were anesthetized with 5% isofluorane and maintained at 2-3% isofluorane during i.t. catheter implantation, modified from Yaksh and Rudy protocol (134). A separate group of mice also underwent surgery for a sham procedure. The sham procedure, involving skin incision and muscle dissection without breakage of the arachnoid membrane to cause leakage of cerebral spinal fluid, was deemed appropriate to control for any postoperative pain. One day following surgery, mice from antisense, sense, and sham conditions began to receive either vehicle (sterile saline) or escalating doses of morphine as described above. *MOR-1K* gene expression levels were measured in tissues collected from separate groups of CXB7/ByJ mice (N=84; 3-4 males and 3-4 females per experimental condition) sacrificed on day 0, on days 1 or 4 following the 8am injection, or on day 5 at 8am. The experimental design is illustrated in Figure 3A.

2.2.5. Behavior

Assessment of Paw Withdrawal Threshold, Mechanical Allodynia, and Mechanical Hyperalgesia

Mice were handled and habituated to the testing environment for 4 days prior to baseline assessments. On test days, mice were placed in plexiglass cages positioned over an elevated wire mesh platform and habituated to the environment for 20 minutes. Paw withdrawal threshold in response to a series of 9 von Frey filaments (with bending forces of 0.03, 0.07, 0.17, 0.40, 0.70, 1.19, 1.50, 2.05, 3.63g; Stoeling, IL) was assessed using the "up-down" method (135), starting with a filament with bending force of 0.70 g. In the absence of a paw withdrawal response, an incrementally stronger filament was presented and in the event of a paw withdrawal, an incrementally weaker

filament was presented. After the initial response threshold was crossed, this procedure was repeated in order to obtain a total of six responses in the immediate vicinity of the threshold. The pattern of withdrawals and absence of withdrawals were noted together with the terminal filament used in the series of six responses. The 50% of the paw withdrawal threshold is calculated as $(10^{[X_f+k\delta]})/10{,}000$, where X_f = value (in log units) of the final von Frey hair used; k = tabular value of pattern of positive (X) and negative (O) responses, and δ = mean difference (in log units) between stimuli. Mechanical allodynia was assessed by presenting a filament with bending force of 0.40 g to the hind paw 10 times for a duration of 1 s with an inter-stimulus interval of 1 s. A significant increase in the percentage frequency of paw withdrawal ([# of paw withdrawals/10] x 100) was defined as mechanical allodynia. Mechanical hyperalgesia was assessed in the same manner, using a filament with a bending force of 1.50 g.

Assessment of Thermal Heat Hyperalgesia

Thermal heat hyperalgesia was evaluated using the hot plate method (136). Mice were placed on a hot plate (Columbus Instruments, OH) maintained at a temperature of 51.5°C for one minute. Each session was videotaped and the total number of aversive responses (paw licks, paw flicks, and jumps) was measured.

2.2.6. Assessment of Gene Expression Levels

Discrete brain and spinal cord samples were collected on days 0, on day 1 and 4 following the 8am morphine administration, and on day 5, 24 hours following morphine cessation. Total RNA from discrete brain regions (medulla, pons, periaqueductal grey, thalamus, hypothalamus, striatum, nucleus accumbens, and frontal lobe), and spinal cord was purified using 1mL TRIzol (Life Technologies, NY) for each tissue sample. Samples were immediately homogenized using a Pro200 homogenizer (Pro Scientific, CT) or Precellys 24 Homogenizer (Bertin Technologies, France) and all subsequent RNA purification steps were performed according to the TRIzol manufacturer recommendations. Purified RNA samples were treated with TURBO DNA-free (Life Technologies, NY) per

manufacturer protocol and concentrations were determined using a Nanodrop-1000 (Thermo Scientific, DE) and reverse transcribed using Transcriptor First Strand cDNA Synthesis kit (Roche, Switzerland) where necessary. Fast Start Universal SYBR Green Master with Rox (Roche, Switzerland) or Power SYBR Green RNA-to-CT 1-Step (Life Technologies, NY) were respectively used per manufacturer protocols to amplify cDNA and RNA, per manufacturer protocols. A 7900HT Fast Real-Time PCR system (Life Technologies, NY) and a StepOnePlus Real-Time PCR system (Life Technologies, NY) were respectively used for measuring cDNA or RNA transcripts amplification. The following primers were used for the detection of the following exon-11 containing MOR-1 splice variants: MOR-1K forward (TCCCCTCTTGAGTGTGACTAATGTC) and reverse (GCCAGAGCAAGGTTGAAAATG); MOR-1L forward (CAGAGCAAGGTTGAAAATGTAGATG) and reverse (AAATCAAAATAGAAAATGGGCTAAGG); MOR-1T forward (GAGCCACATGGAATTGCCTCTGTA) and reverse (GCATCTGCCAGAGCAAGGTTGAAA); forward (GGGCCGATGATGGAAGCTTTCTCTAA) and reverse (GCATCTGCCAGAGCAAGGTTGAAA) primers for splice variants that contain exons 11 and 2. Expression of the target genes was normalized to housekeeping genes RPL7 [forward (TCAATGGAGTAAGCCCAAAG) and reverse (CAAGAGACCGAGCAATCAA)] or GAPDH [forward (TGAAGGTCGGAGTCAACGGATTTGGT) and reverse (CATGTGGGCCATGAGGTCCACCAC)] using the $2^{(-\Delta\Delta CT)}$ method. All primers were purchased from Integrated DNA Technologies (CA).

2.2.7. Statistical Analysis

Baseline responses for paw withdrawal threshold, mechanical allodynia, and mechanical hyperalgesia for each strain were analyzed using one-way ANOVA followed by Bonferroni correction. Subsequent behavioral responses following morphine administration were then analyzed using two-way repeated measures ANOVA with Bonferroni correction for multiple comparisons.

Gene expression was analyzed using a linear mixed model, where the log (10) gene expression of each tissue-replicate assay was the dependent variable and strain was the random effect. For all tests, the criterion for statistical significance level was $p<0.05$. Statistical analyses were performed using Prism (GraphPad Software, CA)

2.3. Results

2.3.1. Strains demonstrate divergent baseline pain profiles.

First, we sought to establish baseline pain responses to mechanical stimuli in C57BL/6J, 129S6, and CXB7/ByJ mice. The C57BL/6J strain was chosen as it is the most studied classic inbred strain, the 129S6 strain was chosen because of its reported resistance to opioid tolerance (137), and the CXB7/ByJ strain was chosen because of its reported decrease in *MOR-1* gene expression (138). For all three strains, male and female mice demonstrated similar behavioral differences to mechanical and thermal heat stimuli (Figure 2.1); hence all behavioral data was pooled together for analysis.

Figure 2.1. Sex-dependent responses to mechanical and thermal heat stimuli across the three strains. Overall, males and females displayed similar behavioral responses to mechanical and thermal heat stimuli within strains. Female C57BL/6J mice demonstrated (A) increased paw withdrawal threshold ($F_{(9,140)} = 12.20$, $p<0.0001$) and (B) increased responses following repeated exposure to an innocuous mechanical stimulus ($F_{(9,140)} = 14.50$, $p<0.0001$). Panels A-D: N=7-8/group. Males are represented in black bars while females are represented by white bars. Data expressed as mean ± SEM.****$p<0.0001$, ***$p<0.001$, *$p<0.05$ different from males.

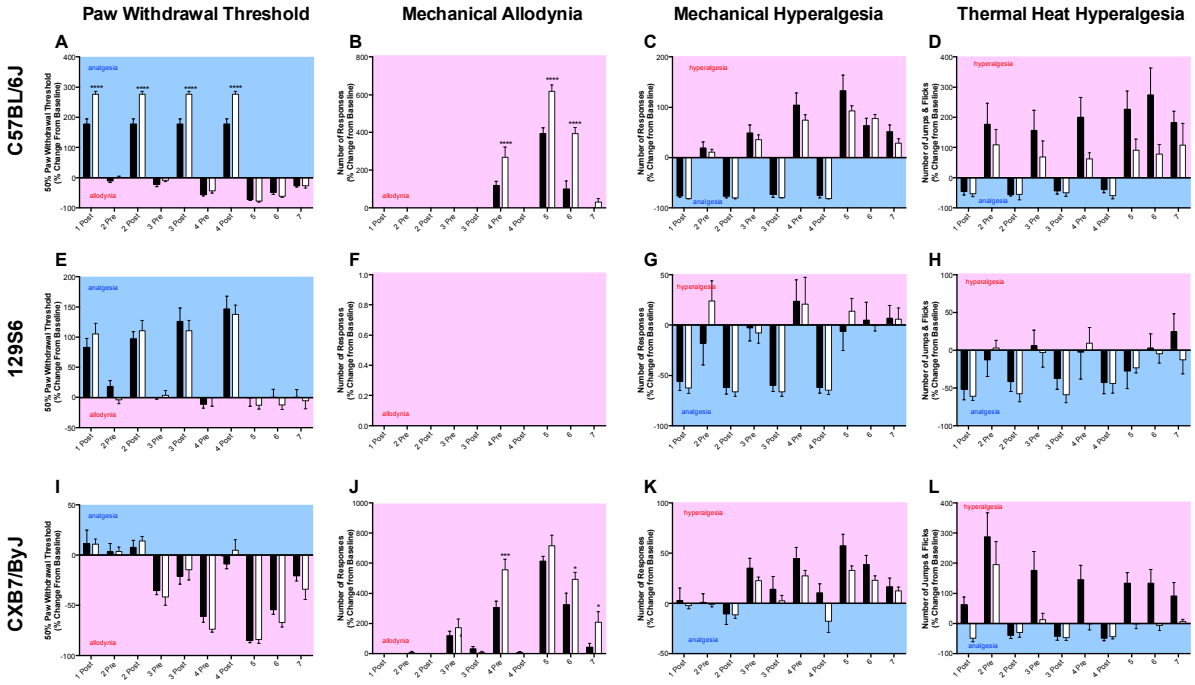
Paw Withdrawal Threshold
Mechanical Allodynia
Mechanical Hyperalgesia
Thermal Heat Hyperalgesia
C57BL/6J
129S6
CXB7/ByJ
A
B
C
D
E
F
G
H
I
J
K
L
analgesia
allodynia
hyperalgesia
50% Paw Withdrawal Threshold (% Change From Baseline)
Number of Responses (% Change from Baseline)
Number of Jumps & Flicks (% Change from Baseline)
1 Post
2 Pre
2 Post
3 Pre
3 Post
4 Pre
4 Post
5
6
7

Our results showed that the strains exhibited baseline differences in mechanical (Figure 2.2A, $F_{(2,43)}$=20.56, p<0.0001; Figure 2.2B, $F_{(2,43)}$=43.77, p<0.0001), and thermal heat pain sensitivity (Figure 2.2C; $F_{(2,43}$=10.64, p=0.0002). Compared to the classic C57BL/6J inbred strain, 129S6 mice were less pain sensitive, exhibiting higher paw withdrawal thresholds and fewer responses to a noxious mechanical stimulus or to thermal heat. In contrast, CXB7/ByJ mice were more pain sensitive, exhibiting lower paw withdrawal thresholds and increased responses to innocuous mechanical or thermal heat stimuli.

Figure 2.2. Strains exhibit divergent behavioral responses to mechanical stimuli at baseline Compared to C57BL/6J mice, 129S6, and CXB7/ByJ mice exhibit differences in (A) paw withdrawal threshold, (B) the number of responses to repeated presentation of a noxious mechanical stimulus sensitivity, and (C) the number of responses to continuous thermal heat. *N*=15-16/group. Data expressed as mean ± SEM. ***$p<0.001$, **$p<0.01$, *$p<0.05$ different from C57BL/6J. $^{###}p<0.001$ different from 129S6.

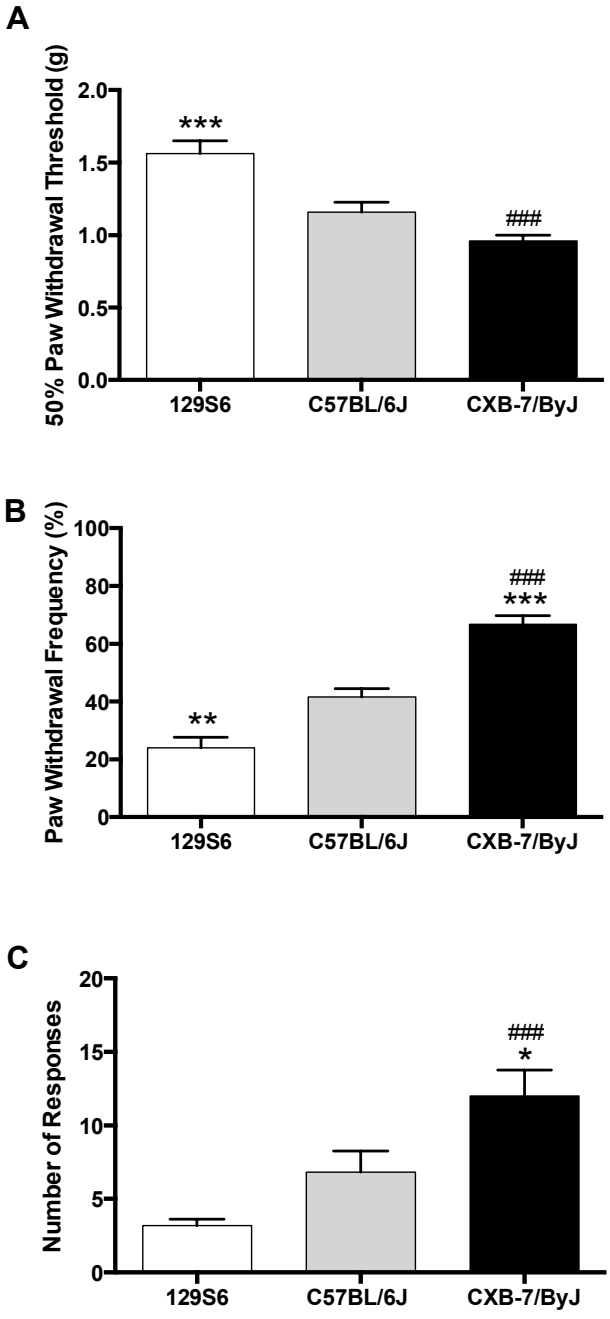
A
50% Paw Withdrawal Threshold (g)
2.0
1.5
1.0
0.5
0.0
***
###
129S6
C57BL/6J
CXB-7/ByJ
B
Paw Withdrawal Frequency (%)
100
80
60
40
20
0
**
###
***
129S6
C57BL/6J
CXB-7/ByJ
C
Number of Responses
20
15
10
5
0
###
*
129S6
C57BL/6J
CXB-7/ByJ

2.3.2. Strains demonstrate divergent pain profiles in a chronic morphine administration paradigm.

Next, we sought to examine the strains' pain responses following morphine administration using a modified murine paradigm for OIH (37). We assessed behavioral responses to mechanical and thermal heat stimuli on days 1-4 during chronic morphine administration and after morphine cessation on days 5-7 (Figure 2.3-2.4). When examining percent change from baseline responses, C57BL/6J, 129S6, and CXB7/ByJ mice exhibited differences in paw withdrawal thresholds over time (Fig. 2.4B; $F_{(18,430)}$=45.38, p<0.0001). C57BL/6J mice showed robust analgesia following morphine administration on days 1-4, then developed allodynia on day 4 prior to morphine administration and on days 5 and 6 following morphine cessation. When compared to C57BL/6J mice, 129S6 mice also showed analgesia following morphine administration on days 1-4, albeit to a lesser degree than C57BL/6J mice, however failed to develop allodynia at later time points (p<0.001). In contrast, CXB7/ByJ mice failed to show analgesia following morphine administration on days 1-4, but did develop allodynia prior to morphine administration on days 3 and 4 and following morphine cessation on days 5 and 6 (p<0.001). Of note, CXB7/ByJ mice also exhibited allodynia following morphine administration on day 3 (p<0.001).

Figure 2.3. Raw data illustrating behavioral responses of 129S6, C57BL/6J, and CXB7/ByJ mice to mechanical and thermal heat stimuli during chronic morphine administration. All three strains exhibit distinct behavioral differences in **(A)** paw withdrawal threshold ($F_{(22,516)} = 71.94$, $p<0.0001$**,** and when assessing responses to the repeated exposure of **(B)** an innocuous mechanical stimulus ($F_{(22,516)} = 35.37, p<0.0001$)**, (C)** a noxious mechanical stimulus ($F_{(22,516)} = 28.54, p<0.0001$), and **(D)** a thermal heat stimulus; $F_{(22,516)} = 4.214$, $p<0.0001$). Panels A-D: *N*=15-16/group. Data expressed as mean ± SEM. * = different from baseline.

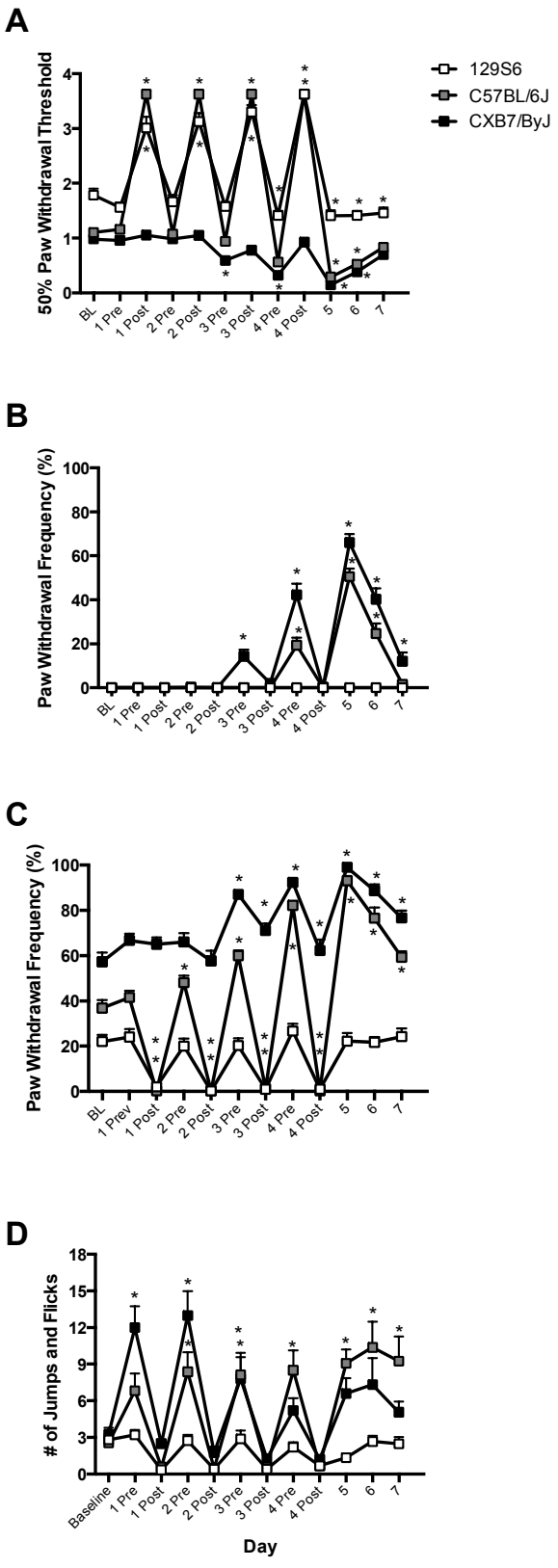
A
50% Paw Withdrawal Threshold
129S6
C57BL/6J
CXB7/ByJ
BL
1 Pre
1 Post
2 Pre
2 Post
3 Pre
3 Post
4 Pre
4 Post
5
6
7
B
Paw Withdrawal Frequency (%)
C
Paw Withdrawal Frequency (%)
1 Prev
D
# of Jumps and Flicks
Baseline
Day

Figure 2.4. Strains exhibit divergent morphine-dependent analgesic and allodynic/hyperalgesic profiles. **(A)** A timeline of chronic morphine administration and the assessments of pain behavior and gene expression are shown. **(B-E)** Compared to C57BL/6J, 129S6 mice exhibit increased paw withdrawal thresholds and fail to develop allodynia or hyperalgesia. In contrast, CXB7/ByJ exhibit decreased paw withdrawal thresholds and increased allodynia and hyperalgesia. For behavioral graphs, blue background indicates a decrease in pain sensitivity (analgesia), and red background indicates an increase in pain sensitivity (allodynia/hyperalgesia). Panels B-D: N=15-16/group. Data expressed as mean ± SEM. ***p<0.001, **p<0.01, *p<0.05 different from C57BL/6J. $^{###}p$<0.001, $^{##}p$<0.01, $^{#}p$<0.05 different from 129S6. Panel E: N=7/group. Data expressed as means ± SEM. *p<0.05 different from baseline.

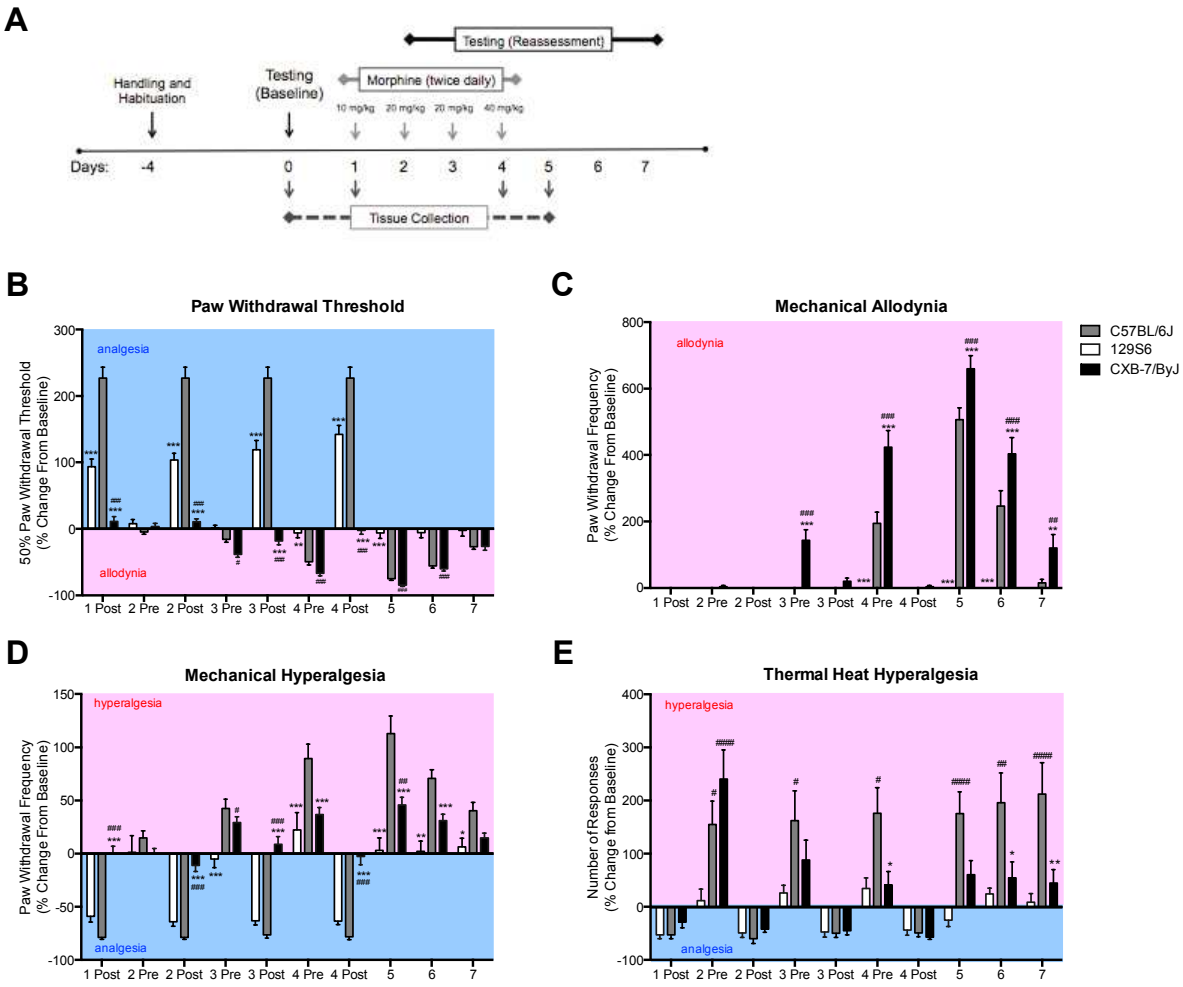
A
Testing (Reassessment)
Handling and Habituation
Testing (Baseline)
Morphine (twice daily)
10 mg/kg
20 mg/kg
20 mg/kg
40 mg/kg
Days: -4 0 1 2 3 4 5 6 7
Tissue Collection
B
Paw Withdrawal Threshold
50% Paw Withdrawal Threshold (% Change From Baseline)
analgesia
allodynia
1 Post 2 Pre 2 Post 3 Pre 3 Post 4 Pre 4 Post 5 6 7
C
Mechanical Allodynia
Paw Withdrawal Frequency (% Change From Baseline)
allodynia
C57BL/6J
129S6
CXB-7/ByJ
D
Mechanical Hyperalgesia
hyperalgesia
analgesia
E
Thermal Heat Hyperalgesia
Number of Responses (% Change from Baseline)
hyperalgesia
analgesia

Strains also exhibited differences in their response to repeated presentation of a normally innocuous punctate mechanical stimulus over time (Fig. 2.4C; $F_{(18,430)}$=32.88, p<0.0001). C57BL/6J mice developed mechanical allodynia prior to morphine administration on day 4 and following morphine cessation on days 5 and 6. Consistent with the paw withdrawal threshold data, 129S6 mice failed to develop mechanical allodynia. CXB7/ByJ mice, however, demonstrated the highest degree of mechanical allodynia, evident prior to morphine administration on days 3 and 4 and following morphine cessation on days 5-7 (p<0.001).

Similarly, strains exhibited differences in their response to repeated presentation of a normally noxious punctate mechanical stimulus over time (Fig. 2.4D; $F_{(18,430)}$=15.19, p<0.0001). C57BL/6J mice showed analgesia following morphine administration on days 1-4, then developed mechanical hyperalgesia prior to morphine administration on days 3 and 4 as well as following morphine cessation on days 5-7. 129S6 mice exhibited analgesia following morphine administration on days 1-4 (p<0.001), however failed to develop mechanical hyperalgesia at later time points. In contrast to the other strains, CXB7/ByJ mice failed to show analgesia following morphine administration, but did develop mechanical hyperalgesia prior to morphine administration on days 3 and 4 as well as following morphine cessation on days 5 and 6 (p<0.001). Consistent with their changes in mechanical allodynia, CXB7/ByJ mice also exhibited mechanical hyperalgesia following morphine administration on day 3 (p<0.001). When assessed for behavioral responses to mechanical stimuli, saline treated controls did not exhibit any changes in paw withdrawal threshold or demonstrate mechanical allodynia or hyperalgesia (Figure 2.5).

Figure 2.5. Raw data illustrating behavioral responses of 129S6, C57BL/6J, and CXB7/ByJ mice to mechanical and thermal heat stimuli during saline administration. Strains exhibit no significant changes from their respective baselines when assessing for (A) paw withdrawal threshold ($F_{(2,516)} = 377.7$, $p<0.0001$)**,** and when assessing responses following repeated exposure to (B) an innocuous ($F_{(2,516)} = 29.08$, $p<0.0001$)**,** or (C) noxious mechanical stimulus ($F_{(2,516)} = 1857$, $p<0.0001$)**.** (D) Unlike 129S6 and C57BL/6J mice, CXB7/ByJ mice exhibited increased responses to thermal heat stimuli ($F_{(2,516)} = 115.2$, $p<0.0001$) starting on day 1 following saline administration that steadily returned to baseline throughout testing. Panels A-D: *N*=15-16/group. Data expressed as mean ± SEM. * = different from baseline.

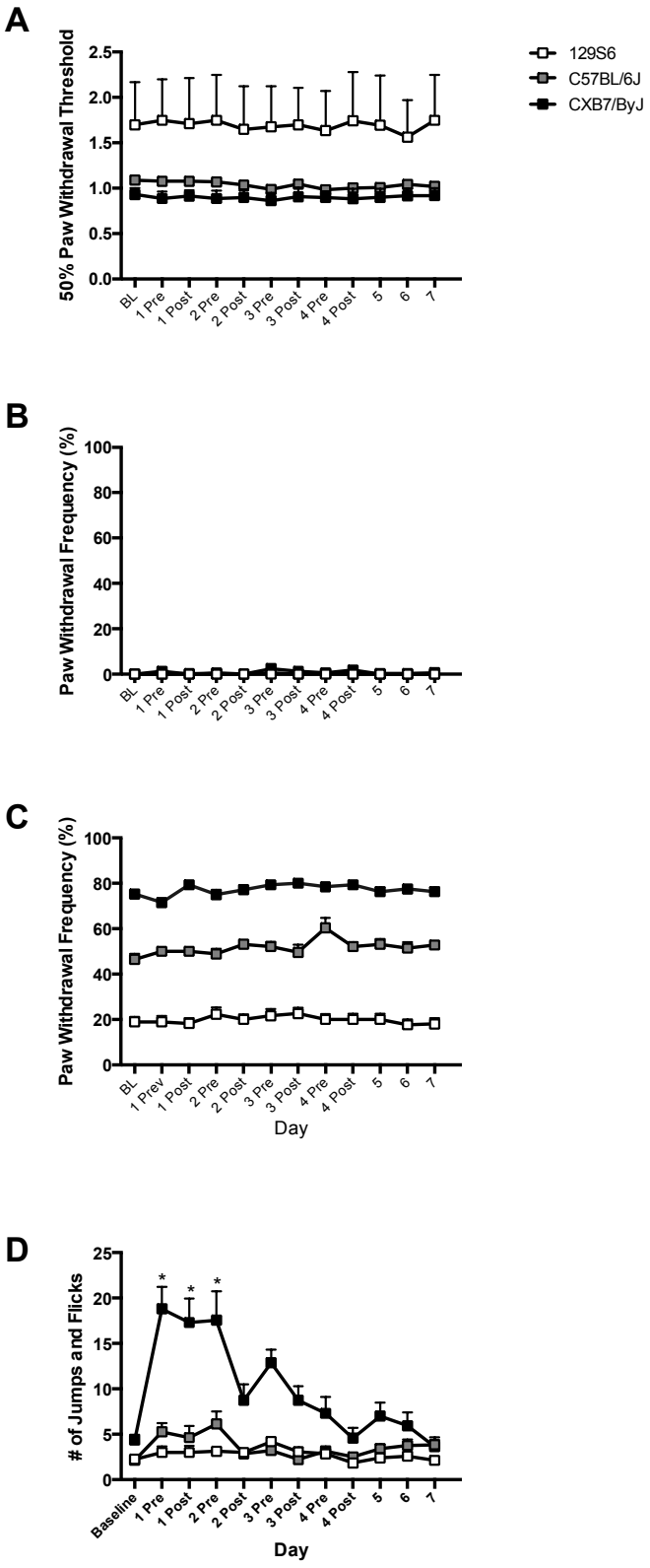
A
50% Paw Withdrawal Threshold
2.5
2.0
1.5
1.0
0.5
0.0
BL
1 Pre
1 Post
2 Pre
2 Post
3 Pre
3 Post
4 Pre
4 Post
5
6
7
129S6
C57BL/6J
CXB7/ByJ
B
Paw Withdrawal Frequency (%)
100
80
60
40
20
0
C
Paw Withdrawal Frequency (%)
1 Prev
Day
D
# of Jumps and Flicks
25
20
15
10
5
0
*
Baseline
Day

Finally, strains differed over time with respect to their response to thermal heat (Fig. 2.4E; $F_{(18,430)}$=3.906, p<0.0001). When compared to 129S6 mice, C57BL/6J mice developed thermal heat hyperalgesia starting on day 2 prior morphine administration and following morphine cessation (p<0.001). CXB7/ByJ mice also developed develop thermal heat hyperalgesia on day 2 and 4 prior to morphine administration and following morphine cessation.

3.3.3. *MOR-1K* gene expression levels parallel OIH profiles.

To determine the relationship between OIH pain profiles and *MOR-1K* gene expression, spinal cord and discrete brain tissues were collected from separate groups of mice at times points corresponding to maximal analgesia and hyperalgesia. Changes in *MOR-1K* gene expression levels across the discrete brain and spinal cord tissues were not significantly different, and thus were normalized and pooled together (Figures 2.6-2.8). C57BL/6J, 129S6, and CXB7/ByJ mice exhibited divergent *MOR-1K* gene expression levels that paralleled their behavioral profiles (Figure 2.9; p=0.011). Compared to C57BL/6J mice, 129S6 mice demonstrated decreased *MOR-1K* gene expression levels on days 1 and 4 (p<0.05), in line with their analgesic responses. In contrast, CXB7/ByJ mice demonstrated increased *MOR-1K* gene expression levels on day 4 (p<0.05), in line with their hyperalgesic responses. Interestingly, *MOR-1K* gene expression levels for both 129S6 and CXB7/ByJ mice returned to near-baseline levels following the cessation of morphine treatment on day 5, suggesting that the observed differences were indeed morphine-dependent. To determine the potential involvement of other MOR-1 splice variants, we measured gene expression levels of other exon-11 containing splice variants (MOR-1G, MOR-1H, MOR-1I, MOR-1J, MOR-1L, MOR-1M, MOR-1N and MOR-1T). The splice variants did not exhibit significant changes in gene expression levels due to morphine administration (Figure 2.10.).

Figure 2.6. Z-scores of *MOR-1K* gene expression levels in discrete tissues of 129S6 mice. Tissue samples from (A) spinal cord, (B) medulla, (C) pons, (D) periaqueductal gray, (E) thalamus, (F) hypothalamus, (G) striatum, (H) nucleus accumbens, and (I) frontal lobe have similar *MOR-1K* gene expression levels in 129S6 mice. Panels A-I: *N*=7/group. Data expressed as Z-score.

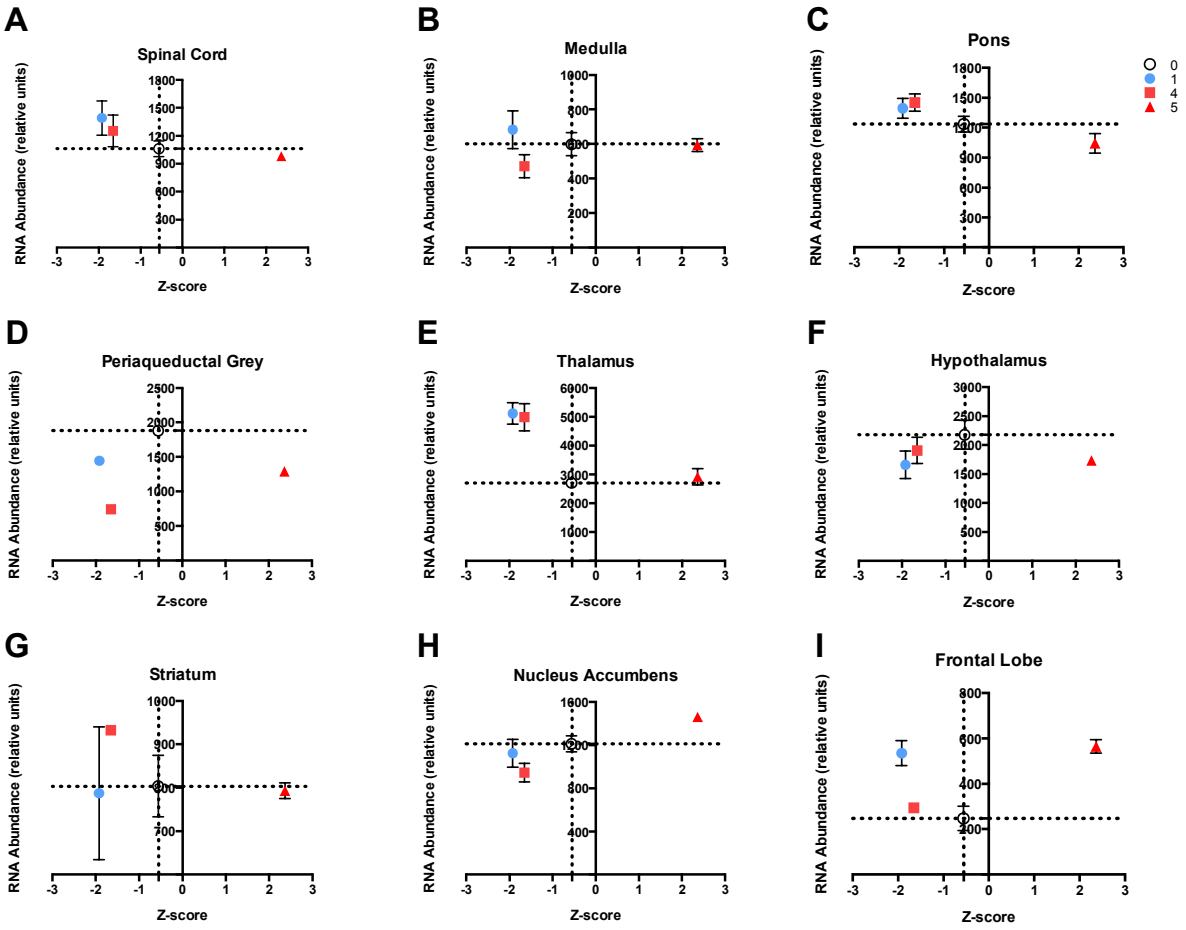
A
Spinal Cord
B
Medulla
C
Pons
D
Periaqueductal Grey
E
Thalamus
F
Hypothalamus
G
Striatum
H
Nucleus Accumbens
I
Frontal Lobe
RNA Abundance (relative units)
Z-score
0
1
4
5

Figure 2.7. Z-scores of *MOR-1K* gene expression levels in discrete tissues of C57BL/6J mice. Tissue samples from (A) spinal cord, (B) medulla, (C) pons, (D) periaqueductal gray, (E) thalamus, (F) hypothalamus, (G) striatum, (H) nucleus accumbens, and (I) frontal lobe have similar *MOR-1K* -gene expression levels in C57BL/6J mice. Panels A-I: *N*=7/group. Data expressed as Z-score

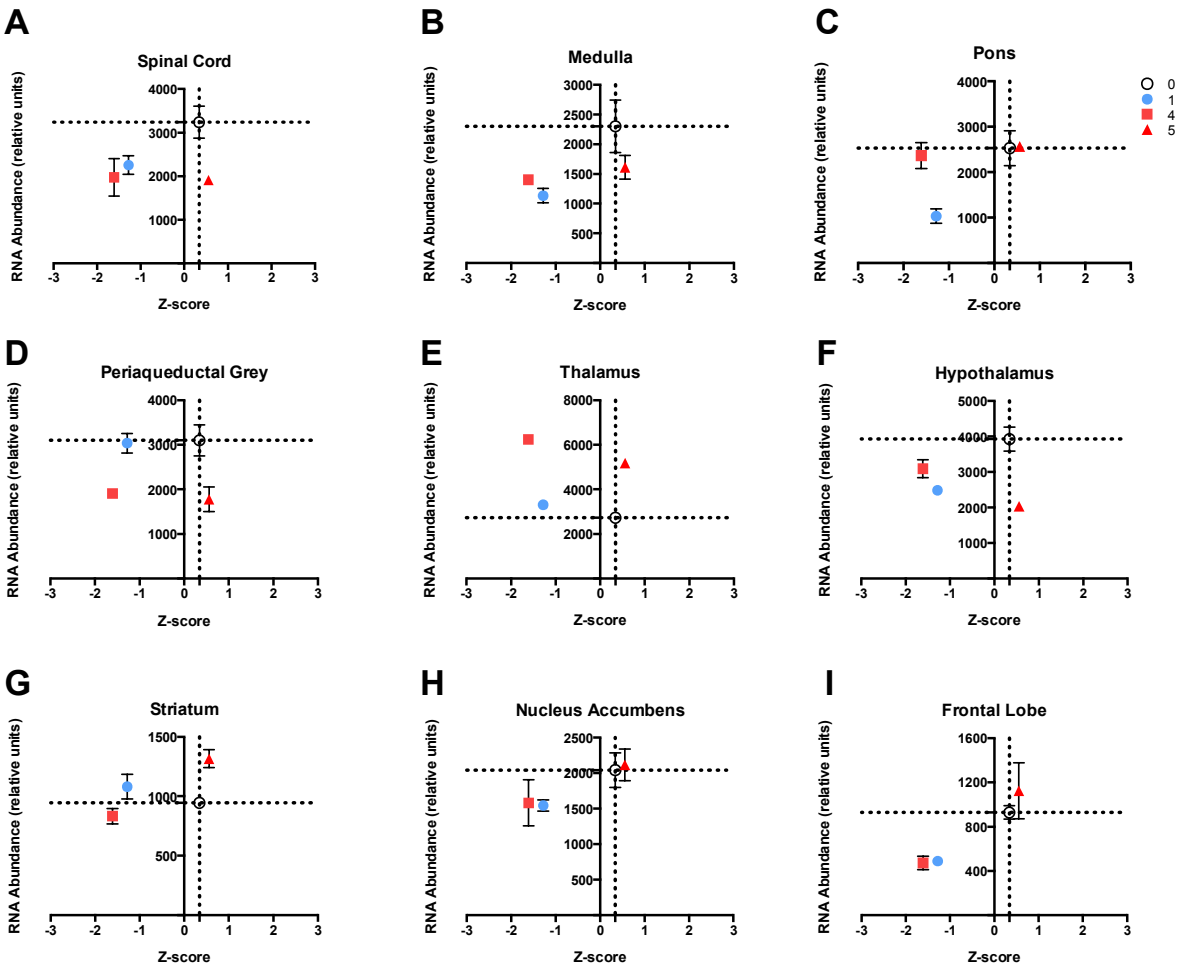
A
Spinal Cord
RNA Abundance (relative units)
Z-score
B
Medulla
RNA Abundance (relative units)
Z-score
C
Pons
RNA Abundance (relative units)
Z-score
0
1
4
5
D
Periaqueductal Grey
RNA Abundance (relative units)
Z-score
E
Thalamus
RNA Abundance (relative units)
Z-score
F
Hypothalamus
RNA Abundance (relative units)
Z-score
G
Striatum
RNA Abundance (relative units)
Z-score
H
Nucleus Accumbens
RNA Abundance (relative units)
Z-score
I
Frontal Lobe
RNA Abundance (relative units)
Z-score

Figure 2.8. Z-scores of *MOR-1K* gene expression levels in discrete tissues of CXB7/ByJ mice. Tissue samples from (A) spinal cord, (B) medulla, (C) pons, (D) periaqueductal gray, (E) thalamus, (F) hypothalamus, (G) striatum, (H) nucleus accumbens, and (I) frontal lobe have similar *MOR-1K* -gene expression levels in CXB7/ByJ mice. Panels A-I: *N*=7/group. Data expressed as Z-score.

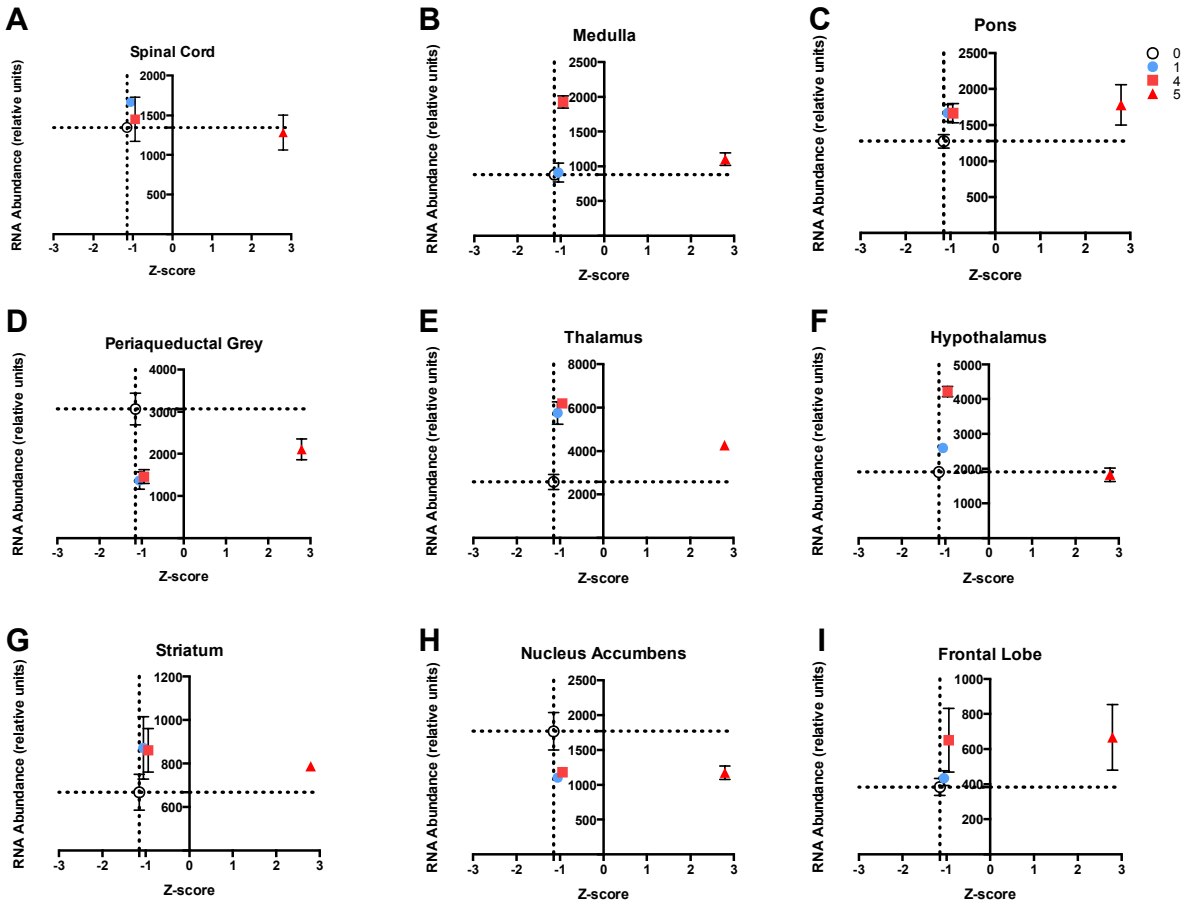
A
Spinal Cord
B
Medulla
C
Pons
0
1
4
5
D
Periaqueductal Grey
E
Thalamus
F
Hypothalamus
G
Striatum
H
Nucleus Accumbens
I
Frontal Lobe
RNA Abundance (relative units)
Z-score

Figure 2.9. Strains exhibit divergent *MOR-1K* gene expression levels that correspond to behavior profiles. 129S6 mice exhibit decreased *MOR-1K* gene expression levels on days 1 and 4, corresponding to their analgesic behavioral profile. In contrast, CXB7/ByJ mice exhibit increased *MOR-1K* gene expression levels on day 4, corresponding to their hyperalgesic behavioral profile.

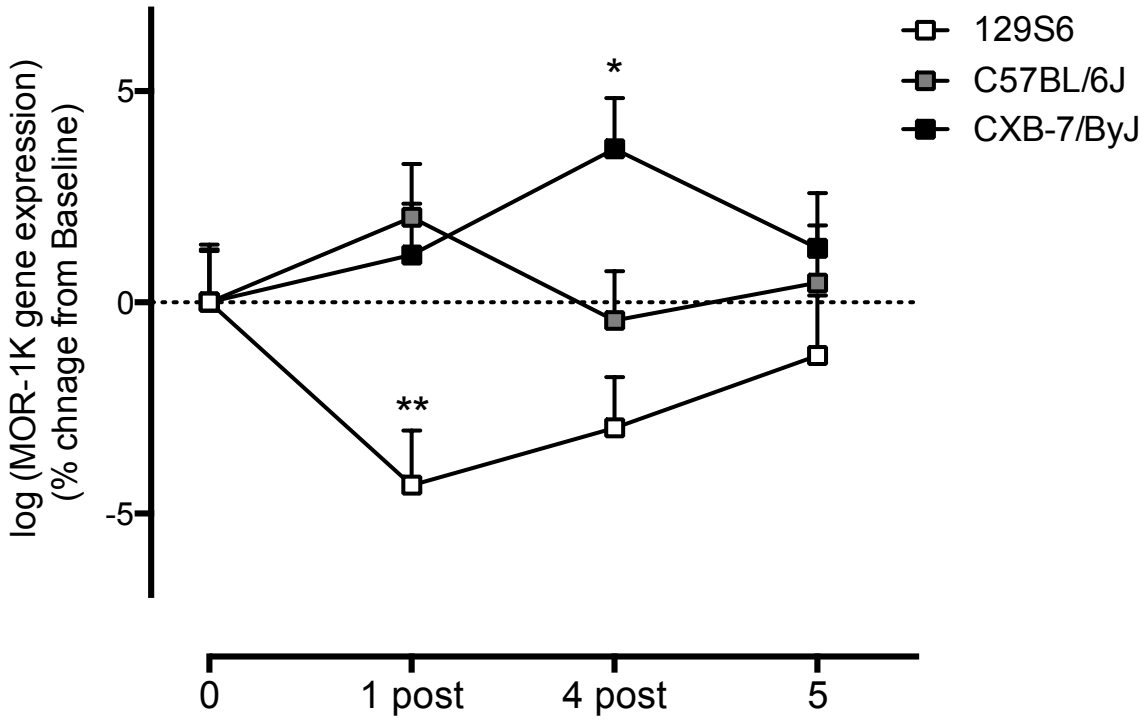
129S6
C57BL/6J
CXB-7/ByJ
log (MOR-1K gene expression)
(% chnage from Baseline)
5
0
-5
*
**
0
1 post
4 post
5

Figure 2.10. Relative quantification of other exon 11 MOR-1 splice variants. (A-C). Chronic morphine administration does not significantly alter the gene expression levels of MOR-1 splice variants that contain exon 11, exon 14, or exon 16. Panels A-I: *N*=7-8/group. Data expressed as Z-score.

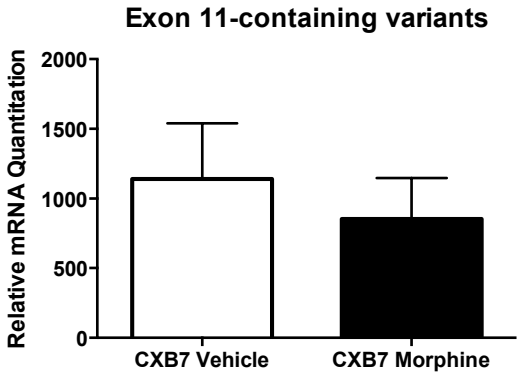
Exon 11-containing variants
Relative mRNA Quantitation
2000
1500
1000
500
0
CXB7 Vehicle
CXB7 Morphine

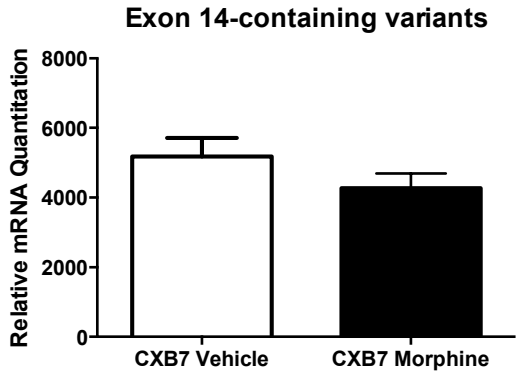
Exon 14-containing variants
Relative mRNA Quantitation
8000
6000
4000
2000
0
CXB7 Vehicle
CXB7 Morphine

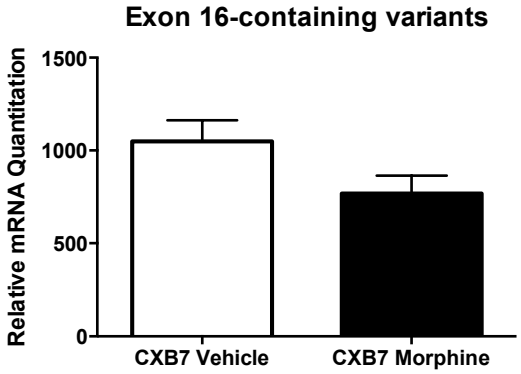
Exon 16-containing variants
Relative mRNA Quantitation
1500
1000
500
0
CXB7 Vehicle
CXB7 Morphine

2.3.4. Sustained delivery of MOR-1K exon 13 antisense siRNA prevents OIH.

The observed correlation between strain-specific pain profiles and MOR-1K gene expression levels suggests that MOR-1K contributes to OIH in genetically susceptible mice. To determine whether MOR-1K is required for the development of OIH in CXB7/ByJ mice, we employed siRNA knockdown. Male and female CXB7/ByJ mice demonstrated similar behavioral phenotypes (Figure 2.11.); thus, all behavioral data was pooled together for analysis. Within the OIH murine paradigm, we found that sustained i.t. delivery of exon 13 antisense siRNA prevented the development of mechanical allodynia (Figure 2.12B; $F_{(2,189)} = 24.69, p<0.0001$, Fig. 2.12C; $F_{(2,189)} = 37.63$, $p<0.0001$) and mechanical hyperalgesia (Fig. 2.12D; $F_{(2,189)} = 54.92$, $p<0.0001$). In contrast, sustained administration of exon 13 sense siRNA or sham surgery did not prevent the development of mechanical pain sensitivity. Of note, we also found that sustained i.t. delivery of the antisense siRNA unmasked morphine analgesia in CXB7/ByJ mice not observed in sense and sham mice or saline-treated controls (Figures 2.13-2.14.) A possible concern with sustained i.t. delivery is the development of inflammation and gliosis in the spinal cord in proximity with the catheter tip (139,140), and its effects on behavioral assessment. Given that CXB7/ByJ mice receiving sense siRNA and sham surgery displayed similar behavioral responses throughout testing, we believe that the use of i.t. catheters for sustained siRNA delivery did not impact the behavioral assessment of OIH.

Figure 2.11. Sex-dependent behavioral responses to mechanical stimuli across Antisense, Sense, and Sham mice. Male and female Antisense mice **(A-C)**, Sense mice **(D-F)**, and Sham mice **(G-I)** exhibited similar responses to mechanical stimuli within their respective treatment groups. Panels A-I: *N*=3-4/group. Data expressed as mean ± SEM.

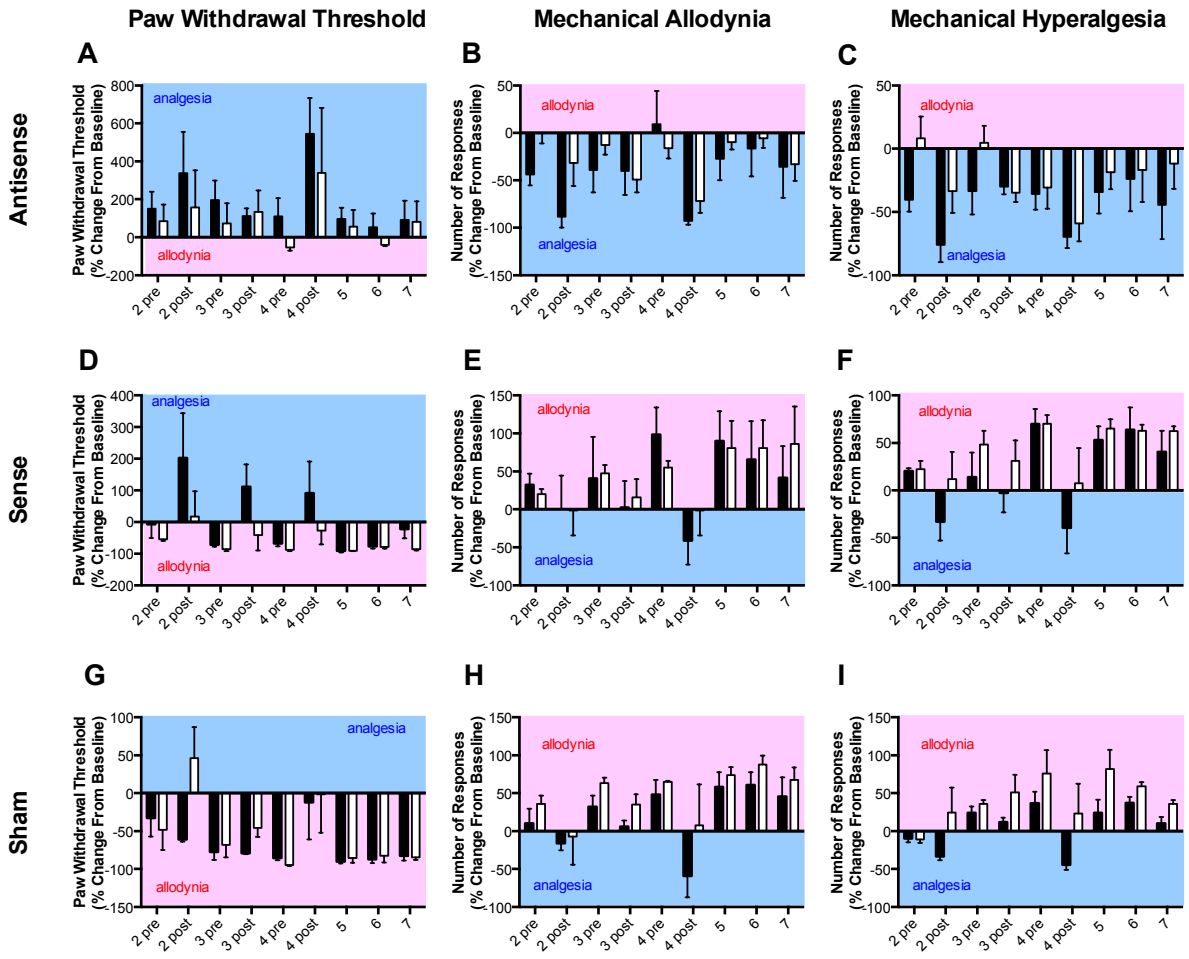
Paw Withdrawal Threshold
Mechanical Allodynia
Mechanical Hyperalgesia
A
B
C
D
E
F
G
H
I
Antisense
Sense
Sham
Paw Withdrawal Threshold (% Change From Baseline)
Number of Responses (% Change From Baseline)
analgesia
allodynia
2 pre
2 post
3 pre
3 post
4 pre
4 post
5
6
7

Figure 2.12. CXB7/ByJ mice treated with exon 13 antisense siRNA fail to develop OIH. (A) A timeline of sustained i.t. siRNA delivery, chronic morphine administration, and assessments of pain behavior and gene expression is shown. CXB7/ByJ mice receiving antisense siRNA exhibit analgesia following morphine administration and cessation, and fail to exhibit **(B)** decreased paw withdrawal thresholds, or increased responses to **(C)** repeated presentation of an innocuous or **(D)** noxious mechanical stimulus. In contrast, mice receiving sense siRNA or sham exhibited analgesia following morphine administration, which was then followed by allodynia/hyperalgesia on days 5-7. Panels B-D: *N*=6-9/group. Data expressed as mean ± SEM.*****p*<0.0001, ****p*<0.001, ***p*<0.01, **p*<0.05 different from Sham..

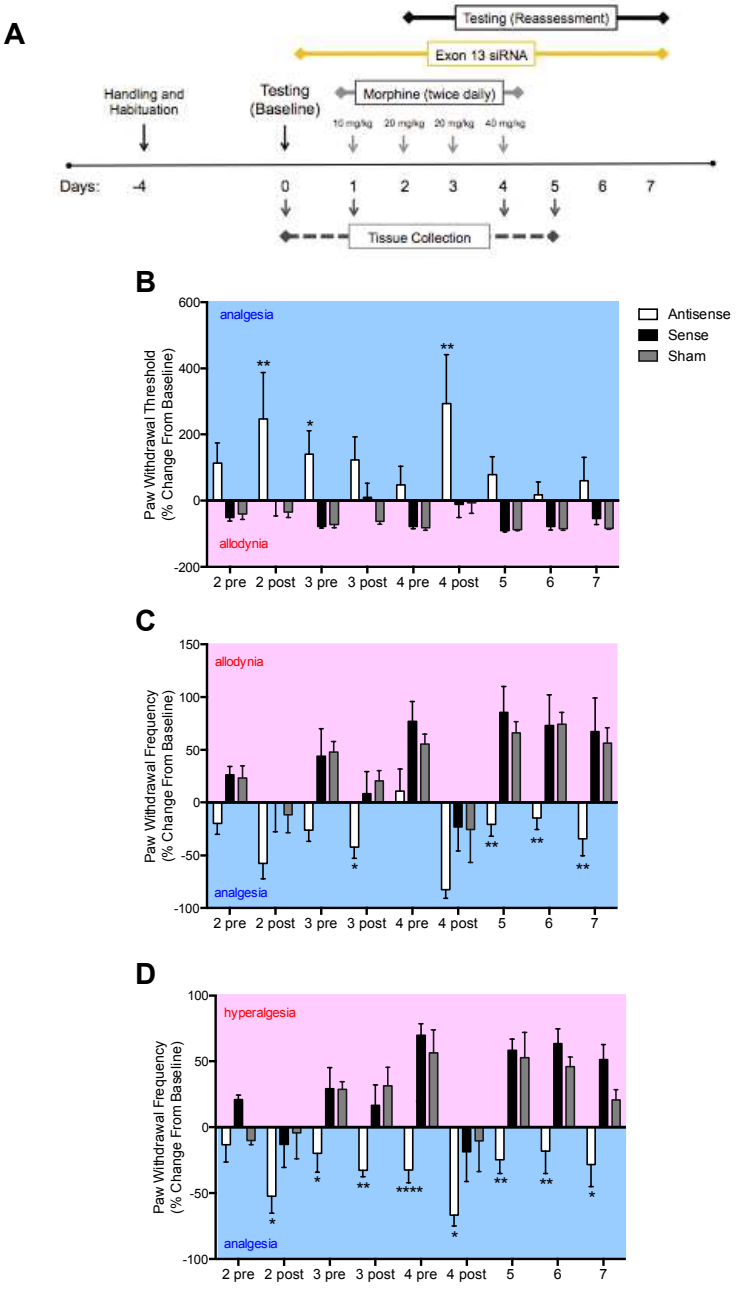
A
Testing (Reassessment)
Exon 13 siRNA
Handling and Habituation
Testing (Baseline)
Morphine (twice daily)
10 mg/kg
20 mg/kg
20 mg/kg
40 mg/kg
Days: -4 0 1 2 3 4 5 6 7
Tissue Collection
B
analgesia
allodynia
Paw Withdrawal Threshold (% Change From Baseline)
600
400
200
0
-200
2 pre 2 post 3 pre 3 post 4 pre 4 post 5 6 7
Antisense
Sense
Sham
C
allodynia
analgesia
Paw Withdrawal Frequency (% Change From Baseline)
150
100
50
0
-50
-100
2 pre 2 post 3 pre 3 post 4 pre 4 post 5 6 7
D
hyperalgesia
analgesia
Paw Withdrawal Frequency (% Change From Baseline)
100
50
0
-50
-100
2 pre 2 post 3 pre 3 post 4 pre 4 post 5 6 7

Figure 2.13. Raw data illustrate behavioral responses of Antisense, Sense, and Sham mice to mechanical stimuli during chronic morphine administration. Antisense mice exhibit **(A)** lower paw withdrawal threshold, **(B)** decreased responses to repeated innocuous **(C)** and noxious stimuli when compared to Sense and Sham mice. Panels A-C: *N*=6-9/group. Data expressed as mean ± SEM. * = different from baseline.

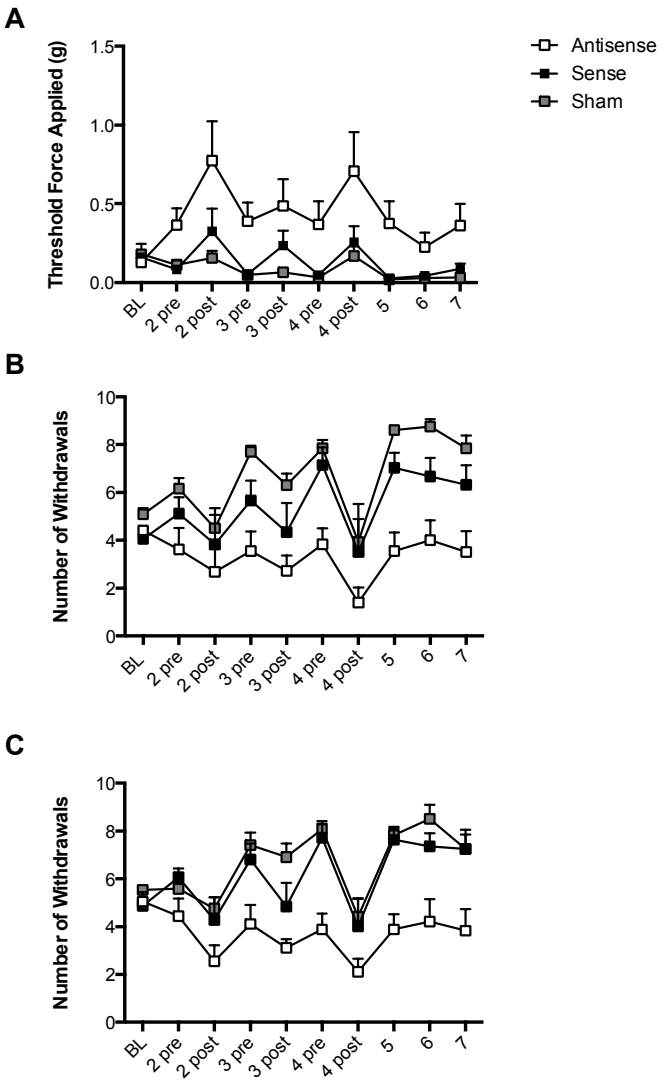
A
Threshold Force Applied (g)
1.5
1.0
0.5
0.0
BL
2 pre
2 post
3 pre
3 post
4 pre
4 post
5
6
7
Antisense
Sense
Sham
B
Number of Withdrawals
10
8
6
4
2
0
BL
2 pre
2 post
3 pre
3 post
4 pre
4 post
5
6
7
C
Number of Withdrawals
10
8
6
4
2
0
BL
2 pre
2 post
3 pre
3 post
4 pre
4 post
5
6
7

Figure 2.14. Raw data illustrate behavioral responses of Antisense, Sense, and Sham mice to mechanical stimuli during saline administration. Antisense, Sense, and Sham mice did not exhibit behavioral differences from their respective baselines when assessing for **(A)** paw withdrawal threshold ($F_{(2,160)} = 34.87$, $p<0.0001$)**, (B)** mechanical allodynia ($F_{(2,160)} = 45.01$, $p<0.0001$)**, (C)** mechanical hyperalgesia ($F_{(2,160)} = 23.43$, $p<0.0001$) during saline administration. Panels A-C: N=6-9/group. Data expressed as mean ± SEM. * = different from baseline.

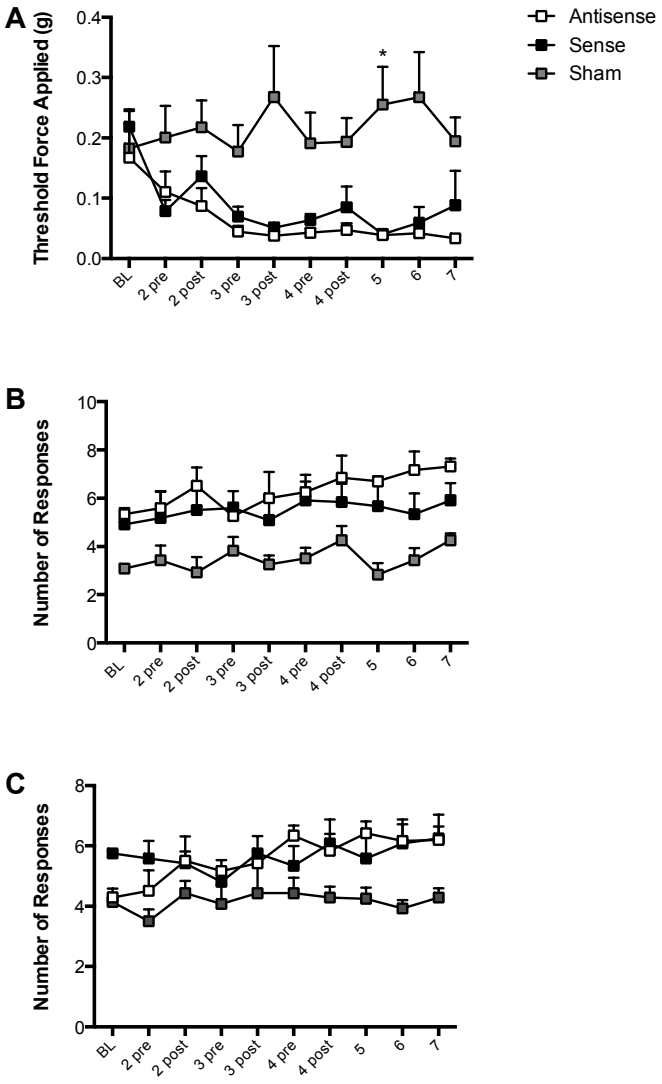
A
Threshold Force Applied (g)
0.4
0.3
0.2
0.1
0.0
*
BL
2 pre
2 post
3 pre
3 post
4 pre
4 post
5
6
7
Antisense
Sense
Sham
B
Number of Responses
10
8
6
4
2
0
C
Number of Responses
8
6
4
2
0

2.3.5. Sustained delivery of MOR-1K exon 13 antisense siRNA decreases MOR-1K gene expression levels.

Finally, we evaluated the efficacy of chronic siRNA administration to suppress MOR-1K gene expression levels in CXB7/ByJ mice. Given that siRNA was administered intrathecally, we examined MOR-1K gene expression within the spinal cord. As predicted, sustained i.t. delivery of antisense siRNA prevented the increase of MOR-1K gene expression levels in the spinal cord (Figure 2.15; $F_{(1,11)}$= 29.05, p=0.0002). In contrast, sustained delivery of sense siRNA failed to block increases in MOR-1K gene expression levels. These findings suggest that MOR-1K located in spinal sites is necessary for the development of OIH.

Figure 2.15. Sustained administration of MOR-1K antisense siRNA reduces MOR-1K gene expression levels. CXB7/ByJ mice receiving antisense siRNA exhibit decreased *MOR-1K* gene expression levels in the spinal cord as compared to those receiving sense siRNA. For all behavioral graphs, blue background indicates a decrease in pain sensitivity (analgesia), and red background indicates an increase in pain sensitivity (allodynia/hyperalgesia). *N*=3-4/group. ***p*<0.01 different from Sense.

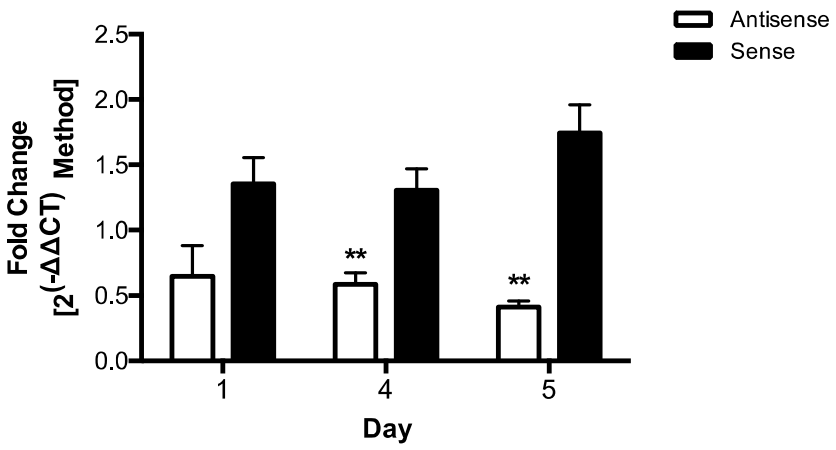
Antisense
Sense
Fold Change
[2^(-ΔΔCT) Method]
2.5
2.0
1.5
1.0
0.5
0.0
**
**
1
4
5
Day

2.4. Conclusion

Here, we provide the first evidence suggesting that in genetically susceptible animals, MOR-1K contributes to the development of OIH. Compared to C57BL/6J and 129S6 mice, CXB7/ByJ mice exhibited the greatest degree of pain following morphine administration alongside increased *MOR-1K* gene expression levels. Reductions in *MOR-1K* gene expression *via* sustained delivery of antisense siRNA not only prevented OIH, but also unmasked morphine analgesia.

The results of this study demonstrate the significance of genetic variability of the mu-opioid receptor in the development of OIH. Of the three mouse strains, CXB7/ByJ mice exclusively exhibited increased pain sensitivity, evident immediately following morphine administration. Their hyperalgesic pain profile also paralleled increased *MOR-1K* mRNA transcript levels. For this reason, we selected this strain to examine the effects of *MOR-1K* knockdown using antisense exon 13 siRNA. CXB7/ByJ mice receiving sustained i.t. delivery of antisense *MOR-1K* siRNA failed to develop OIH and instead exhibited morphine analgesia. Sustained delivery of antisense siRNA significantly reduced *MOR-1K* gene expression levels within the spinal cord. Given that i.t. delivery provides direct access to the spinal cord, we hypothesize that MOR-1K siRNA integrated into primary and secondary order neurons and cleaved *MOR-1K* mRNA transcripts, resulting in decreased *MOR-1K* gene expression levels. As a complement to this experiment, we also sought to determine if MOR-1K overexpression would induce morphine-induced hyperalgesia. Specifically, 129S6 mice, the pain-resistant strain that failed to develop morphine-induced hyperalgesia, received direct *i.t.* injections of adeno-associated virus (AAV) containing canonical MOR-1K plasmid DNA (MOR-1K C) or a SNP containing MOR-1K plasmid DNA (MOR-1K T). Preliminary data demonstrated that when compared to mice that received no vector or empty vector, mice that received either version of MOR-1K exhibited increased mechanical allodynia and hyperalgesia during chronic morphine administration (Appendix 2.1.).

When examining *MOR-1K* gene expression levels in the three mouse strains, we found that C57BL/6J mice exhibited different gene expression patterns during chronic morphine administration when compared to CXB7/ByJ mice. On day 1, C57BL/6J *MOR-1K* gene expression levels were similar to those of the CXB-7/ByJ mice, but on day 4 their expression levels decreased 2.4% while those of the CXB-7/ByJ mice increased 2.5%. It is possible that *MOR-1K* gene expression is negatively regulated in C57BL/6J mice and that is why they exhibit opioid-induced hyperalgesia to a lesser degree than CXB7/ByJ mice. For example, Lu et al provide evidence of microRNA-103/107 downregulation of mu opioid splice variant MOR-1A (141). Further research is needed to investigate the possible strain-specific modulators of MOR-1K expression.

In this study, we observed that, despite a return of *MOR-1K* gene expression to baseline levels, C57BL/6J and CXB7/ByJ mice continued to exhibit OIH following morphine cessation (Fig. 2). This persistence of OIH following opioid cessation has also been observed in other preclinical and clinical studies. In mice, administration of antagonists against the 5-HT3 receptor (5HT3R) (142), N-Methyl-D-aspartate receptor (NMDAR), melanocortin-1 receptor (MC1R) (143) alongside morphine or beta-2-adrenergic receptor (β2AR) (37) prevent the development of OIH. In addition, β2AR-deficient mice fail to develop OIH(37). Clinical studies have also shown that administration the β2AR antagonist propranolol (38) or NMDAR antagonist ketamine (32,144) alongside the fast-acting opioid remifentanil hinders the development of OIH following opioid cessation. Collectively, these findings suggest that MOR-1K may interact with other receptors, including 5HT3R, NMDAR, MC1R, and β2AR, to initiate and maintain OIH.

The study highlights the impact of MOR-1 splice variants in opioid and pain signaling. So far, there are currently thirty-four MOR-1 splice variants in mouse, and twenty splice variants in human (61), numbers which suggest a vast array for functional implications. MOR-1 splice variants other than MOR-1K have been shown to play modulatory roles in opioid signaling. For example, Liu et al have demonstrated that splice variant MOR-1D heterodimerizes with the gastrin-releasing peptide

receptor, resulting in signaling that promotes opioid-induced itch (108). Another MOR-1 splice variant, MOR-1G, has been shown to heterodimerize with the nociceptin receptor ORL-1 to provide a binding site for the novel opioid analgesic 3-iodobenzoyl-6β-naltrexamide (145). Along with modulating opioid analgesia and opioid-related side effects, MOR-1 splice variants have also been shown to stabilize the canonical receptor at the cell membrane (117). These findings demonstrate the influence of splice variants on pain modulation and canonical receptor function. Future research is needed in order to elucidate the functional characteristics of other unexplored MOR-1 splice variants.

Our findings extend previous work examining the effects of genetic variability on opioid analgesia and hyperalgesia. Results from other animal studies have demonstrated strain-specific opioid analgesia efficacy (146) and fentanyl-induced hyperalgesia (147). Likewise, results from human studies have demonstrated that functional variation in the MOR-1 gene locus regulates opioid responses. For example, the MOR-1 A118G gene polymorphism, which leads to reduced MOR signaling (148), is associated with reduced morphine efficacy (149). More recently, the *MOR-1K* rs563649 polymorphism, which results in increased *MOR-1K* translation efficiency, has been associated with increased pain sensitivity and blunted morphine efficacy (128). Combined, these results suggest that genetic susceptibility, particularly in the MOR-1 gene locus, contributes to diminished opioid efficacy and the development of OIH.

In order to understand the mechanisms whereby MOR-1K contributes to OIH, its expression patterns and signaling profiles must be defined. At the tissue level, MOR-1K is expressed in astrocytes within the central nervous system and in perineurial cells within the peripheral nervous system (150), indicating possible influence of glial activation in OIH (151). We have also shown that MOR-1K mRNA is co-expressed with S100, suggesting that the receptor is expressed with satellite glial cells (Appendix 2.2). At the cellular level, MOR-1K is normally expressed intracellularly (65), where it may drive G_s-dependent increases in intracellular cAMP and calcium following active transport or passive diffusion of morphine across the cell membrane (152,153). In the presence of

β2AR, a GPCR also implicated in OIH (38). MOR-1K has been shown to relocate to the cellular membrane *in vitro* (154). Specifically, the authors utilized immunofluorescence to show that MOR-1K and β2AR co-localize within the cell and that both receptors move to the cell membrane. These data suggest the two receptors interact with one another, perhaps by forming a heterodimer. More *in vitro* studies, such as co-immunoprecipitation, are necessary to determine if this is indeed the case. Although its gene expression and signaling profiles are somewhat established, knowledge on MOR-1K protein expression is lacking and needs to be defined. Currently available molecular tools, however, are not selective enough to identify and isolate the MOR-1K protein. Future MOR-1K studies will benefit from the development of antibodies and ligands that specifically target this splice variant.

In conclusion, the present study demonstrates a functional role for MOR-1K in a murine model of OIH. More work is required to determine MOR-1K's downstream effectors and signaling mechanisms as well as to understand its contribution to individual variability in a more comprehensive set of opioid responses. Outcomes from present and future studies will help elucidate the neurobiological mechanisms that drive OIH and, in turn, will inform the development of more rational treatment strategies that alleviate clinical pain while reducing OIH risk.

CHAPTER 3: Determining the Functionality of Strain-specific Mu-opioid Receptor Polymorphisms

3.1. Introduction

When examining the manifestation of OIH in genetically diverse strains of mice, we demonstrated that the three strains demonstrated divergent pain responses following chronic morphine administration that also corresponded to *MOR-1K* gene transcript levels. Specifically, when compared to C57BL/6J, 129S6 mice were pain resistant with decreased *MOR-1K* transcript levels. In contrast, CXB7/ByJ mice were pain sensitive with increased *MOR-1K* transcript levels. We hypothesized that variability in behavioral and gene expression profiles result from strain-specific variability in the MOR-1 gene locus. To test this hypothesis, we examined *OPRM1* sequences from C57BL/6J, 129S6, and CXB7/ByJ strains for possible strain-specific polymorphisms. Furthermore, we utilized bioinformatic databases and cAMP assays to determine the functional impact of polymorphic alleles.

3.2. Materials and Methods

3.2.1. DNA Extraction and Sequencing

Total RNA from discrete brain regions (medulla, pons, periaqueductal grey, thalamus, hypothalamus, striatum, nucleus accumbens, and frontal lobe), and spinal cord was purified using 1mL TRIzol (Life Technologies, NY) for each tissue sample. Samples were immediately homogenized using a Pro200 homogenizer (Pro Scientific, CT) or Precellys 24 Homogenizer (Bertin Technologies, France) and all subsequent RNA purification steps were performed according to the TRIzol manufacturer recommendations. Purified RNA samples were treated with TURBO DNA-free

(Life Technologies, NY) per manufacturer protocol and concentrations were determined using a Nanodrop-1000 (Thermo Scientific, DE) and reverse transcribed using Transcriptor First Strand cDNA Synthesis kit (Roche, Switzerland). Prepared cDNA samples were then amplified using Advantage® HF 2 PCR Kit per manufacturer protocol (Takara Bio USA, CA). Amplified cDNA was sequenced by Genewiz and analyzed using Sequencher 5.1 (Gene Codes Co., MI). Sample sequences were compared to OPRM1 mRNA sequence (NCBI: NM_001039652.1) and MOR-1K cDNA (NCBI: AF260309.1).

3.2.2. Predicting Alterations to Transcription Factor Binding Sites.

A recent genome-wide analysis study investigating the role of OPRM1 polymorphisms in pain in humans demonstrated that a single nucleotide polymorphism (SNP) *rs563649* facilitated increased MOR-1K transcription. Given that the identified murine SNP is also located in exon 13, we sought to determine if it altered existing transcription factor binding sites in the region. Thus, JASPAR CORE database(155) and TFSearch database (Computational Biology Research Consortium, Japan) were used to assess for changes to existing transcription factor binding in MOR-1 and MOR-1K cDNA.

3.2.3. Cyclic AMP Assay

HEK293 cells were transduced with pAAV2-ZsGreen viral vector containing canonical MOR-1K plasmid cDNA, MOR-1K plasmid cDNA containing an exon 13 SNP, or empty vector (Biowit Technologies, Shenzhen, China). The same pAAV2 virus used to express MOR-1K was also used to express MOR-1K in 129S6 mice (Chapter 4) and establishes continuity between both experiments. A separate group of Human Embryonic Kidney (HEK) 293 cells, MOR-1 cDNA was transfected using Fugene HD per manufacturer protocol (Promega, WI). After transduction or transfection, cells were plated into 384 well plates. The seeded plates were treated with morphine or vehicle for 30 min then cAMP levels were detected using HitHunter cAMP Assay for Biologics

(DiscoverX, CA) per manufacturer protocol. The cAMP levels were measured using Cytation5 Cell Imaging Mutli-Mode Reader (BioTek, VT).

3.3. Results

3.3.1. CXB7/ByJ *OPRM1* transcripts contained strain-specific polymorphisms

First, we sought to determine if there were any genetic differences between C57BL/6J, 129S6, and CXB7/ByJ cDNA transcripts. Sequencing of the strains' sequences revealed two single nucleotide polymorphisms, specifically within the CXB7/ByJ transcript. The first polymorphism (Figure 4.1, Table 4.1) was an A → C nucleotide change at position 6788673, located in exon 1 of *OPRM1* transcript. The SNP, already identified as *rs8241991,* is implicated in MOR-1 receptor function. Lee and colleagues found that *rs8241991* altered transcription factor binding to the SP1 binding site, resulting in reduced MOR-1 gene expression levels characteristic of CXB7/ByJ mice (138).

The second polymorphism was a previously unidentified C→ T nucleotide change at position 6679800, located in exon 13. Using JASPAR CORE and TFSearch databases, we found that the SNP is located in an enhancer box, or E-box, regulatory binding site. Due to its sequence, CANNTG, E-box regulatory sequences are capable of being functionally distinct and recruit a variety of basic helix-loop-helix (bHLH) proteins (156). A particular class of bHLH proteins, hypoxia-inducible factor (HIF) proteins, are known modulators of inflammation and pain (157-159) that are influenced by opioid administration(160,161). Given the importance of the E-Box motif in the regulation of pain and opioid function, it is possible that this SNP could alter MOR-1K receptor activity.

Table 3.1. Strain-specific SNPs in *OPRM1* gene.

Rs Number	Position	Region	Variant	Transcript	AA change	Strain
rs8241991	6788673	Exon	A>C	MOR-1	Aspartic acid to alanine	CXB7/ByJ [cite]
Not Listed	6679800	Exon	C>T	MOR-1K		CXB7/ByJ

Figure 3.1. Predicted functional effects of strain-specific polymorphisms. MOR-1 cDNA sequences from 129S6, C57Bl/6J, and CXB-7/ByJ mice were compared. **(A)** CXB-7/ByJ mice possess a strain-specific polymorphism located in the SP 1 binding region of exon 1 that results in reduced MOR-1 gene expression. **(B)** CXB-7/ByJ mice also possess a polymorphism at position 65, in which a T allele replaces the canonical C allele. Transcription factor databases predict that this polymorphism is located within an enhancer-box motif transcription-binding site within exon 13.

A

Alters SP1 binding, reducing MOR-1 expression in CXB-7 mice

B

Alters E-Box motif in CXB-7 mice

3.3.2. Functionality via cyclic AMP assay

Next, we sought to determine if the T allele altered functionality of the MOR-1K receptor. Previous studies have shown that MOR-1K is coupled to the Gs protein and cells transfected with the receptor maintain cAMP levels following morphine administration (65,162). Thus, we used cAMP levels a measure of functional output. To determine potential functionality of the T allele, HEK293 cells were transduced with the pAAV2-ZsGreen virus containing empty vector, the canonical MOR-1K cDNA (MOR-1K C), or the SNP-containing MOR-1K cDNA (MOR-1K T). As a control, another set of cells were transfected with MOR-1 cDNA. Following transduction or transfection, cells were treated with varying concentrations of morphine and cAMP levels were measured. We found that, when compared to empty vector, cells transfected with MOR-1 cDNA exhibited a dose-dependent decrease in cAMP levels following morphine treatment. In contrast, cells transduced with either MOR-1K C or MOR-1K T cDNA exhibited a dose-dependent increase in cAMP levels following morphine treatment (Figure 3.2).

Figure 3.2. Cells expressing MOR-1K demonstrate increased cAMP levels following morphine treatment. . HEK 293 cells expressing MOR-1, MOR-1K C, MOR-1K T, or empty vector were treated with varying concentrations of morphine or vehicle and cAMP levels were measured. When compared to cells expressing empty vector, cells expressing MOR-1 demonstrated a dose-dependent decrease in cAMP levels. In contrast, cells expressing either MOR-1K C or MOR-1K T demonstrated a dose-dependent increase in cAMP levels. There was no significant difference found between the two MOR-1K groups. Data shown as mean ± SEM. N=2 in triplicate.

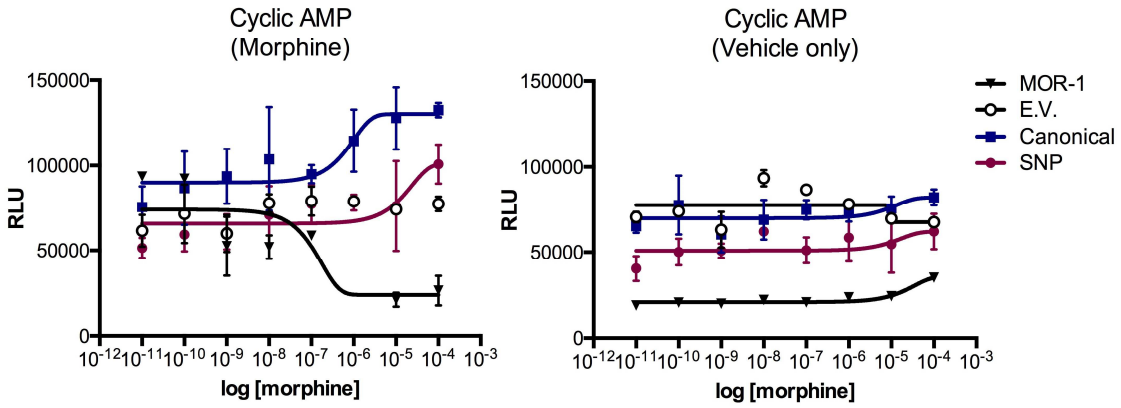
Cyclic AMP
(Morphine)
RLU
150000
100000
50000
0
10-12 10-11 10-10 10-9 10-8 10-7 10-6 10-5 10-4 10-3
log [morphine]
Cyclic AMP
(Vehicle only)
RLU
150000
100000
50000
0
10-12 10-11 10-10 10-9 10-8 10-7 10-6 10-5 10-4 10-3
log [morphine]
MOR-1
E.V.
Canonical
SNP

3.4. Conclusion

Here, we examined the genetic sequences of C57BL/6J, 129S6, and CXB7/ByJ mice for strain-specific polymorphisms. We identified two polymorphisms, specifically in CXB7/ByJ mice. One of the polymorphisms was a previously discovered SNP located in exon 1, and was associated with reduced SP1 binding, resulting in decreased MOR-1 gene expression. The second polymorphism was an unknown SNP located in exon 13. Transcription factor bioinformatic databases indicated that the exon 13 SNP was located in E-box motif site, a regulatory sequence capable of impacting pain and opioid receptor function. In order to determine if this SNP was functional, we sought to determine if the MOR-1K SNP variant would alter cAMP levels. Subsequent assays revealed that cells transduced with the canonical or the SNP containing MOR-1K cDNA demonstrated increased cAMP levels, with no significant differences between the two groups.

It is of interest that *rs824199* is also present in C57BL/6J mice. This strain also demonstrated morphine induced hyperalgesia, but also demonstrated morphine analgesia. The fact that C57Bl/6J and CXB/ByJ mice exhibit different morphine-induced behavioral profiles while expressing the same polymorphism suggests C57BL/6J mice may have genetic compensatory mechanisms to maintain normal levels of MOR-1 expression. Such compensatory features could be expressed in intronic or non-coding regions of the *OPRM1* gene. Full genomic sequencing of *OPRM1* gene from the three strains would allow for a more thorough investigation of genetic polymorphism that impact MOR-1 expression.

Along with *rs824199*, our study found a previously unidentified SNP within exon 13 of OPRM1 gene. This finding resembles the identification of *rs563649* in the human OPRM1 gene. Specifically, Shabalina and colleagues found that *rs563649*, also located with exon 13, was associated with increased pain sensitivity and blunted morphine efficacy in healthy individuals (128). The study also demonstrated that the polymorphism did not alter opioid receptor structure, but altered transcriptional regulation of the splice variant MOR-1K. Given the similar location of the

polymorphism in the OPRM1 gene, we sought to determine if the murine exon 13 SNP also had a functional impact on opioid analgesia as well.

Although the MOR-1K SNP does not appear to alter cAMP function, it may still affect transcriptional regulation of MOR-1K receptor. In order to assess if the MOR-1K SNP alters transcriptional regulation, a luciferase assay may be utilized. Here, 5' regions upstream of the MOR-1K promoter, containing the canonical C allele or T allele, will be inserted into luciferase vectors and transfected into HEK293 cells. Transfected cells will be treated with morphine or vehicle, then assessed for differences in luminescence. The results of this study will inform if altered transcriptional regulation contributes to the CXB7/ByJ strain's morphine-induced pain sensitivity.

CHAPTER 4: Discussion

5.1. The importance of alternative splicing in pain

Pain is a multidimensional system designed to protect organisms from harmful and dangerous environmental stimuli. Acute pain allows us not only to quickly respond to a noxious stimuli but also to learn to avoid such stimuli in the future, thus aiding in the adaptive learning process. Chronic pain, however, is maladaptive, persisting in the absence of noxious stimuli and interfering with normal homeostasis. For both categories of pain, it is important to understand the mechanisms for both types of pain in order to enhance our knowledge and provide solutions.

G-protein coupled receptors (GPCRs) are key in pain transmission, regulation, and modulation. It is evidenced by the large amount of pharmacologic agents that directly target GPCRs for pain management. Because of this, a majority of pharmacologic agents used in acute and chronic pain treatment specifically target key GPCR families, including cannabinoid receptors, serotonergic receptors, alpha and beta adrenergic receptors, and opioid receptors. Although many of these drugs are considered clinical treatment standards, they are not without their faults; these drugs produce unwanted side effects and vary in efficacy depending of the individual patient. These unwanted results are partially due to unintended activation of GPCR splice variants. In order to develop enhanced treatments that provide better outcomes, it is essential to acknowledge that the alternative splice variants of these GPCR also contribute to pain management as well.

Alternative splicing is a regulated genetic process in which a single gene can produce multiple distinct proteins. These proteins can be the result of exon skipping, 3’ or 5’ splice site

insertions, or intron retention. Alternative splicing greatly adds to the diversity of GPCRs by producing functional GPCR splice variants, especially those involved in pain transmission and modulation. The resulting receptors can have a variety of downstream consequences that can aid or attenuate analgesic treatments. An example showcasing the unforeseen impact of GPCR alternative splice variants on pain management is the role of MOR-1K in the development of opioid-induced hyperalgesia.

5.2. Opioid induced hyperalgesia and MOR-1K

Opioids are the most frequently used treatment for acute and chronic pain management. Unfortunately, opioid analgesia is coupled with unwanted side effects such as tolerance, respiratory depression, and addiction. Another unwanted side effect is the paradoxical increase in pain sensitivity known as opioid induced hyperalgesia (OIH). Preclinical research investigating OIH has shown that the disorder is due peripheral and spinal sensitization. Specifically, sustained opioid administration in rodents is associated to increased NMDA receptor activity, decreased glutamate reuptake, and increased glutamate release. Chronic opioid administration also evokes increased inputs from the descending facilitation system that results in increased spinal dynorphin levels. The culmination of these molecular changes lead to increase firing in pro-nociceptive neurons, leading to increased pain transmission and pain perception.

Although the aforementioned mechanisms are key in producing OIH, it is still unclear which receptor is needed to initiate OIH. Given that opioids produce OIH, a mu opioid receptor/ a receptor activated by opioid binding and that also utilizes a excitatory signaling pathway is critical to drive OIH. For this reason, the alternative splice variant MOR-1K is very likely to be possible initiator of OIH.

The splice variant MOR-1K is thought to play a role in OIH due to its genetic association to pain and its signaling profile. When investigating associations between pain and human mu opioid

related genes, Shabalina et al identified SNP *rs563649* within exon 13 in *OPRM1* transcript. Specifically, the authors found that individuals with this polymorphism exhibited higher pain sensitivity and blunted morphine efficacy (128). The study also showed that the SNP increased transcription of its splice variant, MOR-1K. A subsequent cellular study demonstrated that MOR-1K utilizes a excitatory signaling system. Cells transfected with MOR-1K did not reduce cAMP levels, increased intracellular calcium levels and in bound to the excitatory Gs protein(65).

Given its genetic association to pain and its signaling profile, we next sought to determine if MOR-1K contributed to OIH in a genetic-dependent manner. To accomplish this, we used genetically diverse mouse strains: C57BL/6J, a common inbred strain; 129S6, a mouse strain resistant to opioid tolerance; and CXB7/ByJ, a mouse strain with reduced MOR-1 gene expression. Baseline assessment revealed that the strains had divergent pain response, such that 129S6 was the most pain resistant while CXB7 mice were the most pain sensitive.

During chronic morphine administration, strains again demonstrated divergent pain responses to mechanical and thermal heat stimuli. C57BL/6J mice demonstrated increased morphine analgesia that was followed by increased pain sensitivity. 12S6 mice also demonstrated increased analgesia, but failed to develop any pain sensitivity. In contrast, CXB7/ByJ mice exclusively demonstrated increased pain sensitivity following morphine administration. The strains' MOR-1K gene expression also corresponded with their pain profiles. The pain-resistant 129S6 mice demonstrated decreased MOR-1K gene expression during morphine administration while the pain sensitive CXB7/ByJ mice demonstrated increased MOR-1K gene expression. It is important to note that this is a morphine-dependent effect, as the strains' gene expression levels returned to their respective baseline levels on day 5.

To further establish MOR-1K in OIH, we sought to determine the effects of MOR-1K gene knockdown in the pain sensitive CXB7/ByJ mice. MOR-1K gene knockdown was achieved via

chronic administration of exon 13 antisense siRNA. Sustained antisense siRNA administration not only hindered the development of morphine-induced hyperalgesia in CXB7/ByJ mice, but also unmasked morphine analgesia that was previously absent.

5.4. The impact of murine MOR-1K polymorphisms on functionality

The strain–specific behavioral and genetic divergences observed in chapter 3 lead us to inquire if these differences could be due to underlying genetic polymorphism. In order to test this hypothesis, we first sought to determine if there were an genetic polymorphisms between C57BL/6J, 129S6, and CXB7/ByJ mice. Sequencing of the strains' *OPRM1* mRNA transcripts revealed two SNP in CXB7/ByJ mice. The first SNP, identified as *rs8241991,* has been shown to reduced SP1 binding in exon 1, resulting in reduced MOR-1 gene expression(138).

The second SNP discovered is a previously unknown C to T nucleotide change within exon 13. Given that exon 13 is distinct to MOR-1K, we next sought to determine if the presence of the exon 13 SNP would have a functional consequence. Utilizing transcription factor binding site databases, we found that the exon 13 SNP is located in an E-box regulatory motif sequence, a binding site for many transcription factors including HIF-1. Given the implications of HIF-1 in pain and inflammation, it is possible that changes in the exon 13 E-box site may impact MOR-1K receptor function.

In order to assess if the exon 13 SNP alters MOR-1K receptor activity, we assessed for changes in the cAMP levels of cells transduced with virus containing either the canonical MOR-1K transcript or the exon 13 SNP transcript following chronic morphine administration. We found that cells transduced with either variant of MOR-1K demonstrated a dose-dependent increase in cAMP levels but without significant differences within the two groups. Although no differences we found in cAMP levels, it is still possible that the exon 13 SNP may impact functionality in another fashion. Future experiments should focus examining if the SNP alters transcriptional regulation via a luciferase assay.

5.5. Future Directions

The culmination of the presented work has cemented a foundation for the role of MOR-1K in the OIH development, and highlights the importance of GPCR alternative splice variants in pain management. Although the presented work provides a breadth of information about the splice variant MOR-1K, there is still much to learn in order to effectively combat opioid-induced hyperalgesia. For example, the work presented only studied animals received morphine in the absence of any injury or insult. This is contrary to what occurs clinically; those who are at risk of developing OIH take opioids because they suffer from acute or chronic pain. In order for the results to be more applicable to the clinical presentation of OIH, future preclinical investigations of OIH need to done within injury models.

Second, it is necessary to better define MOR-1K's signaling pathway. Gris et al have shown that BE2C cells transfected with MOR-1K bind to G_S protein and are expressed intracellularly. One question that has yet to be answered is if MOR-1K signaling occurs intracellularly or at the membrane. Recent evidence from the Diatchenko lab suggests that MOR-1K may heterodimerize with another receptor in order to signal at the plasma membrane. Samoshkin et al have shown that MOR-1K forms a heterodimer with the beta 2-adrenergic receptor following morphine administration(163). Dever et al have also shown that cells co-transfected with MOR-1K and filamin A, a cytoskeletal protein, express the splice variant at the cell surface. These studies clearly show heterodimerization is necessary for MOR-1K movement to the plasma membrane. Future studies need to focus on demonstrating MOR-1K heterodimerization in mammalian tissue or *in vivo.*

Future experiments also need to examine the relationship/interactions/duality between MOR-1 and MOR-1K signaling. Given that opioids bind to both receptors, it is intriguing that OIH can develop with MOR-1 stimulation. It is essential to determine what happens to MOR-1 receptor availability and signaling during OIH and why MOR-1-induced analgesia does not balance out OIH. A recent study from the Taylor lab may shed some light as to way MOR-1 activation is not enough to

quell OIH. Corder and colleagues have shown MOR-1 remains constitutively active long after exposure to the initial injury (164). Blocking of this activity with naloxone increased pain sensitivity, suggesting that there is a delicate balance between lingering pronociceptive signaling and analgesia produced by MOR-1 constitutive activity. Given that opioid administration induces MOR-1 intracellular translocation (165), it may be possible that an imbalance occurs with reduce MOR-1 expression. This imbalance, combined with previously existing pronociceptive signaling and new MOR-1K signaling, may lead to the development of OIH in post-surgical patients (acute injury) and chronic pain patients (chronic injury).

In line with examining MOR-1K signaling, it is also important to determine if all or specific opioids produce OIH. Thus far, morphine, DAMGO, fentanyl, sufentanil, remifentanil, and methadone have been shown to produce OIH in experimental or clinical settings (166). IBNtxA, a promising new analgesic that doesn't produce respiratory depression, constipation, withdrawal, or addiction, also produces OIH(163). In order to develop more promising opioid therapeutics, it is essential to keep all the unwanted opioid side effect in mind. The data within the present work supports this goal and will inform the development of more rational treatment strategies that alleviate clinical pain while reducing OIH risk.

APPENDIX 2.A.: A Preliminary Study Investigating Virally Mediated MOR-1K Overexpression in 129S6 Mice.

Introduction

In Chapter 2, we found that genetically diverse strains of mice demonstrated divergent behavioral responses and *MOR-1K* gene expression following chronic morphine administration. In particular, we found that the 129S6 strain was the most pain resistant, exhibiting morphine analgesia alongside decreased *MOR-1K* transcript levels. In contrast, the CXB7/ByJ strain was the most pain-sensitive, exclusively exhibiting morphine-induced hyperalgesia alongside increased *MOR-1K* transcript levels. Furthermore, we found that sustained intrathecal administration of antisense exon 13 siRNA prevented the development of morphine-induced hyperalgesia in the pain sensitive CXB7/ByJ mice. As a complement to the siRNA experiment, we next sought to determine if MOR-1K gene over-expression would facilitate the development of OIH in the pain-resistant 129S6 strain. The results from preliminary group of 129S6 suggest the virally directed MOR-1K overexpression produces morphine-induced hyperalgesia. Additionally, mice overexpressing MOR-1K demonstrated morphine-induced increases in glial reactivity and neuronal activation.

Methods and Materials

Ethical Statement

All procedures within this study were approved by the Duke University Institutional Animal Care and Use Committee (protocol number: A010-16-01) and adhered to the guidelines of the Committee for Research and Ethical Issues of the International Association of the Study of Pain (http://www.iasp-pain.org/Education/Content.aspx?ItemNumber=1217). All surgeries were performed under isofluorane anesthesia, and all efforts were made to minimize suffering.

Animals

Male and female 129S6 (http://www.taconic.com/129SVE) mice were obtained from Taconic (Germantown, NY). All mice were 8 -12 weeks old, weighed 20-30 g, were maintained under 12-hour light/dark cycle, and were fed *ad libitum.*

Drugs and Chemicals

Morphine sulfate (Sigma, MO) was dissolved in 0.9% sterile saline (Hospira, IL). Doses of 10 mg/kg, 20 mg/kg, or 40 mg/kg were administered *via* subcutaneous (s.c.) injection in a volume determined by animal weight (1µl/g). A pAAV2-ZsGreen viral vector containing canonical MOR-1K plasmid DNA or MOR-1K plasmid cDNA containing an exon 13 SNP (Biowit Technologies, Shenzhen, China) was administered i.t. via direct injection.

Experimental Design

The effects of MOR-1K over-expression on the development of OIH 129S6 mice.

Prior to chronic morphine administration, 129S6 mice (N=7; 3 males and 4 females) were assessed for baseline responses to mechanical and thermal heat stimuli. Following baseline assessments, mice underwent isoflurane anesthesia to receive direct i.t. injection of pAAV2-ZsGreen viral vector, viral vector containing canonical MOR-1K plasmid cDNA, or viral vector containing exon 13 SNP MOR-1K plasmid cDNA. Mice were anesthetized with 5% isofluorane and maintained at 2-3% isofluorane. One mouse did not receive direct injection of any substance. Two weeks were allowed for proper viral transduction into the spinal cord and dorsal root ganglion. Two weeks following initial direct injection, all mice were re-assessed for responses to mechanical and thermal heat stimuli. Following baseline assessment, mice began to receive escalating doses of morphine on days 1-4 as described above. Separate groups of 129S6 mice ((N=5; 3 males and 2 females)) were sacrificed on day 4 following the 8am injection. The experimental design is illustrated in Figure A2.A.1.

Figure A2.A.1. Timeline of the preliminary 129S6-MOR-1K overexpression experiment.

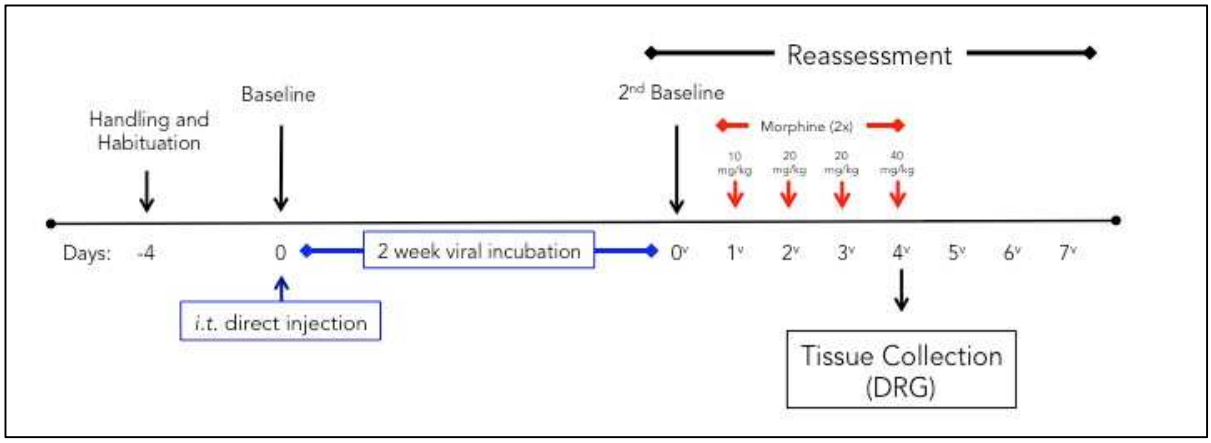
Reassessment
Handling and Habituation
Baseline
2nd Baseline
Morphine (2x)
10 mg/kg
20 mg/kg
20 mg/kg
40 mg/kg
Days: -4
0
2 week viral incubation
0v
1v
2v
3v
4v
5v
6v
7v
i.t. direct injection
Tissue Collection (DRG)

Behavior

Assessment of Paw Withdrawal Threshold, Mechanical Allodynia, and Mechanical Hyperalgesia

Mice were handled and habituated to the testing environment for 4 days prior to baseline assessments. On test days, mice were placed in plexiglass cages positioned over an elevated wire mesh platform and habituated to the environment for 20 minutes. Paw withdrawal threshold in response to a series of 9 von Frey filaments (with bending forces of 0.03, 0.07, 0.17, 0.40, 0.70, 1.19, 1.50, 2.05, 3.63g; Stoeling, IL) was assessed using the "up-down" method (135), starting with a filament with bending force of 0.70 g. In the absence of a paw withdrawal response, an incrementally stronger filament was presented and in the event of a paw withdrawal, an incrementally weaker filament was presented. After the initial response threshold was crossed, this procedure was repeated in order to obtain a total of six responses in the immediate vicinity of the threshold. The pattern of withdrawals and absence of withdrawals were noted together with the terminal filament used in the series of six responses. The 50% of the paw withdrawal threshold is calculated as $(10^{[X_f+k\delta]})/10{,}000$, where X_f = value (in log units) of the final von Frey hair used; k = tabular value of pattern of positive (X) and negative (O) responses, and δ = mean difference (in log units) between stimuli. Mechanical allodynia was assessed by presenting a filament with bending force of 0.40 g to the hind paw 10 times for a duration of 1 s with an inter-stimulus interval of 1 s. A significant increase in the percentage frequency of paw withdrawal ([# of paw withdrawals/10] x 100) was defined as mechanical allodynia. Mechanical hyperalgesia was assessed in the same manner, using a filament with a bending force of 1.50 g.

Assessment of Thermal Heat Hyperalgesia

Thermal heat hyperalgesia was evaluated using the hot plate method (136). Mice were placed on a hot plate (Columbus Instruments, OH) maintained at a temperature of 51.5°C for one minute. Each session was videotaped and the total number of aversive responses (paw licks, paw flicks, and jumps) was measured.

Results

pAAV2-Zsgreen is expressed in DRG

Prior to conducting experiments, it was necessary to first establish that pAAV2-ZsGreen virus penetrated mouse spinal tissue. 129S6 mice were given a direct injection of pAAV2-Zsgreen empty vector to validate viral expression. Following two weeks, we found that the virus was robustly expressed in the DRG (Figure A2.A.2). With this information, we decided to proceed and examine if virally mediated MOR-1K overexpression would induce morphine-induced hyperalgesia in 129S6 mice.

Figure A2.A.2. pAAV2-ZsGreen is expressed in 129S6 mouse dorsal root ganglion. Following isoflurane anesthesia, 129S6 mice received an i.t. direct injection of 10uL of pAAV2-ZsGrean at L5 of the spinal cord. The image was taken at 20X magnification.

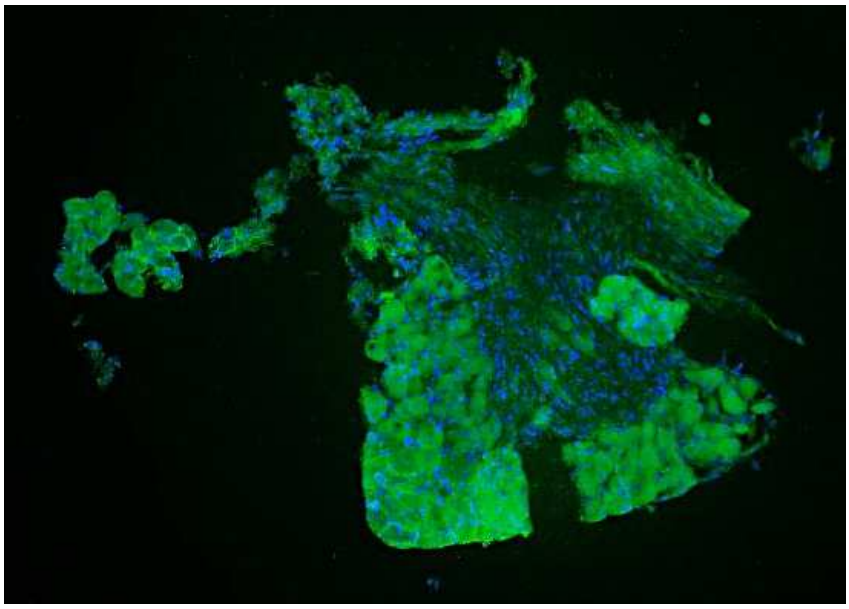

Viral vector mediated MOR-1K overexpression facilitates morphine-induced hyperalgesia

We assessed behavioral responses to mechanical and thermal heat stimuli on prior to and two weeks following *i.t.* direct injection, on days 1-4 during chronic morphine administration, and after morphine cessation on days 5-7 When compared to mice that received empty vector or were untreated, 129S6 mice that received either form of pAAV2-MOR-1K demonstrated decreased paw withdrawal threshold to mechanical stimuli (Figure A2.A.3A) starting on day 1 prior to morphine administration and continuing on day 2, 3, and 4 prior to morphine administration and following morphine cessation. Acutely following morphine administration, 129S6 mice exhibited morphine analgesia regardless of the treatment condition. It is interesting to note that mice that received the MOR-1K T variant exhibited reduced morphine analgesia on day 2, 3, and 4. 129S6 mice that received either form of pAAV2-MOR-1K also exhibited increased responses to a mechanical innocuous stimulus and a mechanical noxious stimulus prior to morphine administration (Figure A2.A.3B-C). These mice also demonstrated increased pain sensitivity to thermal heat stimuli prior to morphine administration (Figure A2.A.3D). Again, it is of note that 129S6 mice that received the MOR-1K T variant exhibited reduced morphine analgesia on days 2, 3, and 4 when assessing for mechanical allodynia and mechanical hyperalgesia.

Figure A2.A.3. Raw data illustrating behavioral responses of pAAV2-MOR1K 129S6 mice to mechanical and thermal heat stimuli during chronic morphine administration. When compared to mice that received empty vector or no vector, mice that received MOR-1K containing virus demonstrated **(A)** decreased mechanical paw withdrawal threshold **(B)** increased mechanical allodynia, **(C)** increased mechanical hyperalgesia and **(D)** thermal heat hyperalgesia following chronic morphine administration. Panels A-D: *N*=1-2/group. Data expressed as mean ± SEM.

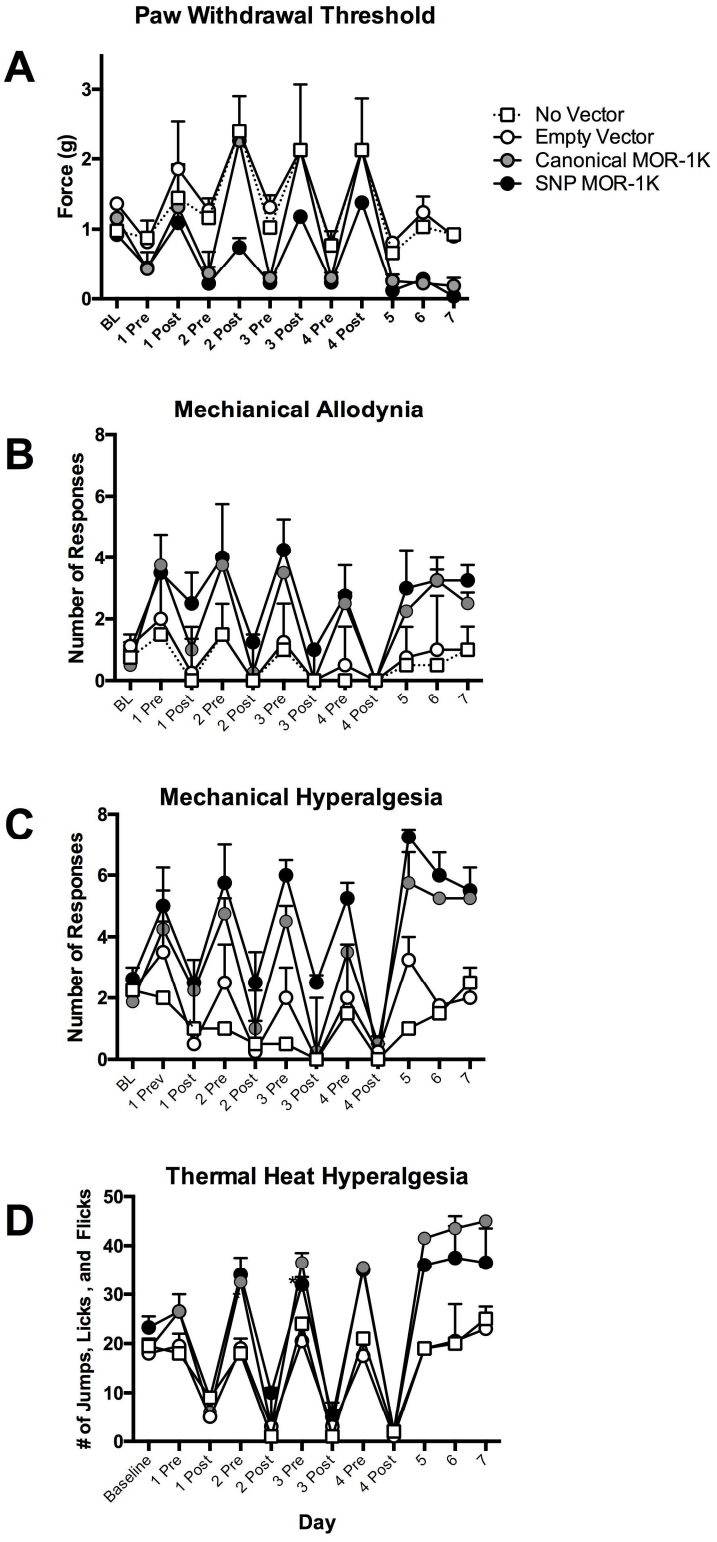
A
Paw Withdrawal Threshold
Force (g)
No Vector
Empty Vector
Canonical MOR-1K
SNP MOR-1K
B
Mechianical Allodynia
Number of Responses
C
Mechanical Hyperalgesia
Number of Responses
D
Thermal Heat Hyperalgesia
# of Jumps, Licks , and Flicks
Day
BL
1 Pre
1 Post
2 Pre
2 Post
3 Pre
3 Post
4 Pre
4 Post
5
6
7
1 Prev
Baseline

Conclusions

Here, in this preliminary study, we provide evidence that virally mediated overexpression of MOR-1K in 129S6 mice may produce morphine-induced hyperalgesia. Specifically, we show that 129S6 mice that received direct i.t. injection of pAAV2 containing either canonical MOR-1K cDNA or SNP MOR-1K cDNA exhibited decreased mechanical paw withdrawal threshold, increased allodynia and hyperalgesia to mechanical stimuli, and increased hyperalgesia to thermal stimuli. To validate the findings in this preliminary study, the existing behavioral groups need to be expanded and a separate behavioral group, in which mice are treated with vehicle, needs to be added as well.

APPENDIX 2.B.: MOR-1K Localization using RNAscope® In Situ Hybridization

Introduction

In order to better understand how MOR-1K signaling contributes to OIH, it is necessary to first establish which cell types express the receptor. Here, we use in situ hybridization, in conjunction with immunohistochemistry, to identify where MOR-1K mRNA is expressed.

Methods and Materials

DRG samples were collected from 129S6 mice following cardiac perfusion with cold 0.1M PBS and 4% paraformaldehyde. Tissues were post-fixed overnight in 4% paraformaldehyde, then cryoprotected sequentially in 10% sucrose/0.1M PBS, 20% sucrose/0.1M PBS, and 30% sucrose/0.1M PBS for 24hrs in each solution at 4°C. The cryoprotected samples were set in Tissue-Tek O.C.T. Compound (Sakura Finetek USA, CA), rapidly frozen in an ethanol/dry ice bath and stored in -80°. Transverse sections (10 μm) were cut using a Microm HM 550 cryostat (Thermo Fisher Scientific, MA) at. The following sections were placed on Superfrost Plus slides (Thermo Fisher Scientific, MA) and stored in -80C. Sections were pretreated and probed for positive control (Mm-Ppib), negative control (negative control probe_dapB), MOR-1K (Mm-Oprm1-MOR-1L-O1), or TRPV1 (Mm-Trpv1) as per the manufacturer's protocol (Advanced Cell Diagnostics, CA). Following in situ hybridization, sections were rinsed in 0.01M PBS, then incubated for 30min in PBS-T. Sections were blocked in PBS-T containing 5% serum for 30 min, then immunolabeled using a primary antibody overnight. Primary antibody mouse monoclonal S100 (1:200, Abcam, MA) was used to stain for satellite glial cells. After several rinses in PBS-T, sections were incubated in biotinylated goat anti-mouse secondary antibody (Vector Laboratories, CA) for 2hrs. Sections were rinsed several times with PBS-T, and then incubated in VECASTAIN Elite Avidin-Biotin Complex solution (Vector Laboratories, CA) for 2hrs. Sections were rinsed in PBS-T, then incubated in ImmPACT SG Peroxidase HRP Substrate (Vector Laboratories, CA) to stain sections blue-gray.

Following several rinses in PBS-T, sections were dried at 60°C for 15 minutes and dipped in xylene. Coverslips were mounted to slides using EcoMount mounting medium (Biocare Medical, CA).

Results

Validation of RNAscope® Positive and Negative Controls

Positive and negative control probes provided by the manufacturer were used to ensure that the protocol was performed appropriately. With the successful staining with the positive and negative controls (Figure A2.B.1), we next stained for MOR-1K and TRPV1 RNA.

Figure A2.B.1. Positive and negative control expression in mouse dorsal root ganglion. DRG was treated with the **(A)** positive control probe, or **(B)** the negative control probe. The image was taken at 20x magnification.

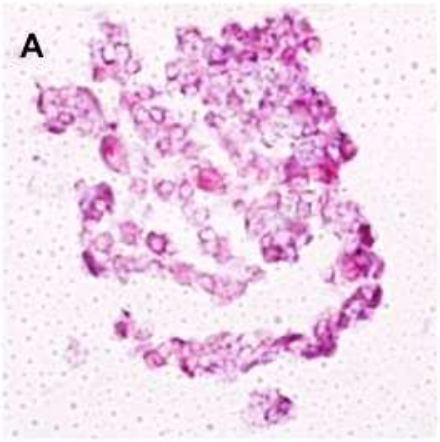
A

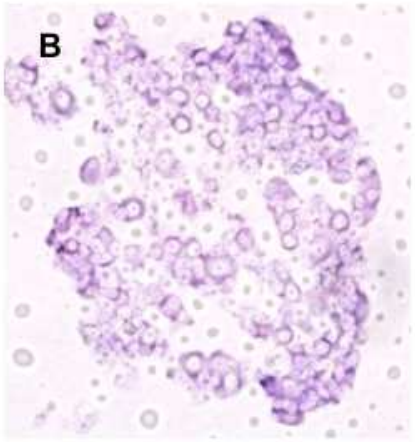
B

MOR-1K RNA expression co-localizes with S100 expression

Initial staining of DRG with MOR-1K RNA probe revealed a delicate, ring like expression surrounding cell bodies in the tissues (Figure A2.B.2). Subsequent histological investigations suggested the observed expression was similar to that of satellite glial cells (SGCs)(167). To confirm that MOR-1K RNA was expressed in SGCs, tissues were first treated with MOR-1K probe, then stained for S100, a marker of SGCs. Visualization of tissues incubated with both the MOR-1K probe and S100 demonstrated co-localization (Figure A2.B.3), suggesting that MOR-1K RNA is expressed in SGCs.

Figure A2.B.2. MOR-1K RNA expression in mouse dorsal root ganglion. Mouse DRG tissue was treated with MOR-1K RNA probe and counterstained with hematoxylin. The image was taken at 20x and 40x magnification.

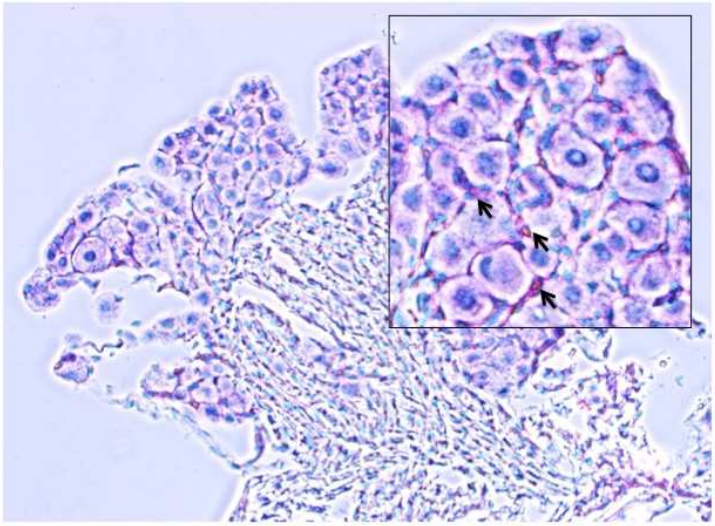

Figure A2.B.3. MOR-1K RNA expression co-localizes with S100 expression. Mouse DRG tissue was incubated with MOR-1K RNA probe and S100 antibody. The image was taken at 20x and 40x magnification.

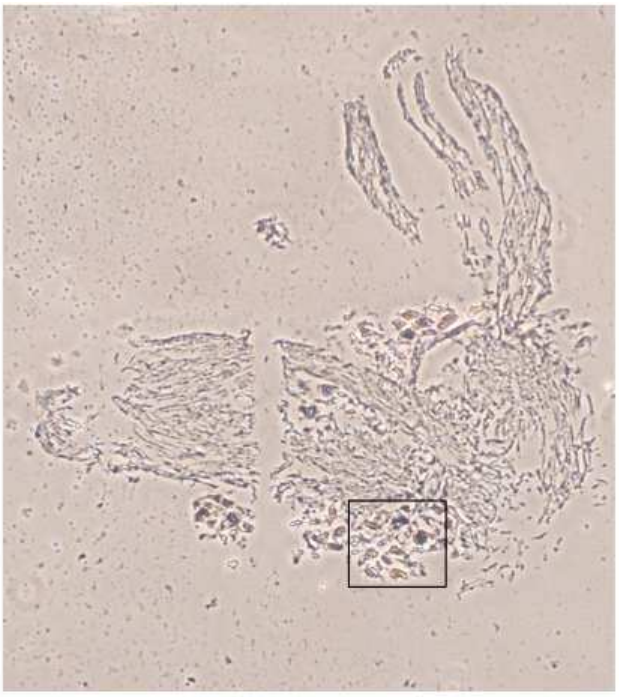

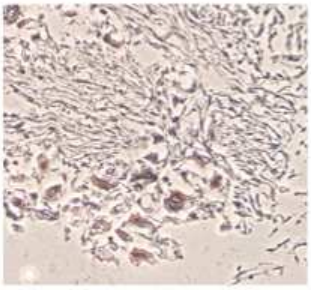

MOR-1K

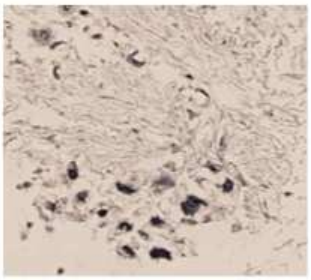

S100

Figure A2.B.4. MOR-1K RNA expression in mouse dorsal root ganglion. Mouse DRG tissue was treated with MOR-1K RNA probe and counterstained with hematoxylin. The image was taken at 20X magnification.

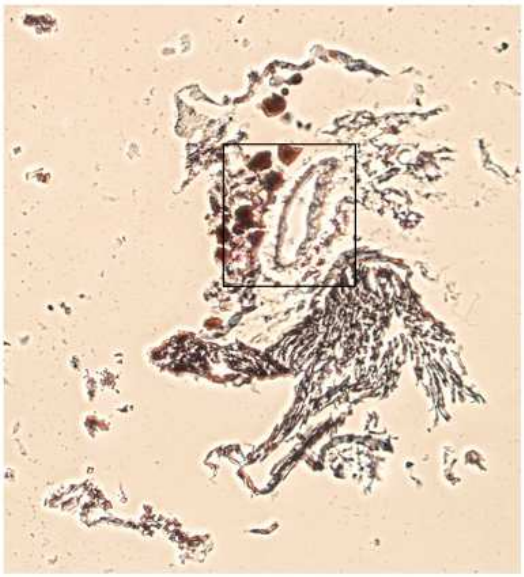

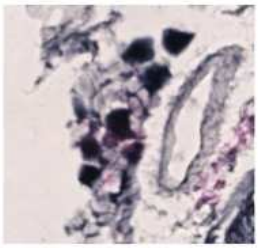

TRPV1

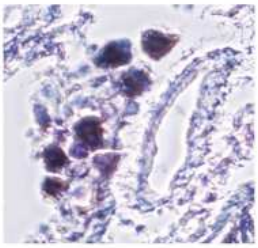

S100

Conclusions

Here, we demonstrate that MOR-1K RNA is expressed in satellite glial cells in DRG. Future research needs to expand MOR-1K localization and examine MOR-1K RNA expression in the spinal cord and in discrete brain regions.

REFERENCES

1. Woolf CJ. Pain: Moving from Symptom Control toward Mechanism-Specific Pharmacologic Management. Ann Intern Med. American College of Physicians; 2004 Mar 16;140(6):441–51.

2. Muley MM, Krustev E, McDougall JJ. Preclinical Assessment of Inflammatory Pain. Munro G, editor. CNS Neurosci Ther. 2016 Feb;22(2):88–101.

3. Campbell JN, Meyer RA. Mechanisms of Neuropathic Pain. Neuron. 2006 Oct;52(1):77–92.

4. Diatchenko L, Nackley AG, Slade GD, Fillingim RB, Maixner W. Idiopathic pain disorders--pathways of vulnerability. Pain. 2006 Aug;123(3):226–30.

5. Fields HL. Mu Opioid Receptor Mediated Analgesia and Reward. In: The Opiate Receptors. Totowa, NJ: Humana Press; 2011. pp. 239–64.

6. McDonald DC, Carlson K, Izrael D. Geographic Variation in Opioid Prescribing in the U.S. The Journal of Pain. 2012 Oct;13(10):988–96.

7. Connor M, Christie MJ. Opioid Receptor Signaling Mechanisms. Clin Exp Pharmacol Physiol. 1999 Jul;26(7):493–9.

8. Arvidsson U, Riedl M, Chakrabarti S, Lee JH, Nakano AH, Dado RJ, et al. Distribution and targeting of a mu-opioid receptor (MOR1) in brain and spinal cord. J Neurosci. 1995 May;15(5 Pt 1):3328–41.

9. Peckys D, Landwehrmeyer GB. Expression of mu, kappa, and delta opioid receptor messenger RNA in the human CNS: a 33P in situ hybridization study. NSC. 1999;88(4):1093–135.

10. Stiene-Martin A, Zhou R, Hauser KF. Regional, developmental, and cell cycle-dependent differences in mu, delta, and kappa-opioid receptor expression among cultured mouse astrocytes. Glia. 1998 Mar;22(3):249–59.

11. Chao CC, Hu S, Shark KB, Sheng WS, Gekker G, Peterson PK. Activation of Mu Opioid Receptors Inhibits Microglial Cell Chemotaxis. … of Pharmacology and …. 1997.

12. McCarthy L, Szabo I, Nitsche JF, Pintar JE, Rogers TJ. Expression of functional mu-opioid receptors during T cell development. J Neuroimmunol. 2001 Mar 1;114(1-2):173–80.

13. Börner C, Stumm R, Höllt V, Kraus J. Comparative analysis of mu-opioid receptor expression in immune and neuronal cells. J Neuroimmunol. 2007 Aug;188(1-2):56–63.

14. Li Z-H, Chu N, Shan L-D, Gong S, Yin Q-Z, Jiang X-H. Inducible expression of functional mu opioid receptors in murine dendritic cells. J Neuroimmune Pharmacol. 2009 Sep;4(3):359–67.

15. Leo S, Nuydens R, Meert TF. Opioid-induced proliferation of vascular endothelial cells. J Pain Res. 2009;2:59–66.

16. Jamison RN, Mao J. Opioid Analgesics. Mayo Clin Proc. 2015 Jul;90(7):957–68.

17. Chu LF, Angst MS, Clark D. Opioid-induced Hyperalgesia in Humans: Molecular Mechanisms and Clinical Considerations. The Clinical journal of pain [Internet]. 2008;24(6):479–96. Available from: http://journals.lww.com/clinicalpain/Abstract/2008/07000/Opioid_induced_Hyperalgesia_in_Humans__Molecular.3.aspx

18. Ali NM. Hyperalgesic response in a patient receiving high concentrations of spinal morphine. Anesthesiology. 1986 Oct;65(4):449.

19. Bekhit MH. Opioid-induced hyperalgesia and tolerance. American journal of therapeutics. 2010;17(5):498.

20. Lee M, Silverman SM, Hansen H, Patel VB, Manchikanti L. A comprehensive review of opioid-induced hyperalgesia. Pain Physician. 2011 Mar;14(2):145–61.

21. Fletcher D, Martinez V. Opioid-induced hyperalgesia in patients after surgery: a systematic review and a meta-analysis. British Journal of Anaesthesia. 2014 May 14;112(6):991–1004.

22. Doverty M, White JM, Somogyi AA, Bochner F, Ali R, Ling W. Hyperalgesic responses in methadone maintenance patients. Pain. 2001 Feb 1;90(1-2):91–6.

23. Hay JL, White JM, Bochner F, Somogyi AA, Semple TJ, Rounsefell B. Hyperalgesia in opioid-managed chronic pain and opioid-dependent patients. J Pain. 2009 Mar;10(3):316–22.

24. Ackerman WE. Paroxysmal opioid-induced pain and hyperalgesia. J Ky Med Assoc. 2006 Sep;104(9):419–23.

25. Schmid CW, Maurer K, Schmid DM, Alon E, Spahn DR, Gantenbein AR, et al. Prevalence of medication overuse headache in an interdisciplinary pain clinic. J Headache Pain. 2013 Dec;14(1):4.

26. Drossman D, Szigethy E. The Narcotic Bowel Syndrome: A Recent Update. Am J Gastroenterol. 2014 Sep 10;2(1):22–30.

27. Meldrum BS. Glutamate as a neurotransmitter in the brain: review of physiology and pathology. J Nutr. 2000 Apr;130(4S Suppl):1007S–15S.

28. Sandkühler J, Gruber-Schoffnegger D. Hyperalgesia by synaptic long-term potentiation (LTP): an update. Curr Opin Pharmacol. 2012 Feb;12(1):18–27.

29. Mao J, Sung B, Ji R-R, Lim G. Chronic Morphine Induces Downregulation of Spinal Glutamate Transporters: Implications in Morphine Tolerance and Abnormal Pain Sensitivity. J Neurosci. Society for Neuroscience; 2002 Sep 15;22(18):8312–23.

30. Ohnesorge H, Feng Z, Zitta K, Steinfath M, Albrecht M, Bein B. Influence of clonidine and ketamine on m-RNA expression in a model of opioid-induced hyperalgesia in mice. PLoS ONE. 2013;8(11):e79567–11.

31. Li X, Angst MS, Clark JD. A murine model of opioid-induced hyperalgesia. Brain Res Mol Brain Res. 2001st ed. 2001 Jan 31;86(1-2):56–62.

32. Angst MS, Koppert W, Pahl I, Clark DJ, Schmelz M. Short-term infusion of the μ-opioid agonist remifentanil in humans causes hyperalgesia during withdrawal. Pain. 2003 Nov;106(1-2):49–57.

33. Koppert W, Sittl R, Scheuber K, Alsheimer M, Schmelz M, Schüttler J. Differential Modulation of Remifentanil-induced Analgesia and Postinfusion Hyperalgesia by S - Ketamine and Clonidine in Humans. Anesthesiology. The American Society of Anesthesiologists; 2003 Jul 1;99(1):152–9.

34. Vanderah T, Suenaga N. Tonic Descending Facilitation from the Rostral Ventromedial Medulla Mediates Opioid-Induced Abnormal Pain and Antinociceptive Tolerance. The Journal of …. 2001.

35. Gardell LR, Wang R, Burgess SE. Sustained morphine exposure induces a spinal dynorphin-dependent enhancement of excitatory transmitter release from primary afferent fibers. The Journal of …. 2002.

36. Vanderah TW, Gardell LR, Burgess SE, Ibrahim M, Dogrul A, Zhong CM, et al. Dynorphin promotes abnormal pain and spinal opioid antinociceptive tolerance. J Neurosci. 2000 Sep 15;20(18):7074–9.

37. Liang D-Y, Liao G, Wang J, Usuka J, Guo Y, Peltz G, et al. A genetic analysis of opioid-induced hyperalgesia in mice. Anesthesiology. 2006 May;104(5):1054–62.

38. Chu LF, Cun T, Ngai LK, Kim JE, Zamora AK, Young CA, et al. Modulation of remifentanil-induced postinfusion hyperalgesia by the β-blocker propranolol in humans. Pain. International Association for the Study of Pain; 2012 May;153(5):974–81.

39. Stone LS, Molliver DC. In Search of Analgesia: Emerging Poles of GPCRs in Pain. Mol Interv. 2009;9(5):234–51.

40. Lundstrom K. An overview on GPCRs and drug discovery: structure-based drug design and structural biology on GPCRs. Methods Mol Biol. 2009;552:51–66.

41. Matsuda LA. Molecular aspects of cannabinoid receptors. Critical reviews in neurobiology. 1997 ed. 1997;11(2-3):143–66.

42. Michelotti GA, Price DT, Schwinn DA. Alpha 1-adrenergic receptor regulation: basic science and clinical implications. Pharmacology & therapeutics. 2001st ed. 2000 Dec;88(3):281–309.

43. Summers RJ, Broxton N, Hutchinson DS, Evans BA. The Janus faces of adrenoceptors: factors controlling the coupling of adrenoceptors to multiple signal transduction pathways. Clin Exp Pharmacol Physiol. 2004 Nov;31(11):822–7.

44. Hannon J, Hoyer D. Molecular biology of 5-HT receptors. Behavioural Brain Research. 2008 Dec 16;195(1):198–213.

45. Alan North R. Opioid receptor types and membrane ion channels. Trends Neurosci. 1986 Jan;9:114–7.

46. Lynch ME, Campbell F. Cannabinoids for treatment of chronic non- cancer pain; a systematic review of randomized trials. British Journal of Clinical Pharmacology. Blackwell Publishing Ltd; 2011 Nov 1;72(5):735–44.

47. Johnston MM, Rapoport AM. Triptans for the Management of Migraine. Drugs. Springer International Publishing; 2010;70(12):1505–18.

48. Terrón JA. Is the 5-HT7 receptor involved in the pathogenesis and prophylactic treatment of migraine? European Journal of Pharmacology. 2002 Mar;439(1-3):1–11.

49. Janice J Kim WIK. 5-HT7 receptor signaling: improved therapeutic strategy in gut disorders. Frontiers in Behavioral Neuroscience. Frontiers Media SA; 2014;8:396.

50. Meuser T, Pietruck C, Gabriel A, Xie G-X, Lim K-J, Pierce Palmer P. 5-HT7 receptors are involved in mediating 5-HT-induced activation of rat primary afferent neurons. Life Sci. 2002 Sep;71(19):2279–89.

51. Rocha-González HI, Meneses A, Carlton SM, Granados-Soto V. Pronociceptive role of peripheral and spinal 5-HT7 receptors in the formalin test. Pain. 2005 Sep;117(1):182–92.

52. Li S-F, Zhang Y-Y, Li Y-Y, Wen S, Xiao Z. Antihyperalgesic effect of 5-HT7 receptor activation on the midbrain periaqueductal gray in a rat model of neuropathic pain. Pharmacol Biochem Behav. 2014 Dec;127:49–55.

53. Boudreau D, Korff Von M, Rutter CM, Saunders K, Ray GT, Sullivan MD, et al. Trends in long-term opioid therapy for chronic non-cancer pain. Pharmacoepidem Drug Safe. John Wiley & Sons, Ltd; 2009 Dec;18(12):1166–75.

54. Hutchinson MR, Zhang Y, Brown K, Coats BD, Shridhar M, Sholar PW, et al. Non-stereoselective reversal of neuropathic pain by naloxone and naltrexone: involvement of toll-like receptor 4 (TLR4). European Journal of Neuroscience. 2008 Jul;28(1):20–9.

55. Max MB, Payne RG, Edwards WT. Principles of Analgesic Use in the Treatment of Acute and Cancer Pain. 4 ed. Greenview, IL; 1999. 1 p.

56. Wang ET, Sandberg R, Luo S, Khrebtukova I, Zhang L, Mayr C, et al. Alternative isoform regulation in human tissue transcriptomes. Nature. 2008 Nov 2;456(7221):470–6.

57. Keren H, Lev-Maor G, Ast G. Alternative splicing and evolution: diversification, exon definition and function. Nat Rev Genet. 2010 May;11(5):345–55.

58. Baralle D. Splicing in action: assessing disease causing sequence changes. Journal of Medical Genetics. 2005 Oct 1;42(10):737–48.

59. Kilpatrick GJ, Dautzenberg FM, Martin GR, Eglen RM. 7TM receptors: the splicing on the cake. Trends in Pharmacological Sciences. 1999 Jul;20(7):294–301.

60. Pan Y-X, Xu J, Xu M, Rossi GC, Matulonis JE, Pasternak GW. Involvement of exon 11-associated variants of the mu opioid receptor MOR-1 in heroin, but not morphine, actions. Proceedings of the National Academy of Sciences. National Acad Sciences; 2009 Mar 24;106(12):4917–22.

61. Pasternak GW, Pan Y-X. Mu Opioids and Their Receptors: Evolution of a Concept. Pharmacol Rev. American Society for Pharmacology and Experimental Therapeutics; 2013;65(4):1257–317.

62. Sato M, Hutchinson DS, Bengtsson T, Floren A, Langel U, Horinouchi T, et al. Functional domains of the mouse beta3-adrenoceptor associated with differential G protein coupling. J Pharmacol Exp Ther. American Society for Pharmacology and Experimental Therapeutics; 2005 Dec;315(3):1354–61.

63. Boise LH, González-García M, Postema CE, Ding L, Lindsten T, Turka LA, et al. bcl-x, a bcl-2-related gene that functions as a dominant regulator of apoptotic cell death. Cell. 1993 Aug 27;74(4):597–608.

64. Cascino I, Fiucci G, Papoff G, Ruberti G. Three functional soluble forms of the human apoptosis-inducing Fas molecule are produced by alternative splicing. J Immunol. 1995 Mar 15;154(6):2706–13.

65. Gris P, Gauthier J, Cheng P, Gibson DG, Gris D, Laur O, et al. A novel alternatively spliced isoform of the mu-opioid receptor: functional antagonism. Molecular Pain. 2010;6(1):33.

66. Lipscombe D, Andrade A, Allen SE. Alternative splicing: Functional diversity among voltage-gated calcium channels and behavioral consequences. Biochimica et Biophysica Acta (BBA) - Biomembranes. 2013 Jul;1828(7):1522–9.

67. Fruhwald J, Camacho Londono J, Dembla S, Mannebach S, Lis A, Drews A, et al. Alternative Splicing of a Protein Domain Indispensable for Function of Transient Receptor Potential Melastatin 3 (TRPM3) Ion Channels. J Biol Chem. American Society for Biochemistry and Molecular Biology; 2012 Oct 26;287(44):36663–72.

68. Zhou Y, Suzuki Y, Uchida K, Tominaga M. Identification of a splice variant of mouse TRPA1 that regulates TRPA1 activity. Nat Commun. Nature Publishing Group; 2013 Sep 6;4.

69. Galiegue S, Mary S, Marchand J, Dussossoy D, Carriere D, Carayon P, et al. Expression of central and peripheral cannabinoid receptors in human immune tissues and leukocyte subpopulations. Eur J Biochem. 1995 ed. 1995 Aug 15;232(1):54–61.

70. Ryberg E, Vu HK, Larsson N, Groblewski T, Hjorth S, Elebring T, et al. Identification and characterisation of a novel splice variant of the human CB1 receptor. FEBS Lett. 2004 ed. 2005 Jan 3;579(1):259–64.

71. Shire D, Carillon C, Kaghad M, Calandra B, Rinaldi-Carmona M, Le Fur G, et al. An amino-terminal variant of the central cannabinoid receptor resulting from alternative splicing. J Biol Chem. 1995 ed. 1995 Feb 24;270(8):3726–31.

72. Cosenza-Nashat MA, Bauman A, Zhao ML, Morgello S, Suh HS, Lee SC. Cannabinoid receptor expression in HIV encephalitis and HIV-associated neuropathologic comorbidities. Neuropathology and applied neurobiology. 2011 ed. Blackwell Publishing Ltd; 2011 Aug;37(5):464–83.

73. Benito C, Nunez E, Tolon RM, Carrier EJ, Rabano A, Hillard CJ, et al. Cannabinoid CB2

receptors and fatty acid amide hydrolase are selectively overexpressed in neuritic plaque-associated glia in Alzheimer's disease brains. Journal of Neuroscience. 2003rd ed. 2003 Dec 3;23(35):11136–41.

74. Yiangou Y, Facer P, Durrenberger P, Chessell IP, Naylor A, Bountra C, et al. COX-2, CB2 and P2X7-immunoreactivities are increased in activated microglial cells/macrophages of multiple sclerosis and amyotrophic lateral sclerosis spinal cord. BMC neurology. 2006 ed. 2006;6(1):12.

75. Liu QR, Pan CH, Hishimoto A, Li CY, Xi ZX, Llorente-Berzal A, et al. Species differences in cannabinoid receptor 2 (CNR2 gene): identification of novel human and rodent CB2 isoforms, differential tissue expression and regulation by cannabinoid receptor ligands. Genes, brain, and behavior. 2009 ed. Blackwell Publishing Ltd; 2009 Jul;8(5):519–30.

76. Chang DJ, Chang TK, Yamanishi SS, Salazar FH, Kosaka AH, Khare R, et al. Molecular cloning, genomic characterization and expression of novel human alpha1A-adrenoceptor isoforms. FEBS Lett. 1998 Jan 30;422(2):279–83.

77. Price RR, Morris DP, Biswas G, Smith MP, Schwinn DA. Acute Agonist-mediated Desensitization of the Human 1a-Adrenergic Receptor Is Primarily Independent of Carboxyl Terminus Regulation: IMPLICATIONS FOR REGULATION OF 1aAR SPLICE VARIANTS. J Biol Chem. 2002 Mar 15;277(11):9570–9.

78. Coge F, Guenin SP, Renouard-Try A, Rique H, Ouvry C, Fabry N, et al. Truncated isoforms inhibit [3H]prazosin binding and cellular trafficking of native human alpha1A-adrenoceptors. Biochem J. 1999 Oct 1;343 Pt 1:231–9.

79. Daniels DV, Gever JR, Jasper JR, Kava MS, Lesnick JD, Meloy TD, et al. Human cloned α1A-adrenoceptor isoforms display α1L-adrenoceptor pharmacology in functional studies. European Journal of Pharmacology. 1999;370(3):337–43.

80. Tseng-Crank J, Kost T, Goetz A, Hazum S, Roberson KM, Haizlip J, et al. The alpha 1C-adrenoceptor in human prostate: cloning, functional expression, and localization to specific prostatic cell types. British Journal of Pharmacology. 1995 ed. 1995 Aug;115(8):1475–85.

81. Strosberg AD. Structure and function of the beta 3-adrenergic receptor. Annu Rev Pharmacol Toxicol. 1997 ed. 1997;37(1):421–50.

82. Soeder KJ, Snedden SK, Cao W, Rocca Della GJ, Daniel KW, Luttrell LM, et al. The beta3-adrenergic receptor activates mitogen-activated protein kinase in adipocytes through a Gi-dependent mechanism. J Biol Chem. 1999 ed. 1999 Apr 23;274(17):12017–22.

83. Sato M, Hutchinson DS, Evans BA, Summers RJ. Functional domains of the mouse beta(3)-adrenoceptor associated with differential G-protein coupling. Biochemical Society transactions. 2007 ed. 2007 Nov;35(Pt 5):1035–7.

84. Kanno T, Yaguchi T, Nishizaki T. Noradrenaline stimulates ATP release from DRG neurons by targeting beta(3) adrenoceptors as a factor of neuropathic pain. Journal of cellular physiology. 2010 ed. Wiley Subscription Services, Inc., A Wiley Company; 2010 Aug;224(2):345–51.

85. Evans BA, Papaioannou M, Hamilton S, Summers RJ. Alternative splicing generates two isoforms of the beta3-adrenoceptor which are differentially expressed in mouse tissues. British Journal of Pharmacology. Blackwell Publishing Ltd; 1999 Jul;127(6):1525–31.

86. Guest, P. C., Salim K, Skynner HA, George SE, Bresnick JN, McAllister G. Identification and characterization of a truncated variant of the 5-hydroxytryptamine(2A) receptor produced by alternative splicing. Brain Res. 2000 Sep 8;876(1-2):238–44.

87. Canton H, Emeson RB, Barker EL, Backstrom JR, Lu JT, Chang MS, et al. Identification, molecular cloning, and distribution of a short variant of the 5-hydroxytryptamine2C receptor produced by alternative splicing. Mol Pharmacol. 1996 Oct;50(4):799–807.

88. Wang Q, O'Brien PJ, Chen CX, Cho DS, Murray JM, Nishikura K. Altered G protein-coupling functions of RNA editing isoform and splicing variant serotonin2C receptors. J Neurochem. 2000 Mar;74(3):1290–300.

89. Blondel O, Gastineau M, Dahmoune Y, Langlois M, Fischmeister R. Cloning, expression, and pharmacology of four human 5-hydroxytryptamine 4 receptor isoforms produced by alternative splicing in the carboxyl terminus. J Neurochem. 1998 Jun;70(6):2252–61.

90. Pindon A, van Hecke G, van Gompel P, Lesage AS, Leysen JE, Jurzak M. Differences in signal transduction of two 5-HT4 receptor splice variants: compound specificity and dual coupling with Galphas- and Galphai/o-proteins. Mol Pharmacol. 2001st ed. 2002 Jan;61(1):85–96.

91. Claeysen S, Faye P, Sebben M, Taviaux S, Bockaert J, Dumuis A. 5-HT4 receptors: cloning and expression of new splice variants. Annals of the New York Academy of Sciences. 1999 ed. 1998 Dec 15;861:49–56.

92. Bender E, Pindon A, van Oers I, Zhang YB, Gommeren W, Verhasselt P, et al. Structure of the human serotonin 5-HT4 receptor gene and cloning of a novel 5-HT4 splice variant. J Neurochem. 2000 ed. 2000 Feb;74(2):478–89.

93. Irving HR, Tochon-Danguy N, Chinkwo KA, Li JG, Grabbe C, Shapiro M, et al. Investigations into the binding affinities of different human 5-HT4 receptor splice variants. Pharmacology. 2010 ed. 2010;85(4):224–33.

94. Brattelid T, Kvingedal AM, Krobert KA, Andressen KW, Bach T, Hystad ME, et al. Cloning, pharmacological characterisation and tissue distribution of a novel 5-HT4 receptor splice variant, 5-HT4(i). Naunyn-Schmiedeberg's Archives of Pharmacology. 2004 ed. 2004 Jun;369(6):616–28.

95. Vilaró MT, Cortés R, Mengod G. Serotonin 5-HT4 receptors and their mRNAs in rat and guinea pig brain: distribution and effects of neurotoxic lesions. The Journal of comparative neurology. 2005 ed. 2005 Apr 18;484(4):418–39.

96. Medhurst AD, Lezoualc'h F, Fischmeister R, Middlemiss DN, Sanger GJ. Quantitative mRNA analysis of five C-terminal splice variants of the human 5-HT4 receptor in the central nervous system by TaqMan real time RT-PCR. Brain Res Mol Brain Res. 2001st ed. 2001 Jun 20;90(2):125–34.

97. Coupar IM, Desmond PV, Irving HR. Human 5-HT(4) and 5-HT(7) receptor splice variants: are they important? Current neuropharmacology. 2007 ed. 2007 Dec;5(4):224–31.

98. Claeysen S, Sebben M, Becamel C, Bockaert J, Dumuis A. Novel brain-specific 5-HT4 receptor splice variants show marked constitutive activity: role of the C-terminal intracellular domain. Mol Pharmacol. 1999 ed. 1999 May;55(5):910–20.

99. Pindon A, Van Hecke G, Josson K, Van Gompel P, Lesage A, Leysen JE, et al. Internalization of human 5-HT4a and 5-HT4b receptors is splice variant dependent. Bioscience reports. 2005 ed. 2004 Jun;24(3):215–23.

100. Mialet J, Berque-Bestel I, Sicsic S, Langlois M, Fischmeister R, Lezoualc'h F. Pharmacological characterization of the human 5-HT(4(d)) receptor splice variant stably expressed in Chinese hamster ovary cells. British Journal of Pharmacology. Blackwell Publishing Ltd; 2000 Oct;131(4):827–35.

101. Vilaro MT, Doménech T, Palacios JM, Mengod G. Cloning and characterization of a novel human 5-HT4 receptor variant that lacks the alternatively spliced carboxy terminal exon. RT-PCR distribution in human brain and periphery of multiple 5-HT4 receptor variants. Neuropharmacology. 2002 Jan;42(1):60–73.

102. Olsen MA, Nawoschik SP, Schurman BR, Schmitt HL, Burno M, Smith DL, et al. Identification of a human 5-HT6 receptor variant produced by alternative splicing. Brain Res Mol Brain Res. 1999 ed. 1999 Feb 5;64(2):255–63.

103. Jasper JR, Kosaka A, To ZP, Chang DJ, Eglen RM. Cloning, expression and pharmacology of a truncated splice variant of the human 5-HT 7 receptor (h5-HT 7(b)). British Journal of Pharmacology. 1997;122(1):126–32.

104. Krobert K, Bach T, Syversveen T, Kvingedal A, Levy F. The cloned human 5-HT 7 receptor splice variants: a comparative characterization of their pharmacology, function and distribution. Naunyn-Schmiedeberg's Archives of Pharmacology. 2001 May 22;363(6):620–32.

105. Mahé C, Bernhard M, Bobirnac I, Keser C, Loetscher E, Feuerbach D, et al. Functional expression of the serotonin 5-HT7 receptor in human glioblastoma cell lines. British Journal of Pharmacology. 2004 ed. 2004 Oct;143(3):404–10.

106. Mahé C, Loetscher E, Dev KK, Bobirnac I, Otten U, Schoeffter P. Serotonin 5-HT7 receptors coupled to induction of interleukin-6 in human microglial MC-3 cells. Neuropharmacology. 2005 ed. 2005 Jul;49(1):40–7.

107. Guthrie CR, Murray AT, Franklin AA, Hamblin MW. Differential agonist-mediated internalization of the human 5-hydroxytryptamine 7 receptor isoforms. Journal of Pharmacology and Experimental Therapeutics. American Society for Pharmacology and Experimental Therapeutics; 2005 Jun;313(3):1003–10.

108. Liu X-Y, Liu Z-C, Sun Y-G, Ross M, Kim S, Tsai F-F, et al. Unidirectional Cross-Activation of GRPR by MOR1D Uncouples Itch and Analgesia Induced by Opioids. Cell. 2011 Oct;147(2):447–58.

109. Peng J, Sarkar S, Chang SL. Opioid receptor expression in human brain and peripheral tissues using absolute quantitative real-time RT-PCR. Drug Alcohol Depend. 2012 Aug 1;124(3):223–8.

110. Xu J, Lu Z, Xu M, Rossi GC, Kest B, Waxman AR, et al. Differential Expressions of the Alternatively Spliced Variant mRNAs of the μ Opioid Receptor Gene, OPRM1 , in Brain Regions of Four Inbred Mouse Strains. PLoS ONE. 2014;9(10):e111267.

111. Wieskopf JS, Pan Y-X, Marcovitz J, Tuttle AH, Majumdar S, Pidakala J, et al. Broad-spectrum analgesic efficacy of IBNtxA is mediated by exon 11-associated splice variants of the mu-opioid receptor gene. Pain. 2014 Oct;155(10):2063–70.

112. Choi HS, Kim CS, Hwang CK, Song KY, Wang W. The opioid ligand binding of human μ-opioid receptor is modulated by novel splice variants of the receptor. Biochem Biophys Res Commun. 2006;343(4):1132–40.

113. Pasternak GW. Insights into mu opioid pharmacology: The role of mu opioid receptor subtypes. Life Sci. 2001 Mar 23;68(2001):2213–9.

114. Pan Y-X. Diversity and complexity of the mu opioid receptor gene: alternative pre-mRNA splicing and promoters. DNA Cell Biol. 2005 Nov;24(11):736–50.

115. Majumdar S, Grinnell S, Le Rouzic V, Burgman M, Polikar L, Ansonoff M, et al. Truncated G protein-coupled mu opioid receptor MOR-1 splice variants are targets for highly potent opioid analgesics lacking side effects. Proceedings of the National Academy of Sciences. 2011 Dec 6;108(49):19778–83.

116. Pan YX, Xu J, Mahurter L, Bolan E, Xu M, Pasternak GW. Generation of the mu opioid receptor (MOR-1) protein by three new splice variants of the Oprm gene. Proceedings of the National Academy of Sciences. 2001;98(24):14084–9.

117. Xu J, Xu M, Brown T, Rossi GC, Hurd YL, Inturrisi CE, et al. Stabilization of the μ-Opioid Receptor by Truncated Single Transmembrane Splice Variants through a Chaperone-like Action. J Biol Chem. 2013 Jul 19;288(29):21211–27.

118. Kaushal S, Ridge KD, Khorana HG. Structure and function in rhodopsin: the role of asparagine-linked glycosylation. Proc Natl Acad Sci USA. National Acad Sciences; 1994 Apr 26;91(9):4024–8.

119. Hawrylyshyn KA, Michelotti GA, Coge F, Guenin SP, Schwinn DA. Update on human alpha1-adrenoceptor subtype signaling and genomic organization. Trends in Pharmacological Sciences. 2004 ed. 2004 Sep;25(9):449–55.

120. Silver K, Walston J, Yang Y, Pratley R, Ravussin E, Raben N, et al. Molecular scanning of the beta-3-adrenergic receptor gene in Pima Indians and Caucasians. Diabetes Metab Res Rev. 1999 May;15(3):175–80.

121. Spronsen A, Nahmias C, Krief S, Briend-Sutren M-M, Strosberg AD, Emorine LJ. The promoter and intron/exon structure of the human and mouse β3- adrenergic- receptor genes. European Journal of Biochemistry. Blackwell Publishing Ltd; 1993 May 1;213(3):1117–24.

122. Nakae A, Nakai K, Tanaka T, Hosokawa K, Mashimo T. Serotonin 2C receptor alternative splicing in a spinal cord injury model. Neuroscience Letters. 2013 Jan 4;532:49–54.

123. Milligan G. Constitutive activity and inverse agonists of G protein-coupled receptors: a current perspective. Mol Pharmacol. American Society for Pharmacology and Experimental Therapeutics; 2003 Dec;64(6):1271–6.

124. Gellynck E, Heyninck K, Andressen KW, Haegeman G, Levy FO, Vanhoenacker P, et al. The serotonin 5-HT7 receptors: two decades of research. Exp Brain Res. Springer Berlin Heidelberg; 2013 Oct;230(4):555–68.

125. Xu J, Faskowitz AJ, Rossi GC, Xu M, Lu Z, Pan Y-X, et al. Stabilization of morphine tolerance with long-term dosing: Association with selective upregulation of mu-opioid receptor splice variant mRNAs. Proceedings of the National Academy of Sciences. National Acad Sciences; 2015 Jan 6;112(1):279–84.

126. Grinnell SG, Majumdar S, Narayan A, Le Rouzic V, Ansonoff M, Pintar JE, et al. Pharmacologic characterization in the rat of a potent analgesic lacking respiratory depression, IBNtxA. J Pharmacol Exp Ther. American Society for Pharmacology and Experimental Therapeutics; 2014 Sep;350(3):710–8.

127. Oladosu FA, Conrad MS, OBuckley SC, Rashid NU, Slade GD, Nackley AG. Mu Opioid Splice Variant MOR-1K Contributes to the Development of Opioid-Induced Hyperalgesia. Taylor B, editor. PLoS ONE. Public Library of Science; 2015;10(8):e0135711.

128. Shabalina SA, Zaykin DV, Gris P, Ogurtsov AY, Gauthier J, Shibata K, et al. Expansion of the human mu-opioid receptor gene architecture: novel functional variants. Oxford University Press; 2009 Mar 15;18(6):1037–51.

129. Latremoliere A, Woolf CJ. Central Sensitization: A Generator of Pain Hypersensitivity by Central Neural Plasticity. The Journal of Pain. 2009 Sep;10(9):895–926.

130. Woolf CJ. Central sensitization: implications for the diagnosis and treatment of pain. Pain. 2011 Mar;152(3 Suppl):S2–15.

131. Cho KJ, Kim HW, Cheon SY, Lee JE, Kim GW. Apoptosis signal-regulating kinase-1 aggravates ROS-mediated striatal degeneration in 3-nitropropionic acid-infused mice. Biochem Biophys Res Commun. 2013 Nov;441(2):280–5.

132. Yu D, Pendergraff H, Liu J, Kordasiewicz HB, Cleveland DW, Swayze EE, et al. Single-stranded RNAs use RNAi to potently and allele-selectively inhibit mutant huntingtin expression. Cell. 2012 Aug 31;150(5):895–908.

133. Schwarz DS, Hutvágner G, Haley B, Zamore PD. Evidence that siRNAs function as guides, not primers, in the Drosophila and human RNAi pathways. Mol Cell. 2002 Sep;10(3):537–48.

134. Yaksh TL, Rudy TA. Chronic catheterization of the spinal subarachnoid space. Physiol Behav. 1976 Dec;17(6):1031–6.

135. Chaplan SR, Bach FW, Pogrel JW, Chung JM, Yaksh TL. Quantitative assessment of tactile

allodynia in the rat paw. J Neurosci Methods. 1994 Jul;53(1):55–63.

136. Menendez L, Lastra A, Hidalgo A, Baamonde A. Unilateral hot plate test: a simple and sensitive method for detecting central and peripheral hyperalgesia in mice. J Neurosci Methods. 2002;113(1):91–7.

137. Kolesnikov Y, Jain S, Wilson R, Pasternak GW. Lack of morphine and enkephalin tolerance in 129/SvEv mice: evidence for a NMDA receptor defect. J Pharmacol Exp Ther. 1998 ed. 1998 Feb;284(2):455–9.

138. Lee P-W, Wu S, Lee Y-M. Differential expression of mu-opioid receptor gene in CXBK and B6 mice by Sp1. Mol Pharmacol. 2004 Dec;66(6):1580–4.

139. Butt MT. Morphologic changes associated with intrathecal catheters for direct delivery to the central nervous system in preclinical studies. Toxicol Pathol. 2011 Jan;39(1):213–9.

140. Mattioli TA, Sutak M, Milne B, Jhamandas K, Cahill CM. Intrathecal Catheterization Influences Tolerance to Chronic Morphine in Rats. Anesth Analg. 2012 Mar;114(3):690–3.

141. Lu Z, Xu J, Xu M, Pasternak GW, Pan Y-X. Morphine regulates expression of μ-opioid receptor MOR-1A, an intron-retention carboxyl terminal splice variant of the μ-opioid receptor (OPRM1) gene via miR-103/miR-107. Mol Pharmacol. 2014 Feb;85(2):368–80.

142. Liang D-Y, Li X, Clark JD. 5-hydroxytryptamine type 3 receptor modulates opioid-induced hyperalgesia and tolerance in mice. Anesthesiology. The American Society of Anesthesiologists; 2011 May;114(5):1180–9.

143. Arout CA, Caldwell M, Rossi G, Kest B. Spinal and supraspinal N-methyl-d-aspartate and melanocortin-1 receptors contribute to a qualitative sex difference in morphine-induced hyperalgesia. Physiol Behav. Elsevier Inc; 2015 Aug 1;147(C):364–72.

144. Joly V, Richebe P, Guignard B, Fletcher D, Maurette P, Sessler DI, et al. Remifentanil-induced postoperative hyperalgesia and its prevention with small-dose ketamine. Anesthesiology. 2005 Jul;103(1):147–55.

145. Majumdar S, Grinnell S, Le Rouzic V, Burgman M, Polikar L, Ansonoff M, et al. Truncated G protein-coupled mu opioid receptor MOR-1 splice variants are targets for highly potent opioid analgesics lacking side effects. Proceedings of the National Academy of Sciences. 2011 Dec 6;108(49):19778–83.

146. Shigeta Y, Kasai S, Han W, Hata H, Nishi A, Takamatsu Y, et al. Association of morphine-induced antinociception with variations in the 5“ flanking and 3” untranslated regions of the mu opioid receptor gene in 10 inbred mouse strains. Pharmacogenet Genomics. 2008 Nov;18(11):927–36.

147. Laboureyras E, Aubrun F, Monsaingeon M, Corcuff J-B, Laulin J-P, Simonnet G. Exogenous and endogenous opioid-induced pain hypersensitivity in different rat strains. Pain Res Manag. 2014 Jul;19(4):191–7.

148. Diatchenko L, Robinson JE, Maixner W. Elucidation of mu-Opioid Gene Structure: How Genetics Can Help Predict Responses to Opioids. Eur J Pain Suppl. 2011 Nov 11;5(2):433–8.

149. Oertel BG, Doehring A, Roskam B, Kettner M, Hackmann N, Ferreirós N, et al. Genetic-epigenetic interaction modulates μ-opioid receptor regulation. 2012 Nov 1;21(21):4751–60.

150. Dever SM, Costin BN, Xu R, El-Hage N, Balinang J, Samoshkin A, et al. Differential expression of the alternatively spliced OPRM1 isoform μ-opioid receptor-1K in HIV-infected individuals. AIDS. 2014 Jan;28(1):19–30.

151. Raffa R, Pergolizzi J Jr. Opioid-Induced Hyperalgesia: Is It Clinically Relevant for the Treatment of Pain Patients. Pain Management Nursing. 2011 In;:1–17.

152. Iwamoto K, Eaton DL, Klaassen CD. Uptake of morphine and nalorphine by isolated rat hepatocytes. J Pharmacol Exp Ther. 1978 Jul;206(1):181–9.

153. Doherty MM, Poon K, Tsang C, Pang KS. Transport Is Not Rate-Limiting in Morphine Glucuronidation in the Single-Pass Perfused Rat Liver Preparation. J Pharmacol Exp Ther. American Society for Pharmacology and Experimental Therapeutics; 2006 May 1;317(2):890–900.

154. Convertino M, Samoshkin A, Maixner W, Diatchenko L, Dokholyan NV. GPCR heterodimerization leads to opioid-induced hyperalgesia. 2nd ed. Study in Multidisciplinary Pain Research 2014. Rome, Italy; 2014.

155. Mathelier A, Fornes O, Arenillas DJ, Chen C-Y, Denay G, Lee J, et al. JASPAR 2016: a major expansion and update of the open-access database of transcription factor binding profiles. Nucleic Acids Research. Oxford University Press; 2016 Jan 4;44(D1):D110–5.

156. Yutzey KE, Konieczny SF. Different E-box regulatory sequences are functionally distinct when placed within the context of the troponin I enhancer. Nucleic Acids Research. Oxford University Press; 1992 Oct 11;20(19):5105–13.

157. Cramer T, Johnson RS. A novel role for the hypoxia inducible transcription factor HIF-1alpha: critical regulation of inflammatory cell function. Cell Cycle. 2003.

158. Manning BD, Cantley LC. AKT/PKB signaling: navigating downstream. Cell. 2007 Jun 29;129(7):1261–74.

159. Milligan ED, Watkins LR. Pathological and protective roles of glia in chronic pain. Nat Rev Neurosci. 2009 Jan;10(1):23–36.

160. Daijo H, Kai S, Tanaka T, Wakamatsu T, Kishimoto S, Suzuki K, et al. Fentanyl activates hypoxia-inducible factor 1 in neuronal SH-SY5Y cells and mice under non-hypoxic conditions in a μ-opioid receptor-dependent manner. European Journal of Pharmacology. 2011 Sep 30;667(1-3):144–52.

161. Koodie L, Ramakrishnan S, Roy S. Morphine Suppresses Tumor Angiogenesis through a HIF-1α/p38MAPK Pathway. The American Journal of Pathology. 2010.

162. Convertino M, Samoshkin A, Viet CT, Gauthier J, Li Fraine SP, Sharif-Naeini R, et al. Differential Regulation of 6- and 7-Transmembrane Helix Variants of μ-Opioid Receptor in Response to Morphine Stimulation. Datta PK, editor. PLoS ONE. Public Library of Science; 2015 Nov 10;10(11):e0142826–15.

163. Samoshkin A, Convertino M, Viet CT, Wieskopf JS, Kambur O, Marcovitz J, et al. Structural and functional interactions between six-transmembrane μ-opioid receptors and β2-adrenoreceptors modulate opioid signaling. Nature Publishing Group. Nature Publishing Group; 2015 Dec 2;:1–13.

164. Corder G, Doolen S, Donahue RR, Winter MK, Jutras BL, He Y, et al. Constitutive μ-Opioid Receptor Activity Leads to Long-Term Endogenous Analgesia and Dependence. Science. American Association for the Advancement of Science; 2013 Sep 20;341(6152):1394–9.

165. Halls ML, Yeatman HR, Nowell CJ, Thompson GL, Gondin AB, Civciristov S, et al. Plasma membrane localization of the μ-opioid receptor controls spatiotemporal signaling. Sci Signal. American Association for the Advancement of Science; 2016 Feb 9;9(414):ra16–6.

166. Roeckel L-A, Le Coz G-M, Gavériaux-Ruff C, Simonin F. Opioid-induced hyperalgesia: Cellular and molecular mechanisms. NSC. IBRO; 2016 Jun 24;:1–23.

167. Hanani M. Satellite glial cells in sensory ganglia: from form to function. Brain Research Reviews. 2005 Jun;48(3):457–76.